REPORT NO.
UCB/EERC-84/10
AUGUST 1984

EARTHQUAKE ENGINEERING RESEARCH CENTER

EARTHQUAKE ANALYSIS AND RESPONSE OF CONCRETE GRAVITY DAMS

by

GREGORY FENVES
ANIL K. CHOPRA

COLLEGE OF ENGINEERING

UNIVERSITY OF CALIFORNIA · Berkeley, California

REPORT DOCUMENTATION PAGE	1. REPORT NO. NSF/CEE-84021	2.	3. Recipient's Accession No. PB85 193902 AS
4. Title and Subtitle Earthquake Analysis and Response of Concrete Gravity Dams			5. Report Date August 1984
			6.
7. Author(s) Gregory Fenves and Anil K. Chopra			8. Performing Organization Rept. No. UCB/EERC-84/10
9. Performing Organization Name and Address Earthquake Engineering Research Center University of California, Berkeley 1301 So. 46th Street Richmond, Calif. 94804			10. Project/Task/Work Unit No.
			11. Contract(C) or Grant(G) No. (C) (G) CEE-8120308 CEE-8401439
12. Sponsoring Organization Name and Address National Science Foundation 1800 G Street, N.W. Washington, D.C. 20550			13. Type of Report & Period Covered
			14.

15. Supplementary Notes

16. Abstract (Limit: 200 words)

First the reservoir bottom materials are modelled approximately by a reservoir bottom that partially absorbs incident hydro-dynamic pressure waves, to show that reservoir bottom absorption provides an important energy radiation mechanism that can significantly affect the earthquake response of concrete gravity dams. A general analytical procedure, based on the substructure method, is then developed to compute the response of concrete gravity dams to arbitrary earthquake ground motion including the simultaneous effects of dam-water interaction, dam-foundation rock interaction and reservoir bottom absorption.

Utilizing the analytical procedure the response of dams to harmonic and earthquake ground motion is computed for a wide range of parameters characterizing the dam, water, foundation rock and reservoir bottom materials.

Finally, a simplified analytical procedure suitable for the preliminary design and safety evaluation of concrete gravity dams is developed. The simplified procedure includes the more important factors influencing the earthquake response of dams. An equivalent single-degree-of-freedom system is developed that approximately represents the fundamental mode response of concrete gravity dams on flexible foundation rock with impounded water and absorptive reservoir bottom materials due to horizontal earthquake ground motion. The equivalent SDF system can then be used in a response spectrum earthquake analysis of the dam.

17. Document Analysis   a. Descriptors

b. Identifiers/Open-Ended Terms

c. COSATI Field/Group

18. Availability Statement Release Unlimited	19. Security Class (This Report)	21. No. of Pages 238
	20. Security Class (This Page)	22. Price

(See ANSI–Z39.18)   See Instructions on Reverse   OPTIONAL FORM 272 (4–77)
(Formerly NTIS–35)
Department of Commerce

EARTHQUAKE ANALYSIS AND RESPONSE OF CONCRETE GRAVITY DAMS

by

Gregory Fenves

Anil K. Chopra

August 1984

ABSTRACT

In order to design earthquake resistant dams and to evaluate the safety of existing dams during future earthquakes, reliable analytical procedures are necessary to predict earthquake induced stresses and deformations. The objectives of this work are to develop efficient techniques for analyzing the earthquake response of concrete gravity dams and investigate how dam-water-foundation rock interaction, and alluvium and sediments that invariably deposit at the bottom of reservoirs, affect the dam response.

In an initial investigation of the fundamental mode response of dams, the reservoir bottom materials are modelled approximately by a reservoir bottom that partially absorbs incident hydrodynamic pressure waves. It is demonstrated that reservoir bottom absorption provides an important energy radiation mechanism that can significantly affect the earthquake response of concrete gravity dams. A general analytical procedure, based on the substructure method, is then developed to compute the response of concrete gravity dams to arbitrary earthquake ground motion including the simultaneous effects of dam-water interaction, dam-foundation rock interaction and reservoir bottom absorption.

Utilizing the analytical procedure the response of dams to harmonic and earthquake ground motion is computed for a wide range of parameters characterizing the dam, water, foundation rock and reservoir bottom materials. It is shown that: (a) the earthquake response of concrete gravity dams is increased by dam-water interaction, but decreased by reservoir bottom absorption with the magnitude of these effects dependent on the flexibility of the foundation rock; (b) dam-water interaction and reservoir bottom absorption both have a profound effect on the response of dams to vertical ground motion, but relatively less effect on the response to horizontal ground motion if foundation-rock flexibility is considered; (c) the significance of the response of concrete gravity dams to vertical ground motion was overestimated in earlier studies that assumed a rigid reservoir bottom; and (d) the compressibility of the water should be considered in the earthquake analysis of concrete gravity dams because the effects of dam-water interaction and reservoir bottom absorption are not properly represented by the assumption of incompressible water.

ACKNOWLEDGEMENTS

vii

1. INTRODUCTION

In order to design earthquake resistant dams and to evaluate the safety of existing dams during future earthquakes, reliable analytical procedures are necessary to predict the earthquake induced stresses and deformations. The early research [5,6] was directed towards the analysis of hydrodynamic effects in the earthquake response of concrete gravity dams. An analytical procedure, based on the substructure method, was developed to compute the earthquake response of dams including the dynamic effects of the impounded water [3]. Utilizing this analytical procedure it was shown that dam-water interaction and water compressibility have a significant influence on the dynamic response of concrete gravity dams [4]; and that the contribution of the vertical component of ground motion to the total response was especially important in the earthquake response of dams because of the large hydrodynamic pressure developed in the lateral direction [2,4].

Subsequently, the substructure method was extended to include the effects of interaction between the dam and flexible foundation rock, which was idealized as a viscoelastic half-plane [8]. Utilizing this analytical procedure it was shown that the response of concrete gravity dams is generally influenced to a significant degree by dam-water interaction and dam-foundation rock interaction [10,11].

In the substructure method formulation, hydrodynamic effects contribute additional frequency-dependent terms in the frequency domain equations of motion for the dam [3]. These hydrodynamic terms can be interpreted as added mass, added damping and added force contributions of the impounded water. They are obtained from the solution of the wave equation for appropriate accelerations at the boundaries of the fluid domain. In the analytical procedure [8] all the hydrodynamic terms, except the added force associated with vertical ground motion, were determined under the assumption that the reservoir bottom is rigid, causing complete reflection of hydrodynamic pressure waves incident at the reservoir bottom. Under this assumption, the hydrodynamic pressure on a rigid dam due to vertical ground motion, and similarly the associated added force, are very large because hydrodynamic pressure waves do not propagate in the upstream direction, resulting in a truly undamped system without any energy loss. This recognition [5] led to a damping boundary condition arising from partial absorption of hydrodynamic pressure waves at the reservoir bottom [25] that was incorporated in subsequent

1

further demonstrated that an absorptive reservoir bottom provides an important energy radiation mechanism, through refraction of pressure waves into the layer of reservoir bottom materials, that should be considered in the earthquake analysis of dams.

Because the effects of reservoir bottom absorption are shown to be significant in Chapter 3, a previously developed general analytical procedure [8], which considers all the important vibration modes in the earthquake response of concrete gravity dams including dam-water-foundation rock interaction, is extended in Chapter 4 to include the effects of absorptive reservoir bottom materials, such as alluvium and sediments. The general analytical procedure is based on the substructure method, wherein each substructure, dam, impounded water, foundation rock and layer of reservoir bottom materials, is idealized in a manner appropriate to its properties and dynamic behavior. The interaction between the impounded water and reservoir bottom materials is approximately modelled by introducing a boundary condition that allows partial absorption of hydrodynamic pressure waves incident on the reservoir bottom. Including reservoir bottom absorption does not change the form of the frequency domain equations for the dam-water-foundation rock system, but it does affect the hydrodynamic terms. Continuum solutions for the hydrodynamic terms including reservoir bottom absorption are presented and numerical methods for their efficient evaluation are discussed.

The objective of Chapter 5 is then to ascertain the manner in which the response of dams is affected by reservoir bottom absorption for a wide range of basic parameters characterizing the dam, impounded water, foundation rock and reservoir bottom materials. The response of an idealized dam monolith to harmonic horizontal or vertical ground motion is presented in the form of frequency response functions. Based on these response results, the effects of reservoir bottom absorption on the response of the dam including its interaction with the impounded water and foundation rock are investigated and shown to influence significantly the response of dams.

Chapter 6 presents the displacement and stress responses of the tallest, non-overflow monolith of Pine Flat concrete gravity dam to Taft ground motion for a range of properties for the reservoir bottom materials and various assumptions for the impounded water and foundation rock. Based on the results from these analyses, the effects of reservoir bottom absorption, dam-water interaction and dam-

2. SYSTEM AND GROUND MOTION

The system considered consists of a concrete gravity dam supported on the horizontal surface of underlying flexible foundation rock and impounding a reservoir of water (Figure 2.1). For computing the response of the dam to intense earthquake ground motion, it is appropriate to consider the two-dimensional vibration of individual dam monoliths. This assumption, based on observations during forced vibration tests of Pine Flat Dam and the earthquake response of Koyna Dam, is discussed elsewhere in detail [8,24]. The system is analyzed under the assumption of linear behavior for the concrete dam, the impounded water and the foundation rock. Thus, the possibilities of concrete cracking [23] or water cavitation [31] are not considered.

The selected monolith or dam cross-section is idealized as a two-dimensional finite element system in order to model arbitrary geometry and elastic material properties of the dam. However, certain restrictions are imposed on the geometry of the dam to permit a continuum solution for hydrodynamic pressure in the impounded water. For the purpose of determining hydrodynamic effects, and only for this purpose, the upstream face of the dam is assumed to be vertical. This assumption is reasonable for actual concrete gravity dams because the upstream face is vertical or almost vertical for most of the height, and the hydrodynamic pressure on the dam face is insensitive to small departures of the face slope from vertical [30], especially if these departures are near the base of the dam, which is usually the case. The water impounded in the reservoir is idealized by a fluid domain of constant depth and infinite length in the upstream direction. The foundation rock underlying the dam and reservoir bottom materials is idealized as a homogeneous, isotropic, viscoelastic half-plane.

The bottom of a reservoir upstream of a dam may consist of highly variable layers of exposed bedrock, alluvium, silt and other sedimentary material. Because these reservoir bottom materials are not adequately modelled by the viscoelastic half-plane idealization of the foundation rock, they are approximately modelled, as described in Chapters 3 and 4, by a boundary condition at the reservoir bottom that allows partial absorption of incident hydrodynamic waves.

Over a period of time, the sediments may deposit to a significant depth in some reservoirs. The thickness of sediment layer can be recognized in the analytical procedure by correspondingly reducing

5
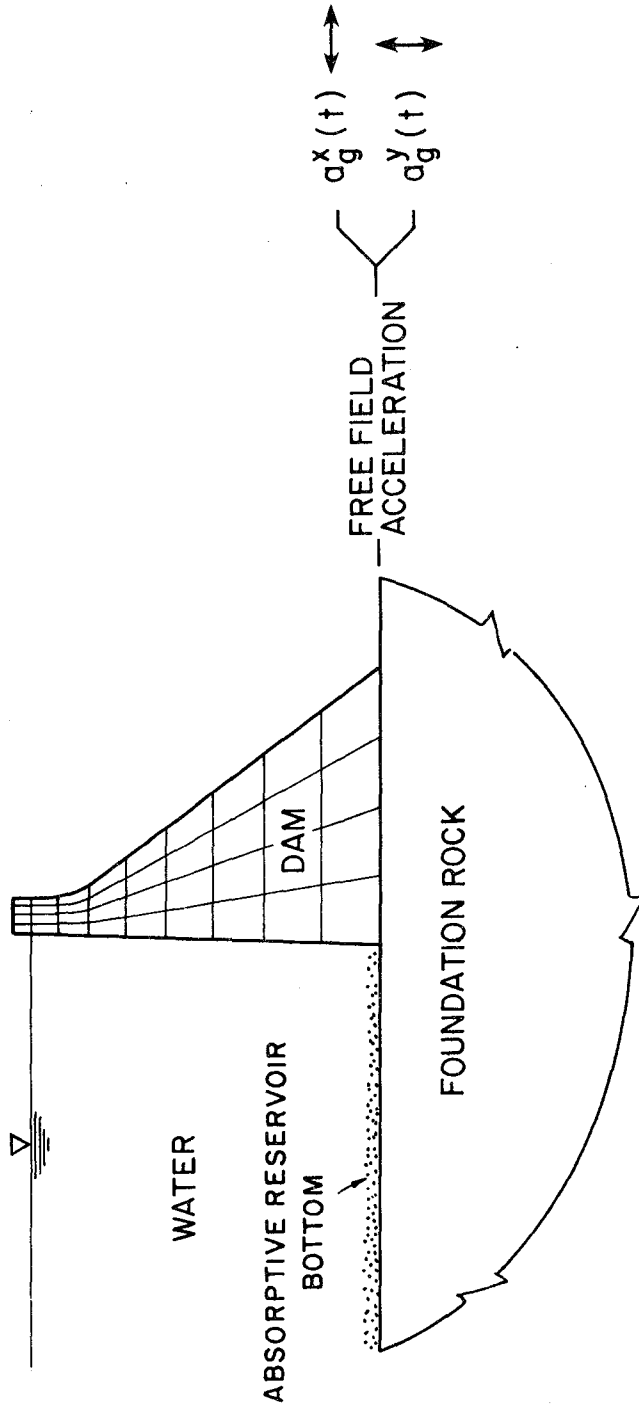
FIGURE 2.1   Dam-water-foundation rock system.

$$M_1 [\ddot{Y}_1^l(t) + 2\xi_1\omega_1 \dot{Y}_1^l(t) + \omega_1^2 Y_1^l(t)] = -L_1^l a_g^l(t) + \int_0^H p^l(0,y,t) \phi_1^{lx}(0,y) \, dy \qquad (3.2)$$

where

$$M \qquad\qquad {}^{\backslash 12} + [\phi_1^{ly}(x,y)]^2 \} \, dxdy \qquad (3.3)$$

is the generalized mass in w

over the cross-sectional are

vibration mode; ω_1 is the f

with an empty reservoir;

and $p^l(0,y,t)$ is the hyd

the dam.

Assuming water (

tude, irrotational moti

where $p(x,y,t)$ is t

of pressure waves i

cal upstream face

conditions for eq

pressure.

The norm

acceleration of

$$(3.6)$$

where ρ is tl

contrary to tʊ

on the reservoir bottom results in a reflected hydrodynamic pressure wave in the water and two refracted waves, dilatational and rotational, in the reservoir bottom materials. The angle of reflection is equal to the angle of incidence and the angles of refraction of the two refracted waves are given by Snell's law. Although the boundary condition given by equation (3.7) allows for proper reflection of hydrodynamic pressure waves for any angle of incidence, the only refracted waves allowed in the layer of reservoir bottom materials are downward, vertically propagating dilatational waves.

The fundamental parameter that characterizes the effects of absorption of hydrodynamic pressure waves at the reservoir bottom is the admittance or damping coefficient q. The wave reflection coefficient α, which is the ratio of the amplitude of the reflected hydrodynamic pressure wave to the amplitude of a vertically propagating pressure wave incident on the reservoir bottom, is related to the damping coefficient [17,25; and Appendix A] by

$$\alpha = \frac{1 - qC}{1 + qC} \tag{3.9}$$

The wave reflection coefficient α is a more physically meaningful description of the behavior of hydro-dynamic pressure waves at the reservoir bottom than is the damping coefficient q. Although the wave reflection coefficient depends on the angle of incidence of the pressure wave at the reservoir bottom, the value α for vertically incident waves, as given by equation (3.9), is used here for convenience. The wave reflection coefficient α may range within the limiting values of 1 and -1. For rigid reservoir bottom materials, $C_r = \infty$ and $q = 0$, resulting in $\alpha = 1$. For very soft reservoir bottom materials, C_r approaches zero and $q = \infty$, resulting in $\alpha = -1$. The material properties of the reservoir bottom medium are highly variable and depend upon many factors. It is believed that α values from 1 to 0 would cover the wide range of materials encountered at the bottom of actual reservoirs. Two typical examples for homogeneous materials are: competent sandstone ($E_r = 2$ million psi, unit weight $= 120$ lb/ft^3) has $\alpha = 0.56$; dense sand ($E_r = 0.2$ million psi, unit weight $= 100$ lb/ft^3) has $\alpha = 0$.

The motion of the dam, as governed by equation (3.2), is affected by the hydrodynamic pressure in the second term on the right side of the same equation; and the hydrodynamic pressure, as governed by equation (3.5) subject to the boundary conditions of equations (3.6) to (3.8), is affected by the

according to equations (3.10) and (3.11), can be separated into boundary conditions for $\bar{p}_0^j(x,y,\omega)$ and $\bar{p}_1(x,y,\omega)$. The frequency response function $\bar{p}_0^x(x,y,\omega)$ for the hydrodynamic pressure due to horizontal ground acceleration of a rigid dam is the solution of equation (3.13) subject to the following boundary conditions:

$$\left.\begin{aligned} \frac{\partial \bar{p}}{\partial x}(0,y,\omega) &= -\rho \\[2mm] \frac{\partial \bar{p}}{\partial y}(x,0,\omega) - i\omega q\, \bar{p}(x,0,\omega) &= 0 \\[2mm] \bar{p}(x,H,\omega) &= 0 \end{aligned}\right\} \qquad (3.15)$$

The frequency response function $\bar{p}_0^y(x,y,\omega)$ for the hydrodynamic pressure due to vertical ground acceleration of a rigid dam is the solution of equation (3.13) subject to the following boundary conditions:

$$\left.\begin{aligned} \frac{\partial \bar{p}}{\partial x}(0,y,\omega) &= 0 \\[2mm] \frac{\partial \bar{p}}{\partial y}(x,0,\omega) - i\omega q\, \bar{p}(x,0,\omega) &= -\rho \\[2mm] \bar{p}(x,H,\omega) &= 0 \end{aligned}\right\} \qquad (3.16)$$

The frequency response function $\bar{p}_1(x,y,\omega)$ for the hydrodynamic pressure due to horizontal acceleration $\phi_1^x(0,y)$ of the upstream face of a dam in its fundamental vibration mode is the solution of equation (3.13) subject to the following boundary conditions:

$$\left.\begin{aligned} \frac{\partial \bar{p}}{\partial x}(0,y,\omega) &= -\rho\,\phi_1^x(0,y) \\[2mm] \frac{\partial \bar{p}}{\partial y}(x,0,\omega) - i\omega q\, \bar{p}(x,0,\omega) &= 0 \\[2mm] \bar{p}(x,H,\omega) &= 0 \end{aligned}\right\} \qquad (3.17)$$

The complex-valued frequency response functions $\bar{p}_0^j(x,y,\omega)$ and $\bar{p}_1(x,y,\omega)$ for hydrodynamic pressure can be obtained using standard solution methods for boundary value problems. They are derived in Appendix B and summarized below for the upstream face of the dam $(x=0)$:

$$\mu_n(\omega) = \omega_n^r / C \tag{3.22a}$$

$$\omega_n^r = \frac{2n-1}{2} \pi \frac{C}{H} \tag{3.22b}$$

where ω_n^r are the natural vibration frequencies of the impounded water with rigid reservoir bottom; and

$$Y_n(y,\omega) = \cos\mu_n y \tag{3.23}$$

Furthermore, equation (3.18) reduces to the expressions derived earlier [2,3,25] for a rigid reservoir bottom (Appendix C).

The substitution of equation (3.14) into equation (3.12) leads to the frequency response function for the fundamental modal coordinate for a dam subjected to the l-component of harmonic free-field ground acceleration $(l = x,y)$:

$$\bar{Y}_1^l(\omega) = \frac{-[L_1^l + B_0^l(\omega)]}{-\omega^2\{M_1 + \text{Re}[B_1(\omega)]\} + i\omega\{2M_1\xi_1\omega_1 - \omega\,\text{Im}[B_1(\omega)]\} + \omega_1^2 M_1} \tag{3.24}$$

in which

$$B_0^l(\omega) = -\int_0^H \bar{p}_0^l(0,y,\omega)\,\phi_1^x(0,y)\,dy \tag{3.25a}$$

$$B_1(\omega) = -\int_0^H \bar{p}_1(0,y,\omega)\,\phi_1^x(0,y)\,dy \tag{3.25b}$$

where $\bar{p}_0^l(0,y,\omega)$ and $\bar{p}_1(0,y,\omega)$ were presented in equation (3.18). The effects of dam-water interaction and reservoir bottom absorption are contained in equation (3.24) through the frequency-dependent terms $B_0^l(\omega)$ and $B_1(\omega)$. Hydrodynamic effects can be interpreted as modifying the properties of the dam by introducing an added force $B_0^l(\omega)$, an added mass represented by the real-valued component of $B_1(\omega)$, and an added damping represented by the imaginary-valued component of $B_1(\omega)$. The added mass arises from the portion of the impounded water that reacts in phase with the motion of the dam. The added damping arises from the radiation of pressure waves in the upstream direction, away from the dam, and from their refraction and absorption into the absorptive reservoir bottom materials.
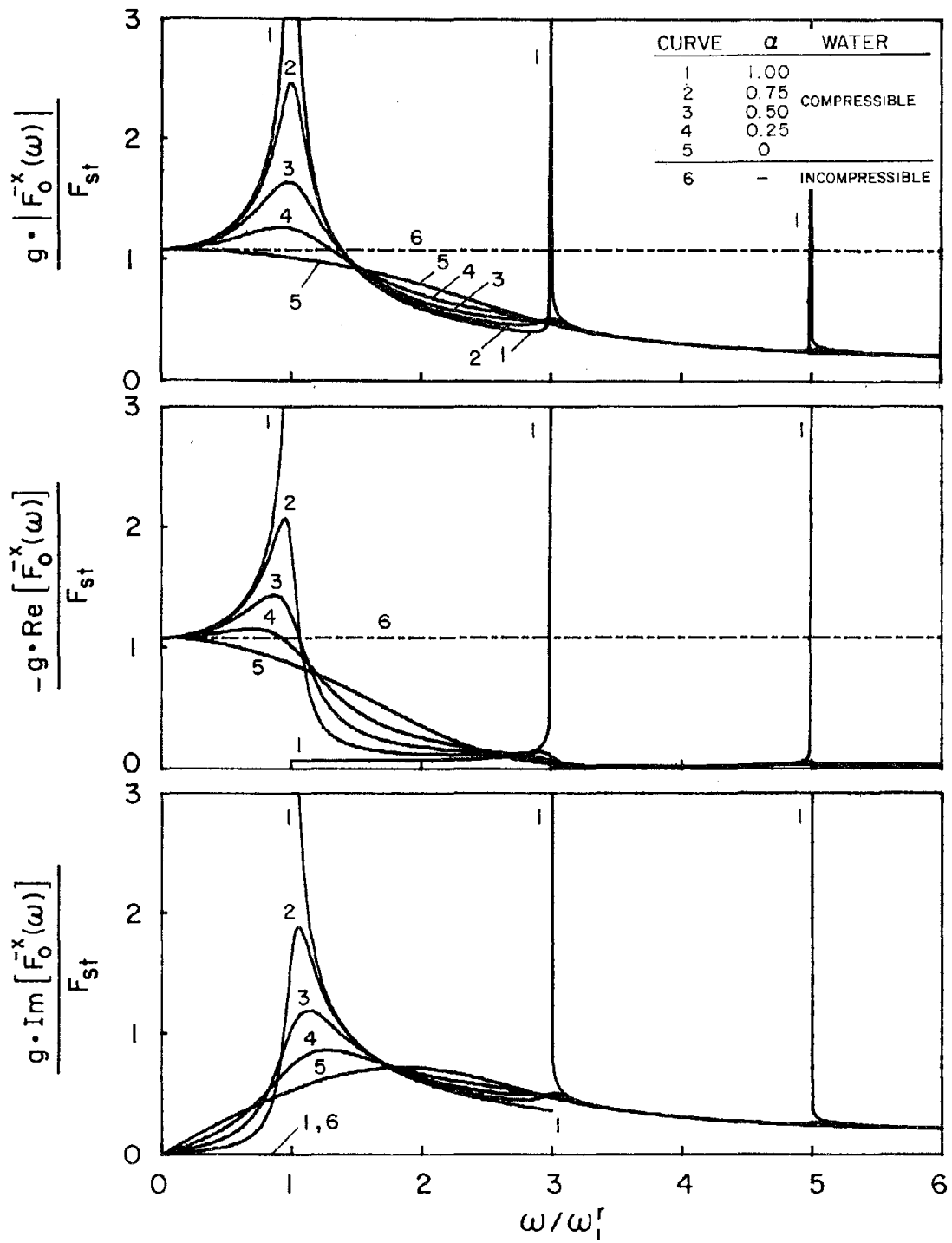
FIGURE 3.1   Influence of reservoir bottom absorption on the hydrodynamic force on a rigid dam due to harmonic horizontal ground motion.

the upstream direction of the infinitely-long fluid domain, resulting in radiation of energy. As the excitation frequency increases past ω_n^r, the hydrodynamic force contribution of the nth mode changes from a pressure function that decays exponentially to one that propagates in the upstream direction, thus reducing the real-valued component of $\bar{F}_0^x(\omega)$ and increasing its imaginary-valued component (Figure 3.1). With increasing excitation frequency, a larger number of modes are associated with the propagating pressure waves, leading to increased energy radiation and hence smaller hydrodynamic force [Figure 3.1(a)] -- except for the local resonances at the natural vibration frequencies of the impounded water.

Because of reservoir bottom absorption, the frequency-dependent eigenvalues $\mu_n(\omega)$ of the impounded water are complex-valued for all excitation frequencies. Consequently, the contribution of the nth natural vibration mode of the impounded water to the hydrodynamic force due to horizontal ground motion is complex-valued for all excitation frequencies; wherein the imaginary-valued component arises from the radiation of energy due to propagation of pressure waves in the upstream direction and their refraction into the absorptive reservoir bottom. As a result, if the reservoir bottom is absorptive, $\bar{F}_0^x(\omega)$ contains a 90° out-of-phase component even for excitation frequencies less than ω_1^r [Figure 3.2(c)]. Because of the additional energy radiation that results from reservoir bottom absorption, the hydrodynamic force is bounded for all excitation frequencies, the fundamental resonant peak is reduced and the higher resonant peaks are virtually eliminated. The additional energy radiation has little influence on the resonant frequencies of the impounded water.

The hydrodynamic pressure due to vertical ground motion is independent of the upstream x-coordinate [5] because pressure waves do not propagate in the upstream direction, resulting in a truly undamped system if the reservoir bottom is rigid. The frequency response function $\bar{F}_0^y(\omega)$ for hydrodynamic force due to vertical ground motion is real-valued, in-phase or opposite-phase relative to the ground acceleration, for all excitation frequencies. Reservoir bottom absorption leads to an imaginary-valued component associated with radiation of energy because pressure waves refract into the absorptive reservoir bottom for all excitation frequencies. This radiation damping reduces the response for all frequencies and results in bounded resonant response peaks.

component does not exist for any excitation frequency. It is apparent that, whereas the modulus of the hydrodynamic force with an absorptive reservoir bottom may be predicted reasonably well for lower excitation frequencies by neglecting water compressibility, this assumption does not recognize the radiation of energy due to pressure waves propagating in the upstream direction and refracting into the layer of reservoir bottom materials. For higher excitation frequencies, the incompressible solution greatly overestimates the hydrodynamic force because energy radiation due to wave propagation in the upstream direction is especially significant. Thus, it may be concluded that the analytically predicted effects of reservoir bottom absorption are not properly represented by neglecting compressibility of the impounded water. The conflicting conclusions from experimental data may in part be due to unreliable measurements of the phase angle between hydrodynamic force and acceleration of the piston.

3.5 Dam Response

3.5.1 Basic System Parameters

The non-dimensional form of equation (3.24) shows that, if $\overline{Y}_1(\omega) = -\omega^2\, \overline{Y}_1'(\omega)$ is expressed as a function of the excitation frequency parameter ω/ω_1 for a dam of fixed cross-sectional geometry and Poisson's ratio, it depends on three system parameters: $\Omega_r = \omega_1'/\omega_1$, the ratio of the fundamental natural vibration frequency of the impounded water to that of the dam alone; H/H_s, the ratio of water depth to dam height; and α, the wave reflection coefficient for the reservoir bottom materials. As seen in equation (3.22b), $\omega_1' = \pi C/2H$, and it can be shown that $\omega_1 = \gamma C_s/H_s$, where γ is a dimensionless factor that only depends on the cross-sectional geometry of the dam and Poisson's ratio, $C_s = \sqrt{E_s/\rho_s}$, E_s is the Young's modulus of elasticity and ρ_s is the density of the concrete in the dam; therefore

$$\Omega_r = \frac{\pi}{2\gamma}\, \frac{C}{C_s}\, \frac{H_s}{H} \tag{3.26}$$

For fixed values of γ, C, ρ_s and H/H_s, the frequency ratio Ω_r is proportional to $1/\sqrt{E_s}$. Thus Ω_r decreases with increasing E_s, or dam stiffness, and *vice versa*. If the reservoir is empty or the impounded water is assumed to be incompressible, $\overline{Y}_1(\omega)$ expressed as a function of ω/ω_1 is independent of E_s and α. Also, the incompressible water case is equivalent to $\Omega_r = \infty$.

3.5.3 Effects of Reservoir Bottom Absorption

Frequency response functions for dams subjected to horizontal and vertical ground motions are presented in Figures 3.3 to 3.6 for two selected values of $\Omega_r = 0.67$ and 1.0. Each plot contains response curves for the dam with full reservoir for five values of α and the response curve for the dam with an empty reservoir. The latter is the familiar response curve for a single degree-of-freedom system with frequency-independent mass, stiffness and damping parameters. The response of the dam with impounded water, however, is affected by the frequency-dependent hydrodynamic terms in the equations of motion for the dam, resulting in complicated shapes for the response curves.

The response behavior is especially complicated if the hydrodynamic pressure waves are completely reflected at the reservoir bottom ($\alpha = 1$) because at excitation frequencies equal to ω_m^r, the natural vibration frequencies of the impounded water, the added hydrodynamic mass and force are both unbounded. As determined by a limiting process, however, the response function due to horizontal ground motion, has bounded values at ω_m^r, which appear as local dips or increases in the response curve. Because of dam-water interaction, the resonant behavior is particularly complicated in the neighborhood of ω_1^r and ω_1 where two resonant peaks can occur (Figure 3.3) or only a single resonant peak may appear (Figure 3.5). In contrast, the response function due to vertical ground motion is dominated by the unbounded response values at excitation frequencies equal to ω_n^r (Figures 3.4 and 3.6). In the neighborhood of ω_n^r, the added mass is controlled by the term $[\omega^2 - (\omega_n^r)^2]^{-\frac{1}{2}}$ and the added force due to the vertical ground motion by $[\omega^2 - (\omega_n^r)^2]^{-1}$; because the latter term tends to infinity as ω approaches ω_n^r faster than the first term, the response is unbounded [18]. These unbounded peaks are not the result of resonance in the usual sense, which is associated with the denominator in equation (3.24) attaining a minimum, but are caused by the unbounded added force.

Reservoir bottom absorption reduces the added force associated with both ground motion components and the added mass to bounded values at ω_n^r. Consequently, the dips at ω_n^r in the response function due to horizontal ground motion are eliminated; and the unbounded values at ω_n^r in the response function due to vertical ground motion are reduced to bounded peaks, which disappear for the smaller values of α.
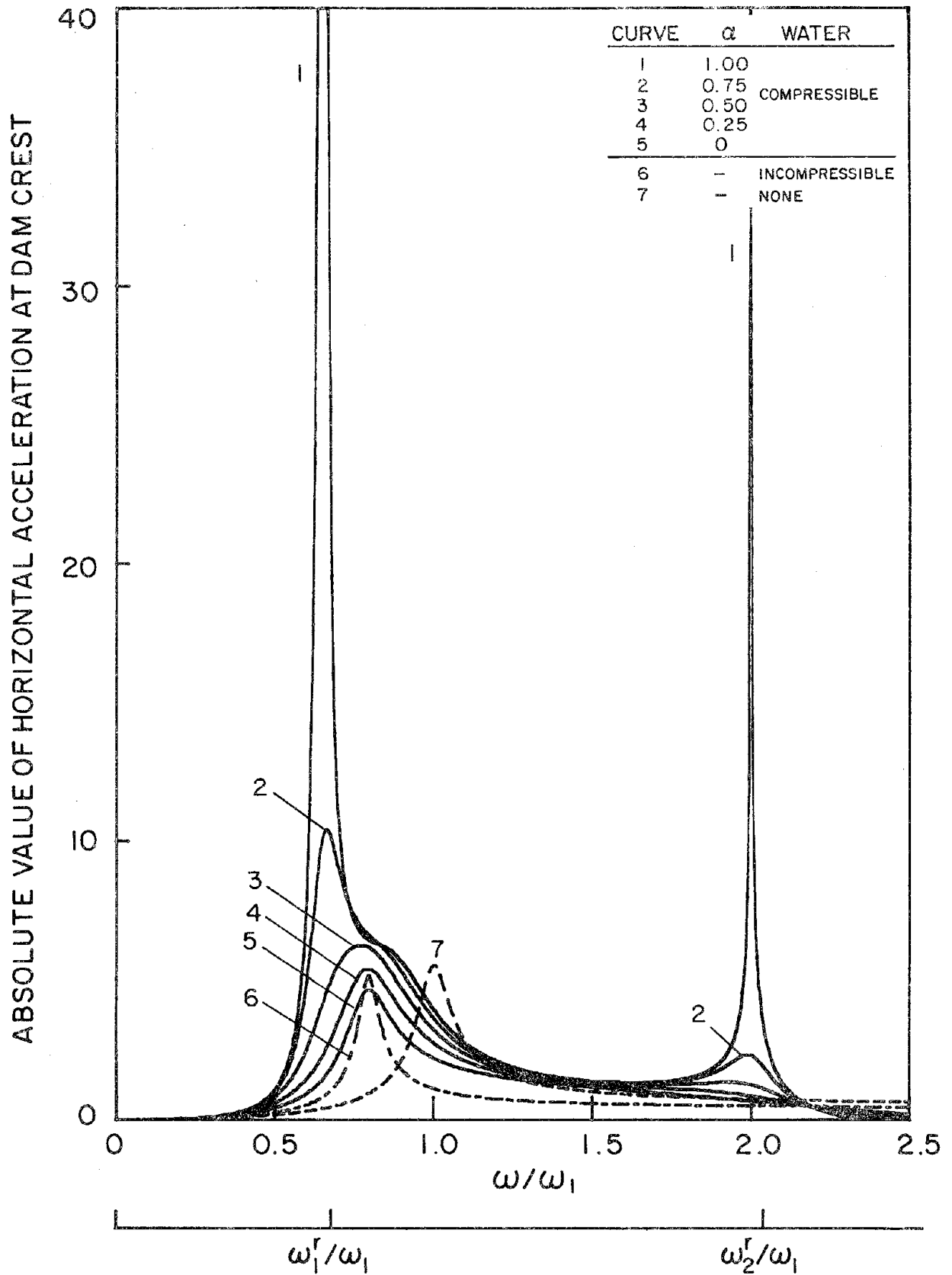
FIGURE 3.4   Influence of reservoir bottom absorption on dam response due to harmonic vertical ground motion. Frequency ratio $\Omega_r = 0.67$
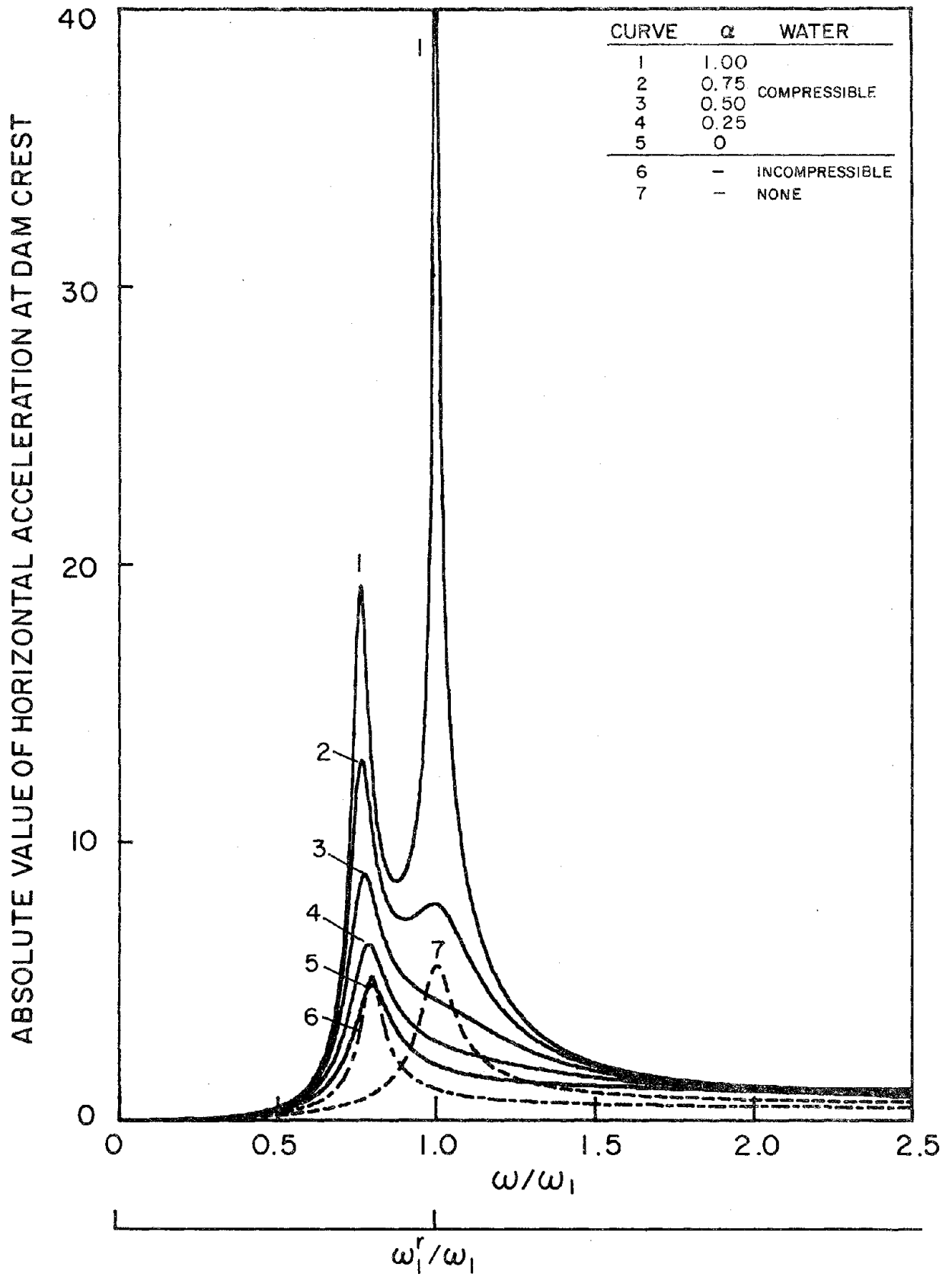
FIGURE 3.6   Influence of reservoir bottom absorption on dam response due to harmonic vertical ground motion. Frequency ratio $\Omega_r = 1.0$

3.5.4 Influence of the Frequency Ratio Ω_r

The response of the dam with an empty reservoir, when presented in the form of Figures 3.7 to 3.10, is independent of the Young's modulus E_s for the dam concrete. Similarly, the response curves including hydrodynamic effects do not vary with E_s if water compressibility is neglected [6]. However, the results presented in Figures 3.7 to 3.10 demonstrate that the frequency ratio Ω_r, or correspondingly the E_s value, affects the response functions if water compressibility is included. The fundamental resonant frequency of the dam decreases to a greater degree relative to ω_1 for the smaller values of Ω_r, i.e. larger values of E_s. This decrease in resonant frequency also depends on reservoir bottom absorption, being less pronounced for a wave absorptive reservoir bottom than for a rigid reservoir bottom.

Wave absorption at the reservoir bottom affects the resonant peak and bandwidth in an especially significant way. Comparison of Figures 3.7 and 3.9 for the response of the dam to horizontal ground motion shows that decreasing Ω_r, or increasing E_s, leads to larger resonant response over a narrower bandwidth for a rigid reservoir bottom (Figure 3.7); but causes smaller resonant response over a wider bandwidth for an absorptive reservoir bottom (Figure 3.9). This opposite trend in response results from the manner in which the effective damping at resonance is altered by reservoir bottom absorption. Two mechanisms contribute to the effective damping of the dam-water system: energy dissipation in the dam alone, represented by the viscous damping ratio ξ_1; and added damping due to radiation and absorption of hydrodynamic pressure waves, represented by the term $\mathrm{Im}[B_1(\omega)]$ in equation (3.24). The added damping at the resonant frequency of the dam-water system is zero if the reservoir bottom is rigid, because pressure waves do not refract into rigid reservoir bottom materials, nor do they propagate in the upstream direction at the resonant frequency, as it is less than ω_1^r. As Ω_r decreases, or E_s increases, the added mass at the resonant frequency increases, which proportionally decreases the viscous damping ratio in the dam. Because the added damping is zero at the resonant frequency, the effective damping decreases with decreasing Ω_r, leading to larger resonant response (Figure 3.7). If reservoir bottom absorption is included, however, the added damping is greater than zero at the resonant frequency of the dam-water system because the natural vibration modes of the impounded water contribute to energy radiation by propagation of pressure waves upstream and refraction into the
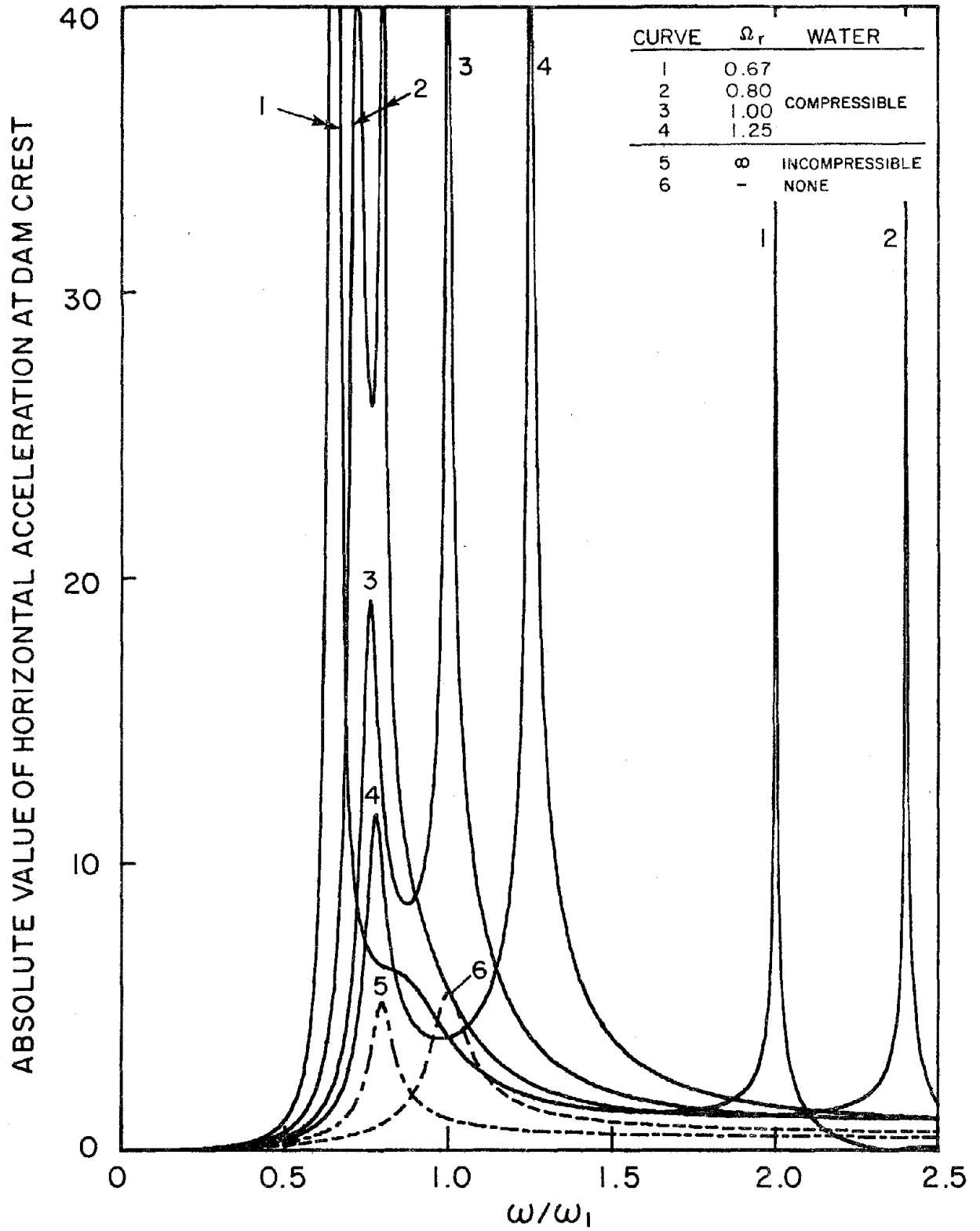
FIGURE 3.8 Influence of the frequency ratio Ω_r on dam response due to harmonic vertical ground motion with rigid reservoir bottom $(\alpha = 1)$.
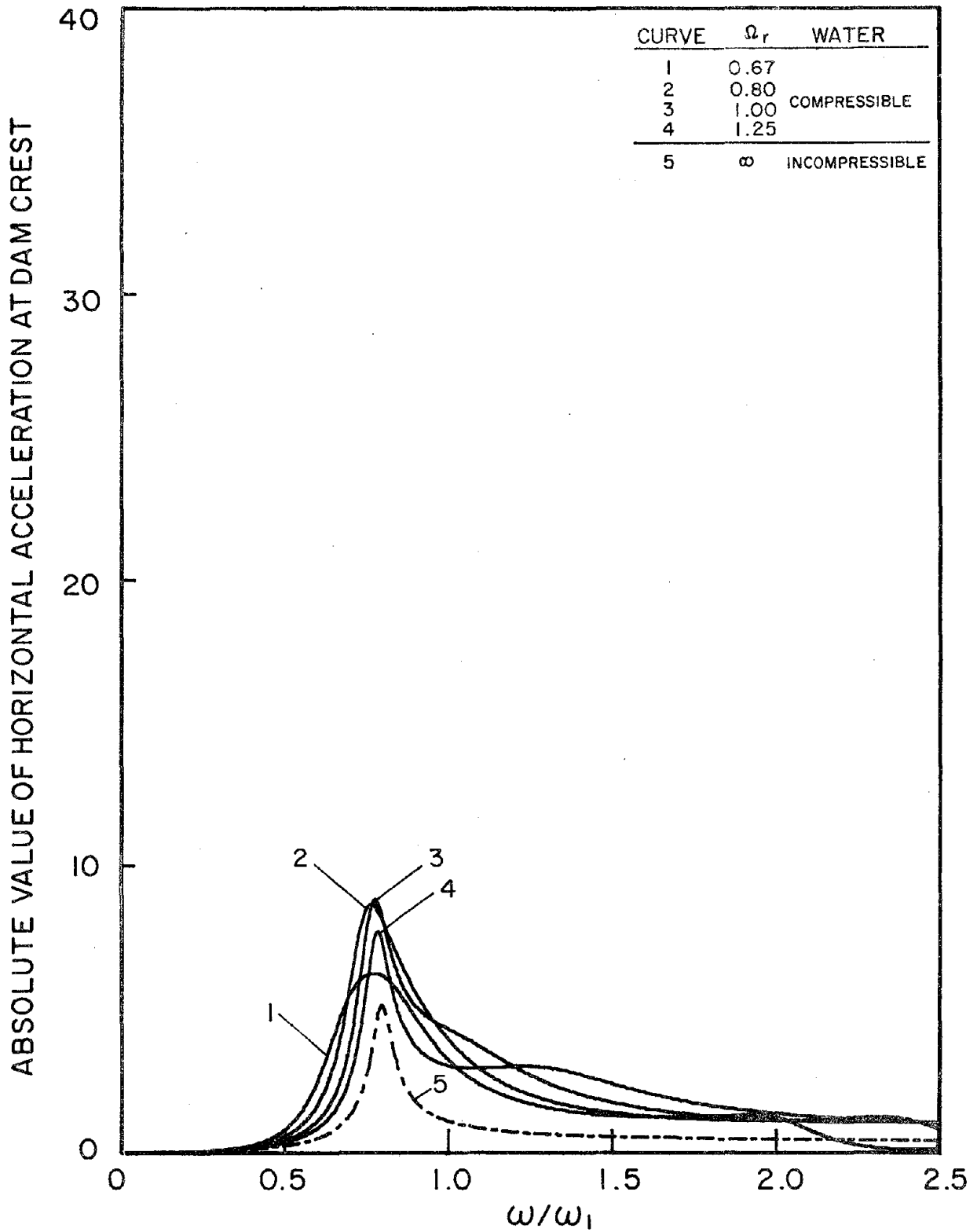
FIGURE 3.10   Influence of the frequency ratio Ω_r on dam response due to harmonic vertical ground motion with absorptive reservoir bottom.   Wave reflection coefficient $\alpha = 0.5$

dam response essentially as an incompressible fluid if the dam is flexible enough. Water compressibility assumes significance in the response of concrete gravity dams because E_s is generally in the range of 2 to 5 million psi for which the corresponding frequency ratio Ω_r varies between 1.2 and 0.7.

3.5.5 Comparison of Responses to Horizontal and Vertical Ground Motion

Comparing the response of the dam to horizontal and vertical ground motions (Figures 3.7 and 3.8) it is apparent -- consistent with common view -- that the response of a dam with an empty reservoir to vertical ground motion is relatively small because the L_1^l term [equation (3.4)] is much smaller for vertical ground motion ($l=y$) than for horizontal ground motion ($l=x$). With water impounded in the reservoir, the dam response is affected by the added hydrodynamic mass, damping and force terms in equation (3.24). Because the added mass and damping are independent of the excitation direction, the response functions due to horizontal and vertical ground motion display the same resonant frequency and effective damping. However, as discussed in Section 3.4, the hydrodynamic force on a rigid dam, and hence the added force $B_0^l(\omega)$, strongly depends on the excitation direction, thus leading to considerably different response due to the two components of ground motion.

This effect is summarized in Table 3.1 where the ratio of the resonant amplitude of horizontal crest displacement of the dam with a full reservoir to that with an empty reservoir is presented for several values of the frequency ratio Ω_r and two values of the wave reflection coefficient α: 1.0 and 0.5. In Table 3.1, the unbounded peaks that occur at excitation frequencies equal to ω_n^r in the response to vertical ground motion with rigid reservoir bottom are ignored because they are not resonant peaks in the usual sense caused by the denominator of equation (3.24) attaining a minimum, but are caused by unbounded values of $B_0^y(\omega)$. Whereas hydrodynamic effects result in increased response of the dam to either ground motion component (Table 3.1), if water compressibility is included the increase is greater in the response to vertical ground motion because the effective earthquake force L_1^y is small and the added force $B_0^y(\omega)$, which is comparatively large, dominates the numerator of equation (3.24). The added force is comparatively large because it is the result of hydrodynamic pressures acting in the

horizontal direction, same as the direction of primary displacement in the fundamental vibration mode of the dam, whereas L_1^y is the result of effective earthquake forces acting in the vertical direction. In contrast, for horizontal ground motion both the effective earthquake force and hydrodynamic pressure act in the horizontal direction, so $B_0^x(\omega)$ does not dominate L_1^x.

Hydrodynamic effects cause a larger increase in response to vertical ground motion than in response to horizontal ground motion, as the ratios of the responses to the two ground motion components show in Table 3.2. Thus, it is apparent that dam response to vertical ground motion is relatively more important if hydrodynamic effects are included. As seen in Tables 3.1 and 3.2, the significance of the response to vertical ground motion depends on Ω_r and α; increasing with decreasing Ω_r, i.e. as water compressibility effects become more significant; increasing for larger α i.e., as the energy radiated through an absorptive reservoir bottom decreases; and the response is sensitive to α only for systems with smaller Ω_r values.

4. GENERAL ANALYTICAL PROCEDURE

4.1 Introduction

The response results presented in Chapter 3 demonstrated that absorptive reservoir bottom materials can significantly affect the fundamental mode response of dams with impounded water due to harmonic ground motion. Consequently, the effects of reservoir bottom materials should be included in the earthquake analysis of dams. With this motivation, a general analytical procedure [8], based on the substructure method, is extended to include the effects of absorptive reservoir bottom materials on the response of concrete gravity dams to earthquake ground motion. As in the previous analytical procedure [8], the effects of dam-water interaction and dam-foundation rock interaction are included.

4.2 Frequency Domain Equations

4.2.1 Dam Substructure

The equations of motion for the dam idealized as a planar, two-dimensional finite element system (Figure 2.1) are:

$$\mathbf{m}_c \ddot{\mathbf{r}}_c + \mathbf{c}_c \dot{\mathbf{r}}_c + \mathbf{k}_c \mathbf{r}_c = -\mathbf{m}_c \mathbf{1}_c^x a_g^x(t) - \mathbf{m}_c \mathbf{1}_c^y a_g^y(t) + \mathbf{R}_c(t) \tag{4.1}$$

in which $\mathbf{m}_c$, $\mathbf{c}_c$ and $\mathbf{k}_c$ are the mass, damping and stiffness matrices for the finite element system; $\mathbf{r}_c$ is the vector of nodal point displacements relative to the free-field ground displacement (Figure 4.1):

$$\mathbf{r}_c^T = \; < r_1^x \; r_1^y \; r_2^x \; r_2^y \; \cdots \; r_n^x \; r_n^y \; \cdots \; r_{N+N_b}^x \; r_{N+N_b}^y \; >$$

where r_n^x and r_n^y are the x- and y-components of displacements of nodal point n; N is the number of nodal points above the dam base; N_b is the number of nodal points at the base; and

$$\{\mathbf{1}_c^x\}^T = \; < 1 \; 0 \; 1 \; 0 \; \cdots \; 1 \; 0 \; \cdots \; 1 \; 0 >$$

$$\{\mathbf{1}_c^y\}^T = \; < 0 \; 1 \; 0 \; 1 \; \cdots \; 0 \; 1 \; \cdots \; 0 \; 1 >$$

The force vector $\mathbf{R}_c(t)$ includes hydrodynamic forces $\mathbf{R}_h(t)$ at the upstream face of the dam and forces $\mathbf{R}_b(t)$ on the base of the dam due to interaction between the dam and the foundation rock.

39

For harmonic ground acceleration $a_g^l(t) = e^{i\omega t}$ in the $l = x$ (horizontal) or $l = y$ (vertical) direction, the displacements and forces can be expressed in terms of their complex-valued frequency response functions: $r_c(t) = \bar{r}_c^l(\omega) e^{i\omega t}$, $R_c(t) = \bar{R}_c^l(\omega) e^{i\omega t}$, $R_h(t) = \bar{R}_h^l(\omega) e^{i\omega t}$ and $R_b(t) = \bar{R}_b^l(\omega) e^{i\omega t}$. The vector $\bar{r}_c^l(\omega)$ contains the frequency response functions for the x- and y-components of displacement, $(r_n^x)^l$ and $(r_n^y)^l$, $n = 1, 2, \cdots N + N_b$, due to the l-component of ground motion. Partitioning r_c into r, for nodal points above the base, and r_b, for nodal points on the base (Figure 4.1), and assuming constant hysteretic damping in the dam, equation (4.1) can be expressed as [8]:

$$
\left\{ -\omega^2 \begin{bmatrix} m & 0 \\ 0 & m_b \end{bmatrix} + (1 + i\eta_s) \begin{bmatrix} k & k_b \\ k_b^T & k_{bb} \end{bmatrix} \right\} \begin{Bmatrix} \bar{r}^l(\omega) \\ \bar{r}_b^l(\omega) \end{Bmatrix} = - \begin{Bmatrix} m\underline{1}^l \\ m_b\underline{1}_b^l \end{Bmatrix} + \begin{Bmatrix} \bar{R}_h^l(\omega) \\ \bar{R}_b^l(\omega) \end{Bmatrix}
\tag{4.2}
$$

where η_s is the constant hysteretic damping factor for the dam concrete. The hydrodynamic forces R_h will be expressed later in terms of the acceleration of the upstream face of the dam by analysis of the fluid domain substructure. Also, the dam-foundation rock interaction forces R_b will be expressed in terms of the interaction displacements at the base by analysis of the foundation rock substructure.

4.2.2 Foundation Rock Substructure

The complex-valued, dynamic stiffness matrix $\underline{S}(\omega)$ for the foundation-rock region relates forces and displacements [8]:

$$
\begin{bmatrix} \underline{S}_{rr}(\omega) & \underline{S}_{rq}(\omega) \\ \underline{S}_{rq}^T(\omega) & \underline{S}_{qq}(\omega) \end{bmatrix} \begin{Bmatrix} \bar{r}_f(\omega) \\ \bar{q}(\omega) \end{Bmatrix} = \begin{Bmatrix} \bar{R}_f(\omega) \\ \bar{Q}_h(\omega) \end{Bmatrix}
\tag{4.3}
$$

The forces and corresponding displacements, relative to the free-field ground motion, at the surface of the foundation-rock region (Figure 4.1) are expressed in terms of their complex-valued frequency response functions. The forces and displacements at the foundation-rock surface under the dam base due to dam-foundation rock interaction are $R_f(t) = \bar{R}_f(\omega) e^{i\omega t}$ and $r_f(t) = \bar{r}_f(\omega) e^{i\omega t}$. Similarly, the hydrodynamic forces and displacements at the reservoir bottom are $Q_h(t) = \bar{Q}_h(\omega) e^{i\omega t}$ and $q(t) = \bar{q}(\omega) e^{i\omega t}$. Beyond a certain distance upstream of the dam, the hydrodynamic forces Q_h acting at

$$\left\{ -\omega^2 \begin{bmatrix} \mathbf{m} & \underline{0} \\ \underline{0} & \mathbf{m}_b \end{bmatrix} + (1+i\eta_s) \begin{bmatrix} \mathbf{k} & \mathbf{k}_b \\ \mathbf{k}_b^T & \mathbf{k}_{bb} \end{bmatrix} + \begin{bmatrix} \underline{0} & \underline{0} \\ \underline{0} & \underline{S}_f(\omega) \end{bmatrix} \right\} \begin{Bmatrix} \bar{\mathbf{r}}^l(\omega) \\ \bar{\mathbf{r}}_b^l(\omega) \end{Bmatrix} =$$

$$-\begin{Bmatrix} \mathbf{m}\underline{1}^l \\ \mathbf{m}_b\underline{1}_b^l \end{Bmatrix} + \begin{Bmatrix} \bar{\mathbf{R}}_h^l(\omega) \\ -\underline{S}_{rq}\underline{S}_{qq}^{-1}\bar{\mathbf{Q}}_h^l(\omega) \end{Bmatrix} \tag{4.9}$$

The vector $\bar{\mathbf{R}}_h^l(\omega)$ of frequency response functions for hydrodynamic forces at the upstream face of the dam contains non-zero terms corresponding only to the x-degrees of freedom (DOF). The vector $\bar{\mathbf{Q}}_h(\omega)$ of frequency response functions for hydrodynamic forces at the reservoir bottom contains non-zero terms corresponding only to the y-DOF. Later, $\bar{\mathbf{R}}_h^l(\omega)$ and $\bar{\mathbf{Q}}_h(\omega)$ will be expressed in terms of the accelerations of the upstream face of the dam and the reservoir bottom by analysis of the fluid domain substructure.

4.2.4 Reduction of Degrees of Freedom

Equation (4.9) represents a set of $2(N+N_b)$ frequency-dependent, complex-valued equations. Enormous computational effort would be required for repeated solution of these equations for many values of the excitation frequency. Thus, it is important to reduce the number of degrees of freedom.

An approach based on the Ritz concept is effective in the reduction of the number of DOF in interacting structural systems [8]. The displacements $\mathbf{r}_c$ relative to the free-field ground motion are expressed as linear combinations of J Ritz vectors of an associated dam-foundation rock system:

$$\mathbf{r}_c(t) = \sum_{j=1}^{J} Z_j(t)\psi_j \tag{4.10}$$

where $Z_j(t)$ is the generalized coordinate that corresponds to the jth Ritz vector ψ_j. For harmonic ground acceleration, equation (4.10) can be expressed in terms of the complex-valued frequency response functions for the generalized coordinates:

$$\bar{\mathbf{r}}_c^l(\omega) = \sum_{j=1}^{J} \bar{Z}_j^l(\omega)\psi_j \tag{4.11}$$

shown later.

Introducing the transformation of equation (4.11) into equation (4.9), premultiplying by ψ_n^T and

using the orthogonality properties of the eigenvectors of the associated dam-foundation rock system

with respect to the stiffness and mass matrices of equation (4.13), results in:

$$\mathbf{S}(\omega)\,\overline{\mathbf{Z}}^I(\omega) = \mathbf{L}^I(\omega) \tag{4.17}$$

where the elements of the matrix $\mathbf{S}$ and the vector $\mathbf{L}^I$ are:

$$S_{nj}(\omega) = [-\omega^2 + (1+i\eta_s)\lambda_n^2]\delta_{nj} + \psi_n^{fT}[\underline{\tilde{S}}_f(\omega) - (1+i\eta_s)\underline{\tilde{S}}_f(0)]\psi_j^f \tag{4.18a}$$

$$\mathbf{L}_n^I = -\psi_n^T\mathbf{m}_c\mathbf{1}_c^I + \{\psi_n^f\}^T\overline{\mathbf{R}}_h^I(\omega) - \psi_{bn}^T\underline{S}_{rq}(\omega)\,\underline{S}_{qq}^{-1}(\omega)\,\overline{\mathbf{Q}}_h(\omega) \tag{4.18b}$$

for $n,j=1,2,3\cdots J$; $\overline{\mathbf{Z}}^I(\omega)$ is the vector of frequency response functions $\overline{Z}_j^I(\omega)$ for the generalized

coordinates; δ_{nj} is the Kronecker delta function; and ψ_n^f is a subvector of ψ_n that contains only the ele-

ments corresponding to the nodal points at the upstream face of the dam.

Equations (4.17) and (4.18) represent J simultaneous, complex-valued equations in the general-

ized coordinates for each excitation frequency ω. These equations need to be solved over a range of

values of the excitation frequency to compute the frequency response functions. Fortunately, accurate

solutions can be obtained by including only a small number of Ritz vectors, typically less than ten,

which profoundly reduces the computational effort [9].

4.2.5 Fluid Domain Substructure

Boundary Value Problem. -- The unknown hydrodynamic forces $\mathbf{R}_h(t)$ and $\mathbf{Q}_h(t)$, whose frequency

response functions appear in equation (4.18b), can be expressed in terms of accelerations of the

upstream face of the dam and the reservoir bottom by analysis of the fluid domain. Assuming water to

be linearly compressible and neglecting its viscosity, the small amplitude, irrotational motion of water is

governed by the two-dimensional wave equation:

$$\frac{\partial^2 p}{\partial x^2} + \frac{\partial^2 p}{\partial y^2} = \frac{1}{C^2}\frac{\partial^2 p}{\partial t^2} \tag{4.19}$$

where $p(x,y,t)$ is the hydrodynamic pressure (in excess of hydrostatic pressure) and C is the velocity

The frequency response function $\bar{p}'(x,y,\omega)$ for the hydrodynamic pressure in the impounded water is the solution of equation (4.20) subject to the boundary conditions in equations (4.21) to (4.23) and the radiation condition in the upstream direction (negative x-direction). After solving for $\bar{p}'(x,y,\omega)$, the frequency response functions $\bar{R}_h'(\omega)$ and $-\bar{Q}_h(\omega)$ in equation (4.18b) are given as vectors of the nodal forces statically equivalent to the pressure function $\bar{p}'(0,y,\omega)$ at the upstream face of the dam and the pressure function $\bar{p}'(x,0,\omega)$ at the reservoir bottom, respectively.

Absorptive Reservoir Bottom. -- The boundary condition in equation (4.22) contains three terms that contribute to the total acceleration of the reservoir bottom: the vertical free-field ground acceleration, the modification of the free-field motion due to interaction between the impounded water and the foundation rock, and the modification of the free-field motion due to interaction between the dam and the foundation rock. Grouping the terms in equation (4.22) that are functions of the hydrodynamic pressure (or force) on the left side of the equation, gives a more convenient form for the boundary condition at the reservoir bottom:

$$\frac{\partial}{\partial y}\bar{p}(x,0,\omega) - \rho\omega^2 \bar{q}_h(x,\omega) = -\rho[\delta_{yl} + \sum_{j=1}^{J}\chi_j(x)\bar{\bar{Z}}_j'(\omega)], \qquad l=x,y \qquad (4.24)$$

The right side of equation (4.24) is identical to the right side of the boundary condition at the reservoir bottom presented in reference 8, but the left side now contains an additional term that includes the effects of water-foundation rock interaction.

By idealizing the foundation-rock region as a viscoelastic half-plane, the dam-foundation rock interaction effects were rigorously represented in the analytical formulation of the preceding sections. This idealization is not appropriate for representing the effects of interaction between the impounded water and the foundation rock because these effects should be dominated by the overlying alluvium and sediments, possibly deposited to a significant depth, that are highly saturated and have a small shear modulus. A hydrodynamic pressure wave impinging on such materials will partially reflect back into the water and partially refract, primarily as a dilatational wave, into the layer of reservoir bottom materials. Because of the considerable energy dissipation that results from hysteretic behavior and

is given by

$$C(\omega) = -i\left[\frac{1}{\rho_r C_r} \frac{1}{\omega}\right] \qquad (4.29)$$

Because the thickness of the sediment layer is not recognized explicitly, this compliance function is applied at the reservoir bottom. The compliance function $C(\omega)$ is imaginary-valued for all excitation frequencies, so the wave absorptive model of the reservoir bottom materials introduces an additional damping mechanism into the system.

The substitution of equations (4.25) and (4.29) into equation (4.24) gives the boundary condition at the absorptive reservoir bottom:

$$[\frac{\partial}{\partial y} - i\omega q]\bar{p}(x,0,\omega) = -\rho[\delta_{yl} + \sum_{j=1}^{J}\chi_j(x)\bar{Z}_j'(\omega)], \qquad l=x,y \qquad (4.30)$$

where $q = \rho/\rho_r C_r$. This boundary condition allows for proper reflection of hydrodynamic pressure waves for any angle of incidence. However, the only refracted waves allowed in the reservoir bottom materials are downward, vertically propagating dilatational waves.

As discussed in Section 3.2, the fundamental parameter that characterizes the effects of absorption of hydrodynamic pressure waves into the reservoir bottom materials is the admittance or damping coefficient q. The wave reflection coefficient α, which is defined as the ratio of the amplitude of the reflected hydrodynamic pressure wave to the amplitude of a vertically propagating pressure wave incident on the reservoir bottom, is related to the damping coefficient q by equation (3.9).

Solution for Hydrodynamic Pressure Terms. -- The frequency response function $\bar{p}'(x,y,\omega)$ for the hydrodynamic pressure in the impounded water is the solution of equation (4.20) subject to the boundary conditions in equations (4.21), (4.30) and (4.23) and the radiation condition. The linear form of the governing equation and boundary conditions allows $\bar{p}'(x,y,\omega)$ to be expressed as:

$$\bar{p}'(x,y,\omega) = \bar{p}_0'(x,y,\omega) + \sum_{j=1}^{J}\bar{Z}_j'(\omega)[\bar{p}_j'(x,y,\omega) + \bar{p}_j^b(x,y,\omega)] \qquad (4.31)$$

In equation (4.31), the frequency response function $\bar{p}_0^x(x,y,\omega)$ for the hydrodynamic pressure due to

$$\frac{\partial}{\partial x}\bar{p}(0,y,\omega) = 0$$

$$[\frac{\partial}{\partial y} - i\omega q]\bar{p}(x,0,\omega) = -\rho \chi_j(x)$$

$$\bar{p}(x,H,\omega) = 0$$

(4.35)

The complex-valued frequency response functions $\bar{p}_0^l(x,y,\omega)$ and $\bar{p}_j^f(x,y,\omega)$ can be obtained using standard solution methods for boundary value problems. They are derived in Appendix B and summarized below for the upstream face of the dam $(x=0)$:

$$\bar{p}_0^x(0,y,\omega) = -2\rho H \sum_{n=1}^{\infty} \frac{\mu_n^2(\omega)}{H[\mu_n^2(\omega) - (\omega q)^2] + i(\omega q)} \frac{I_{0n}(\omega)}{\sqrt{\mu_n^2(\omega) - \omega^2/C^2}} Y_n(y,\omega)$$

(4.36a)

$$\bar{p}_0^y(0,y,\omega) = \frac{\rho C}{\omega} \frac{1}{\cos\frac{\omega H}{C} + iqC\sin\frac{\omega H}{C}} \sin\frac{\omega(H-y)}{C}$$

(4.36b)

$$\bar{p}_j^f(0,y,\omega) = -2\rho H \sum_{n=1}^{\infty} \frac{\mu_n^2(\omega)}{H[\mu_n^2(\omega) - (\omega q)^2] + i(\omega q)} \frac{I_{jn}(\omega)}{\sqrt{\mu_n^2(\omega) - \omega^2/C^2}} Y_n(y,\omega)$$

(4.36c)

where the eigenvalues $\mu_n(\omega)$ satisfy equation (3.20) and the eigenfunctions $Y_n(y,\omega)$ are defined by equation (3.21), and

$$I_{0n}(\omega) = \frac{1}{H}\int_0^H Y_n(y,\omega)\, dy$$

(4.37a)

$$I_{jn}(\omega) = \frac{1}{H}\int_0^H \psi_j(y)\, Y_n(y,\omega)\, dy$$

(4.37b)

The solution of equation (4.20) with the boundary conditions in equation (4.35) may be obtained by use of a Fourier transform with respect to the spatial x-coordinate. Such a general solution is not necessary, however, because the resulting pressure function $\bar{p}_j^b(x,y,\omega)$ has little effect on the response of the dam, as will be discussed in the next section.

Hydrodynamic Force Vectors. -- The frequency response functions for $\mathbf{R}_h(t)$, the vector of hydro-dynamic forces at the upstream face of the dam, and $\mathbf{Q}_h(t)$, the vector of hydrodynamic forces at the

contained in the hydrodynamic terms: $\bar{\mathbf{R}}_0^l(\omega)$, $\bar{\mathbf{R}}_j^l(\omega)$, $\bar{\mathbf{R}}_j^p(\omega)$, $\bar{\mathbf{Q}}_0^l(\omega)$, $\bar{\mathbf{Q}}_j^l(\omega)$ and $\bar{\mathbf{Q}}_j^p(\omega)$.

It can be argued and shown through numerical examples that several terms in equation (4.40) are relatively small and can be dropped without introducing significant error [8,9]. One group of terms arises from the hydrodynamic forces $\mathbf{Q}_0^l$, $\mathbf{Q}_j^l$ and $\mathbf{Q}_j^p$ at the reservoir bottom that are due to the various excitations mentioned earlier. The other such term involves the hydrodynamic forces $\mathbf{R}_j^p$ at the upstream face of the dam due to deformational motions of the reservoir bottom.

Dropping these terms from equations (4.40) leads to the final form for the elements of $\tilde{\mathbf{S}}$ and $\tilde{\mathbf{L}}$:

$$\tilde{S}_{nj}(\omega) = [-\omega^2 + (1+i\eta_s)\lambda_n^2]\delta_{nj} + \psi_n^T[\underline{S}_j(\omega) - (1+i\eta_s)\underline{S}_j(0)]\psi_j$$

$$+ \omega^2\{\psi_n^l\}^T\bar{\mathbf{R}}_j^l(\omega) \tag{4.41a}$$

$$\tilde{L}_n^l = -\psi_n^T\mathbf{m}_c\mathbf{1}_c^l + \{\psi_n^l\}^T\bar{\mathbf{R}}_0^l(\omega) \tag{4.41b}$$

Equations (4.39) and (4.41) represent J complex-valued equations in the frequency response functions $\bar{Z}_j^l(\omega)$, $j=1,2,\cdots J$, for the generalized coordinates that correspond to the Ritz vectors included in the analysis. The matrix $\tilde{\mathbf{S}}(\omega)$ and vector $\tilde{\mathbf{L}}(\omega)$ are determined according to equation (4.41) for each excitation frequency ω of interest and equation (4.39) is solved to give $\bar{Z}_j^l(\omega)$. Repeated solution for the excitation frequencies covering the range over which the earthquake ground motion and structural response have significant components leads to the complete frequency response functions for the generalized coordinates.

Equations (4.39) and (4.41) are identical to equations (52) and (53) in reference 8, where a rigid reservoir bottom was assumed for all retained hydrodynamic terms except $\bar{\mathbf{R}}_0^l(\omega)$. As derived here, reservoir bottom absorption also affects the other hydrodynamic terms $\bar{\mathbf{R}}_0^x(\omega)$ and $\bar{\mathbf{R}}_j^l(\omega)$, as seen in equations (4.36a) and (4.36c), but it does not change the form of the frequency domain equations.

4.3 Response to Arbitrary Ground Motion

The response of the dam to arbitrary ground motion can be computed once the complex-valued frequency response functions $\bar{Z}_j^l(\omega)$, $l=x,y$, $j=1,2,\cdots J$, for the generalized coordinates have been obtained from the solution of equations (4.39) and (4.41) for excitation frequencies in the range of

functions $\bar{p}_0^I(0,y,\omega)$ and $\bar{p}_j^I(0,y,\omega)$ by the principle of virtual displacements. Two aspects of the functions $\bar{p}_0^x(0,y,\omega)$ and $\bar{p}_j^f(0,y,\omega)$ that lead to a large amount of computational effort in their evaluation are examined in this section with the objective of developing an efficient analytical procedure.

4.4.1 Number of Vibration Modes of the Impounded Water

The frequency response functions $\bar{p}_0^x(0,y,\omega)$ and $\bar{p}_j^f(0,y,\omega)$ defined in equations (4.36a) and (4.36c) are summations of the contributions of an infinite number of natural vibration modes of the impounded water. In practice, the sums must be truncated at a finite number. The computational effort required to evaluate the hydrodynamic terms is directly proportional to the number of vibration modes in the sums, so only the significant vibration modes should be included. The sums should at least include the contributions of all the vibration modes of the impounded water with natural vibration frequencies less than the maximum excitation frequency ω_{max} considered in the analysis. The natural vibration frequencies of the impounded water are functions of the wave reflection coefficient α, but their dependence on α is slight, as shown in Section 3.4. Consequently, the criterion for determining the number of included vibration modes can be stated in terms of the natural vibration frequencies ω_n^r of the impounded water with rigid reservoir bottom as the smallest value of n that satisfies:

$$\omega_n^r > \omega_{max} \tag{4.46}$$

A few additional vibration modes should be included in the summations to ensure convergence of the hydrodynamic terms for excitation frequencies near ω_{max}. Several numerical experiments indicated that five additional modes are sufficient. Thus, from equations (4.46) and (3.22b), the number N_w of included vibration modes is given by

$$N_w = \frac{1}{2}\frac{\omega_{max}}{\omega_1^r} + 5 \tag{4.47}$$

Equation (4.47) shows that the number N_w of included vibration modes increases as the depth of the impounded water increases and the maximum excitation frequency increases.
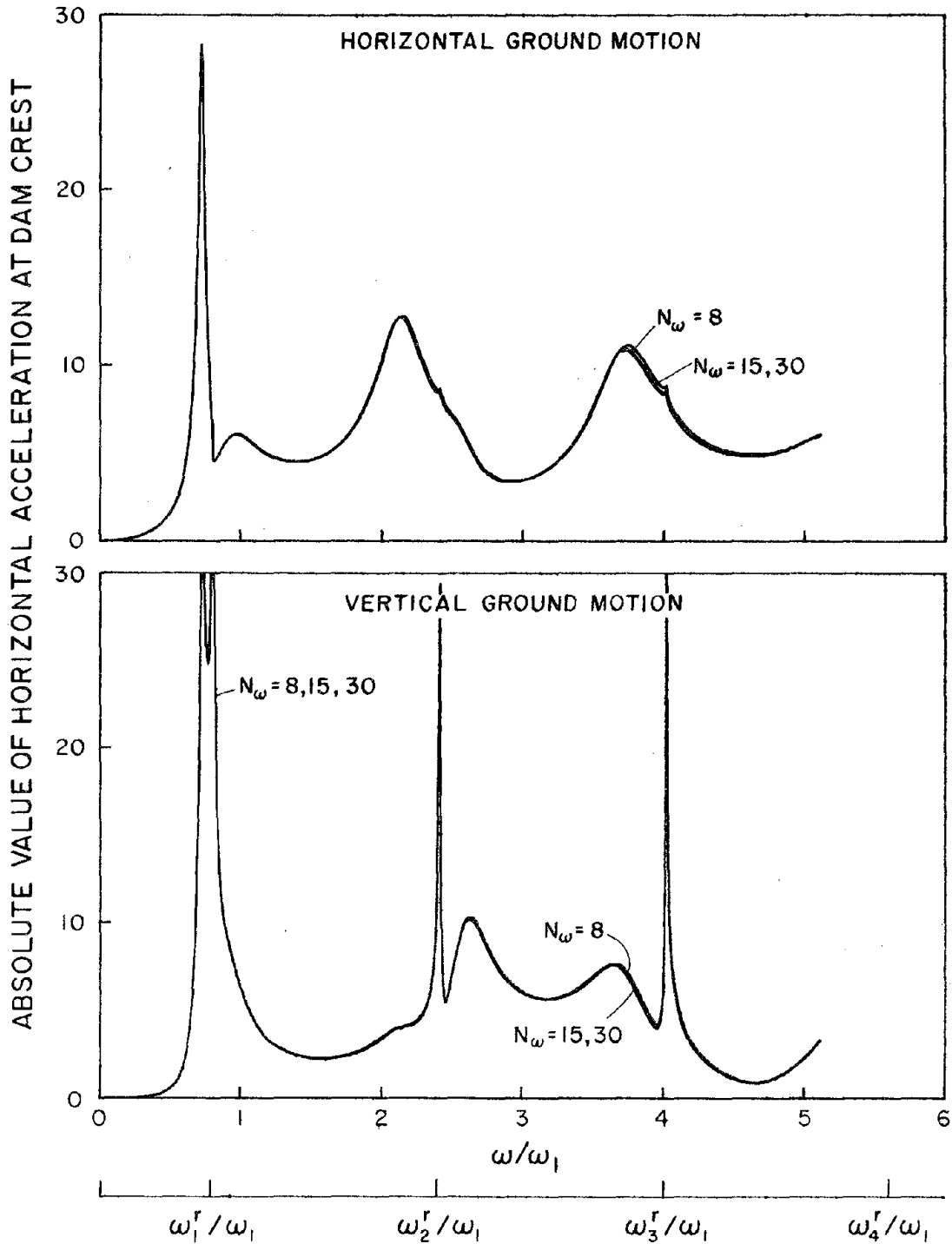
FIGURE 4.2 Influence of N_w, the number of vibration modes of the impounded water included in the analysis, on response of dams with full reservoir on rigid foundation rock, due to harmonic ground motion.
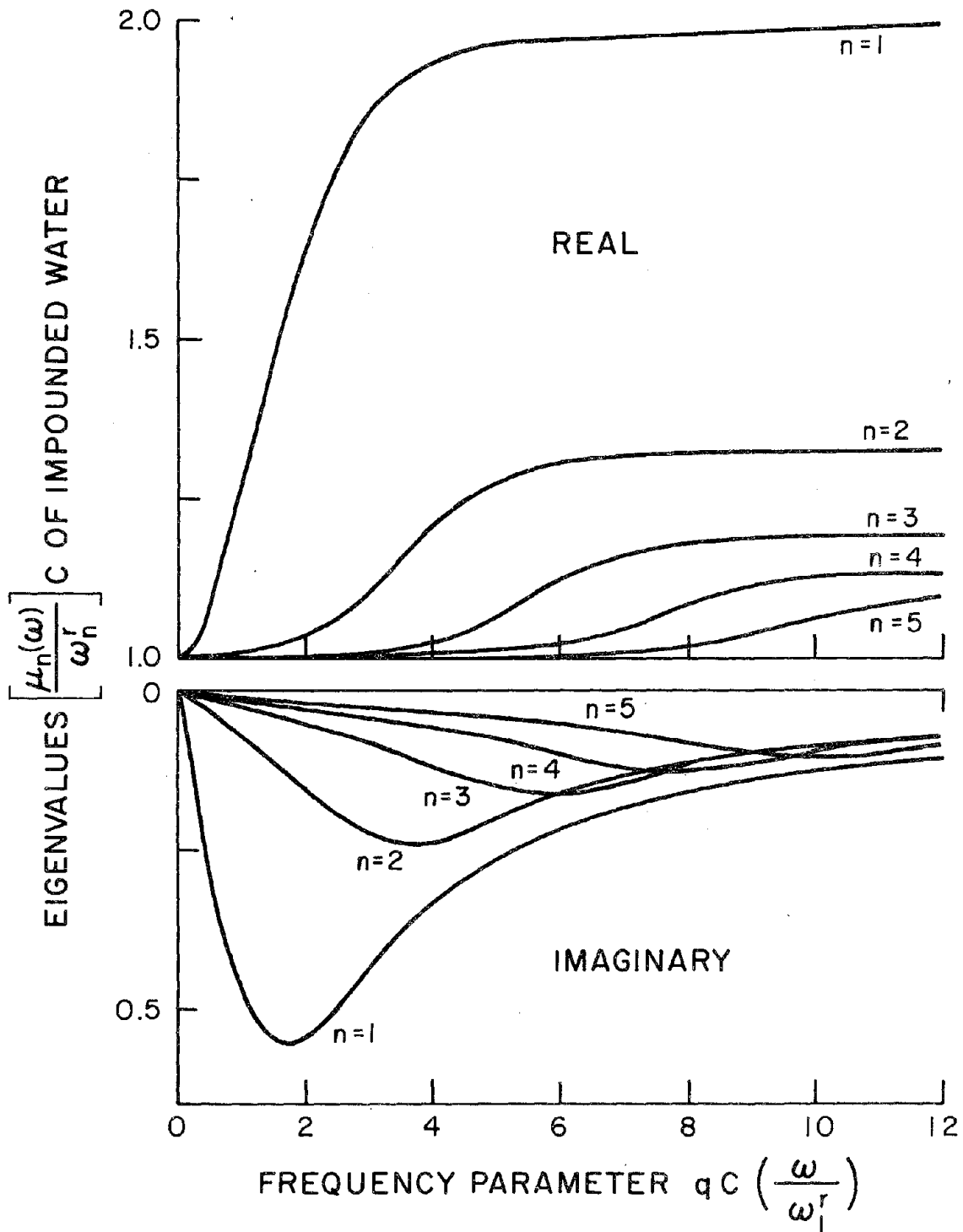
FIGURE 4.3   Variation of $\mu_n(\omega)$, the eigenvalues of the impounded water considering reservoir bottom absorption, with excitation frequency ω.
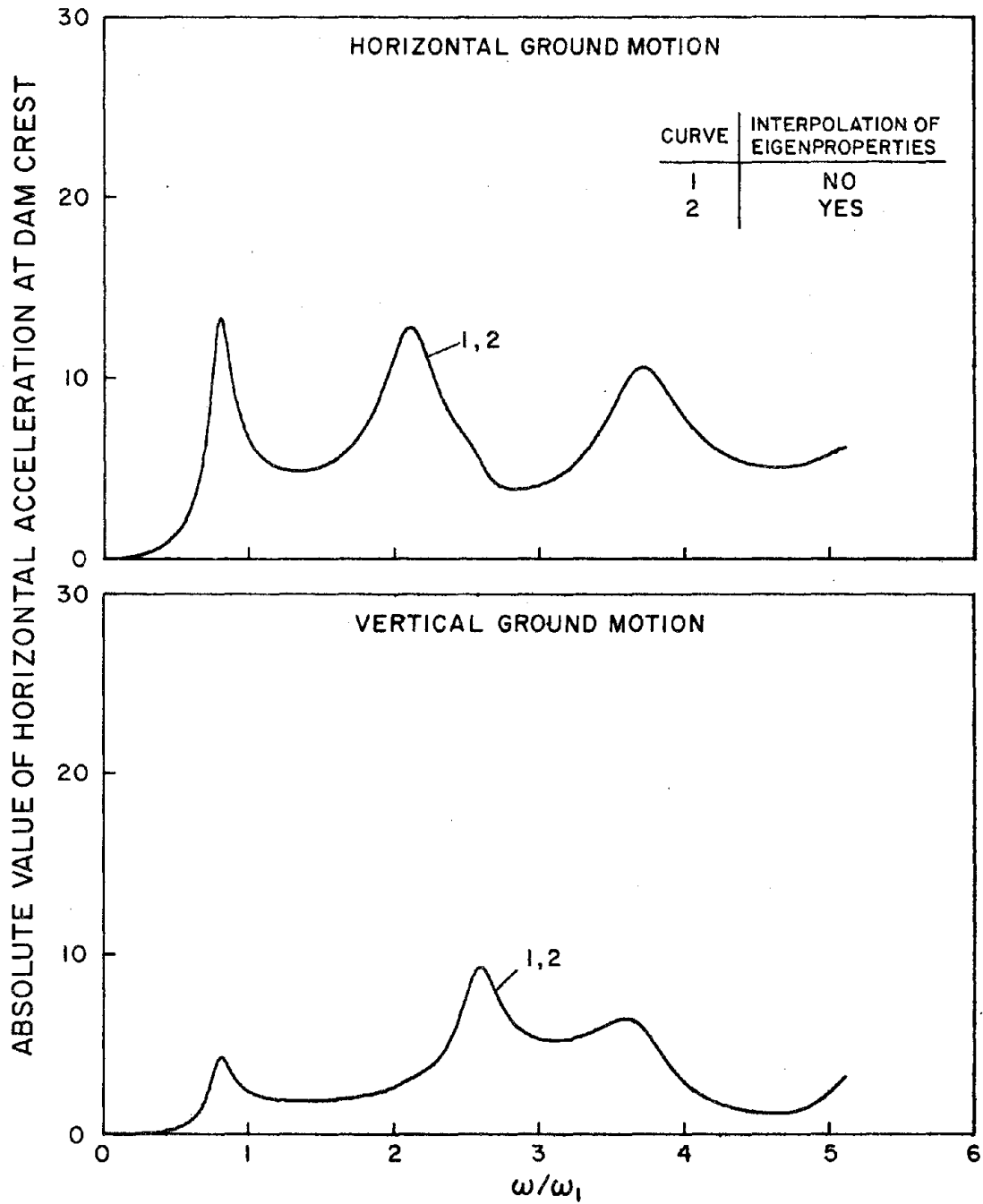
FIGURE 4.4   Influence of linear interpolation of eigenproperties of the impounded water on response of dams due to harmonic ground motion. Results presented for full reservoir, rigid foundation rock and wave reflection coefficient $\alpha=0$.

5. COMPLEX-VALUED FREQUENCY RESPONSE FUNCTIONS

5.1 Introduction

This chapter presents the response of an idealized concrete gravity dam due to harmonic ground motion in the form of complex-valued frequency response functions. The response is computed using the general analytical procedure developed in Chapter 4. In contrast to Chapter 3, which only considered the fundamental mode response, the results presented in this chapter include all the significant vibration modes of the dam. Response results are presented for a wide range of the important parameters that characterize the properties of the dam, foundation rock, impounded water and reservoir bottom materials. Based on the frequency response functions, the effects of reservoir bottom absorption on the response of dams, including interaction with the impounded water and foundation rock, are investigated.

5.2 System, Cases Analyzed and Response Quantities

5.2.1 Dam-Water-Foundation Rock System

The idealized monolith considered in Chapter 3 as representative of concrete gravity dams has a triangular cross-section with a vertical upstream face and a downstream face slope of 0.8 to 1. The dam is assumed to be homogeneous and isotropic with linear elastic properties for the mass concrete: Poisson's ratio =0.2, unit weight =155 lb/ft^3, and the Young's modulus of elasticity E_s is varied over a practical range: E_s=2, 4 and 5 million psi. Energy dissipation in the dam concrete is represented by constant hysteretic damping factor of η_s=0.10. This value corresponds to a viscous damping ratio of 0.05 in all natural vibration modes of the dam on rigid foundation rock with an empty reservoir.

The finite element idealization of the dam monolith, shown in Figure 5.1, consists of twenty elements and twenty-six nodal points. This idealization has forty-two degrees of freedom if the foundation rock is assumed to be rigid, and fifty-two degrees of freedom if foundation-rock flexibility is considered.

The dam monolith is supported on the surface of foundation rock idealized as a homogeneous, isotropic, viscoelastic half-plane. The material properties of the foundation rock are: Poisson's ratio

63
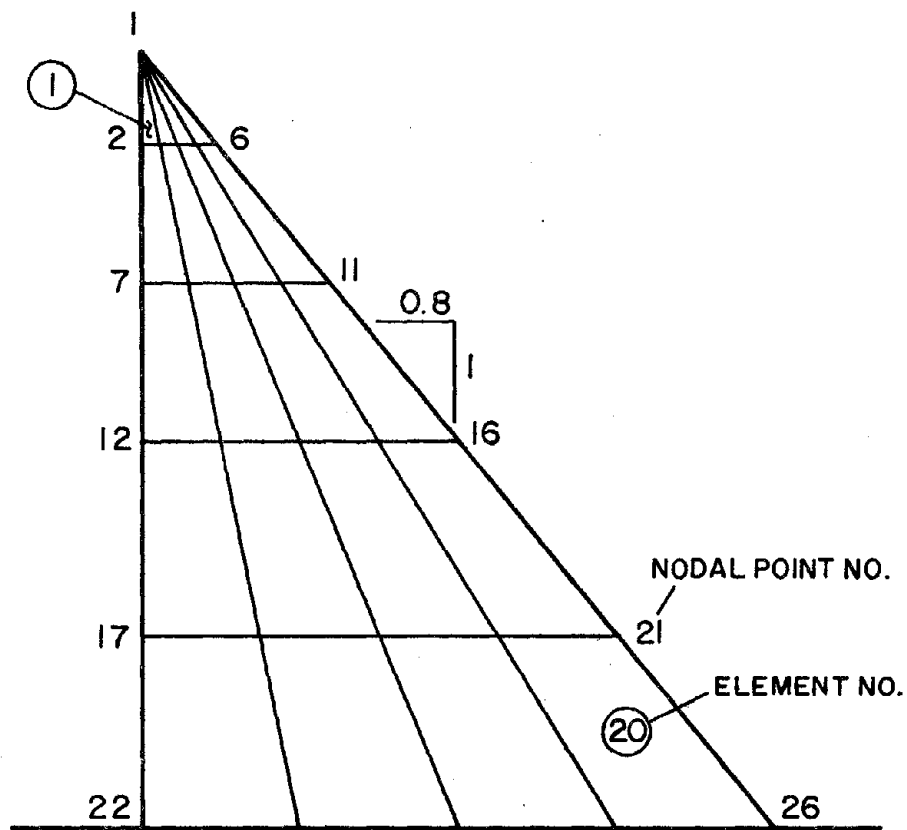
FIGURE 5.1 Finite element idealization of the dam monolith.

Table 5.1 -- Cases of the Idealized

Dam-Water-Foundation Rock System Analyzed

Case	Dam E_s (million psi)	Foundation Rock Condition	E_f/E_s	Impounded Water Condition	H/H_s	Reservoir Bottom Condition	α
1	any*	rigid	∞	none	0	-	-
2	4	rigid	∞	full	1	rigid	1.0
3	4	rigid	∞	full	1	absorptive	0.75
4	4	rigid	∞	full	1	absorptive	0.5
5	4	rigid	∞	full	1	absorptive	0
6	5	rigid	∞	full	1	rigid	1.0
7	5	rigid	∞	full	1	absorptive	0.5
8	2	rigid	∞	full	1	rigid	1.0
9	2	rigid	∞	full	1	absorptive	0.5
10	any*	rigid	∞	full,incompressible	1	rigid	any[†]
11	any*	flexible	1	none	0	-	-
12	4	flexible	1	full	1	rigid	1.0
13	4	flexible	1	full	1	absorptive	0.75
14	4	flexible	1	full	1	absorptive	0.5
15	4	flexible	1	full	1	absorptive	0
16	4	flexible	2	full	1	rigid	1.0
17	4	flexible	2	full	1	absorptive	0.5
18	4	flexible	1/4	full	1	rigid	1.0
19	4	flexible	1/4	full	1	absorptive	0.5

* Response results for these cases, when presented in normalized form, are valid for all E_s.
† Response results for the case neglecting water compressibility are independent of α.
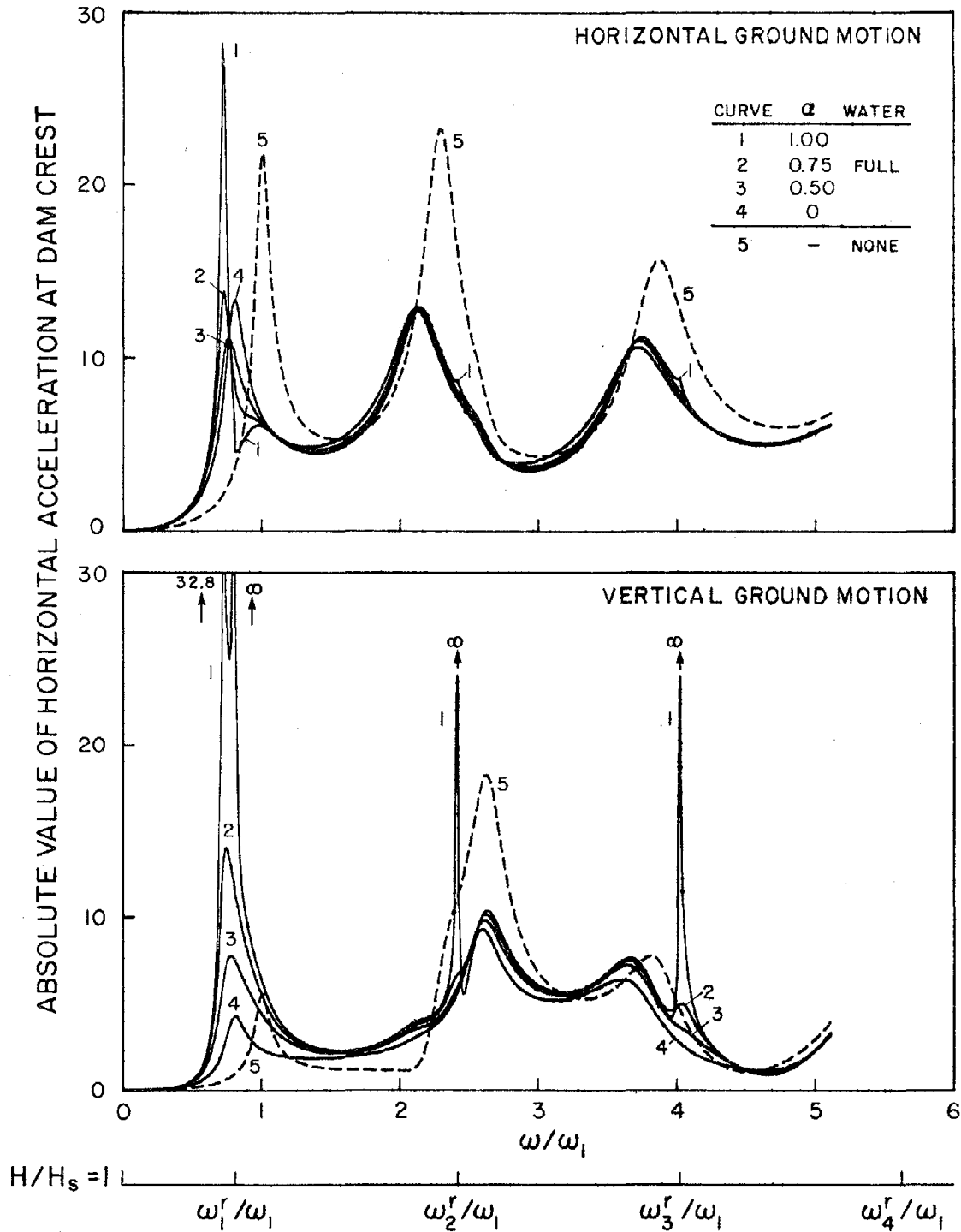
FIGURE 5.2   Hydrodynamic effects in response of dams due to harmonic ground motion. Results presented for full reservoir with varying values of the wave reflection coefficient α (Cases 2, 3, 4 and 5 of Table 5.1), and for no water (Case 1).

absorption eliminates the unbounded response values due to vertical ground motion and the dips in the response function for horizontal ground motion.

Thus, reservoir bottom absorption primarily affects the dam response for excitation frequencies less than ω_1^r, where material damping in the dam concrete is normally the only energy dissipation mechanism present if the foundation rock is assumed to be rigid. For higher frequencies the upstream radiation of energy dominates the energy radiation into the absorptive reservoir bottom, essentially eliminating its effect.

5.3.2 Influence of Young's Modulus E_s

The frequency response function for the dam, when presented in dimensionless form, is independent of the Young's modulus E_s for the dam concrete if there is no impounded water or its compressibility is neglected [6]. The frequency response functions for Cases 2, 4, 6, 7, 8 and 9 due to horizontal and vertical ground motion, presented in Figures 5.3 and 5.4, respectively, demonstrate that the E_s value affects the response if water compressibility is included. Most affected is the fundamental resonant frequency $\tilde{\omega}_r$, the response in the neighborhood of this frequency, and the response of the dam with rigid reservoir bottom due to vertical ground motion for excitation frequencies close to ω_n^r -- because of the response singularities discussed earlier. As E_s increases, the normalized fundamental resonant frequency ratio $\tilde{\omega}_r/\omega_1$ of the dam decreases due to dam-water interaction. This decrease in the resonant frequency ratio also depends on reservoir bottom absorption, being less pronounced for a wave absorptive reservoir bottom than for a rigid reservoir bottom [compare Figure 5.3(a) to (b), and Figure 5.4(a) to (b)].

Reservoir bottom absorption affects the amplitude and frequency bandwidth of the fundamental resonant peak in an especially significant way. The response to horizontal ground motion shows that increasing E_s causes larger resonant response over a narrower bandwidth for a rigid reservoir bottom [Figure 5.3(a)]; but causes smaller resonant response over a wider bandwidth for a wave absorptive reservoir bottom [Figure 5.3(b)]. This opposite response behavior results from the manner in which the effective damping at the resonant frequency is influenced by reservoir bottom absorption, as
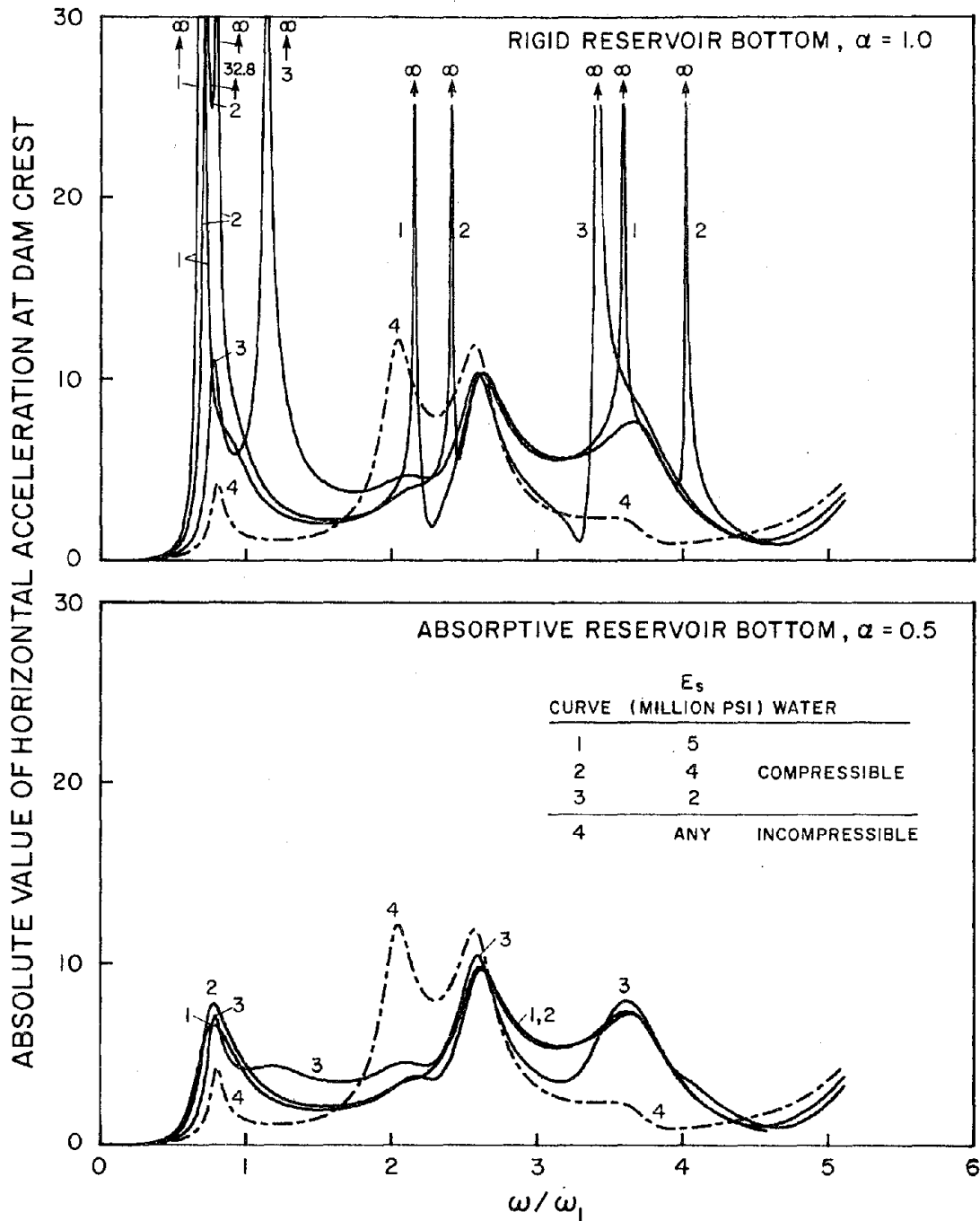
FIGURE 5.4. Influence of Young's modulus E_s for dam concrete on response of dams with full reservoir due to harmonic vertical ground motion. Results presented for rigid reservoir bottom (Cases 2, 6 and 8 of Table 5.1), absorptive reservoir bottom (Cases 4, 7 and 9) and incompressible water (Case 10).

horizontal ground motion, but little influence on the response to vertical ground motion. As seen above, the value of E_s can significantly affect the fundamental resonant frequency and the response function for excitation frequencies near it. For larger excitation frequencies, however, the frequency response functions for both components of ground motion are are less affected by the E_s value, irrespective of whether the reservoir bottom is rigid or absorptive.

5.3.3 Effects of Water Compressibility

To understand how compressibility of the impounded water affects the dam with a full reservoir, the response obtained by neglecting water compressibility (Case 10) is also plotted in Figures 5.3 and 5.4. If water compressibility is neglected dam-water interaction results in frequency-independent, real-valued added force and added mass; there is no added damping. With decreasing E_s, the effects of water compressibility on the fundamental resonant response become smaller. Although this trend is straightforward for horizontal ground motion (Figure 5.3), it is more complicated for the response to vertical ground motion (Figure 5.4) because of the unbounded response peaks for excitation frequencies equal to ω_n^r if the reservoir bottom is rigid.

Contrary to an earlier recommendation based on the tank experiments [20] described in Section 3.4, in the range of E_s values encountered in concrete gravity dams, the effects of wave absorption at the reservoir bottom on dam response are not properly represented by analysis that neglects water compressibility [Figures 5.3(b) and 5.4(b)]. Although such an analysis provides a good approximation to the fundamental resonant frequency $\tilde{\omega}_r$, the fundamental resonant response to horizontal ground motion is overestimated because incompressible water does not allow radiation of energy upstream or through the reservoir bottom; and the amplitude of the higher resonant peaks are overestimated by even a greater margin. Therefore, water compressibility should be considered in the earthquake analysis of concrete gravity dams.
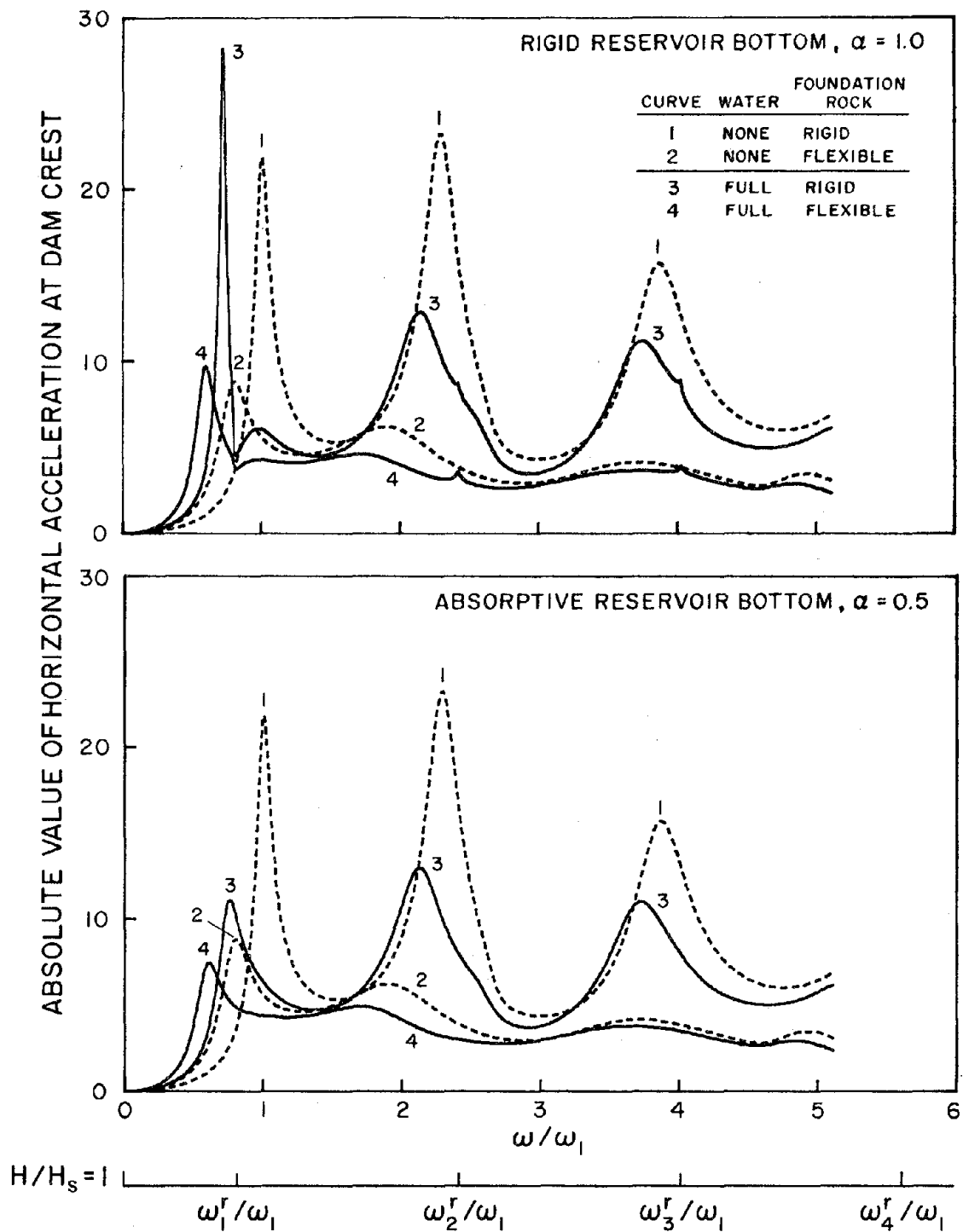
FIGURE 5.5 Response of dams due to harmonic horizontal ground motion for four conditions: dam on rigid foundation rock with no water (Case 1 of Table 5.1); dam on flexible foundation rock with no water (Case 11); dam on rigid foundation rock with full reservoir (Cases 2 and 4); and dam on flexible foundation rock with full reservoir (Cases 12 and 14).

4); and dam on flexible foundation rock with full reservoir (Cases 12 and 14). As noted earlier [11], interaction between the dam and flexible foundation rock affects the response of the dam in a simpler manner than does dam-water interaction (compare curve 2 to 3). This is because the impedances of the half-plane idealization for the foundation-rock region are slowly-varying, smooth functions of excitation frequency without resonant frequencies, whereas the added hydrodynamic force, mass and damping are frequency-dependent functions with peaks at ω_r^r. Dam-foundation rock interaction reduces the fundamental resonant frequency $\tilde{\omega}_f$ of the dam, and reduces the amplitude of the fundamental resonant peak and increases the bandwidth at resonance because of radiation and material damping in the foundation-rock region. Similarly, dam-foundation rock interaction reduces the higher resonant frequencies, although to a lesser degree than the fundamental resonant frequency, and substantially reduces the amplitude of the higher resonant peaks. As shown earlier [11], for decreasing values of E_f/E_s, which for fixed E_s means decreasing foundation rock modulus, each resonant frequency of the dam decreases; the resonant amplitude at each of these frequencies decreases and the bandwidth at resonance increases, implying an increase in the apparent damping of the structure. Dam-foundation rock interaction, as also shown earlier [11], affects the response of the dam to horizontal and vertical ground motions in a similar manner.

5.4.2 Hydrodynamic and Reservoir Bottom Absorption Effects

The effects of dam-water interaction and of dam-foundation rock interaction on the dynamic response of the dam can be observed from the remaining response functions presented in Figures 5.5 and 5.6. The effects of dam-water interaction on the dam response to either ground motion component are qualitatively similar for rigid and flexible foundation rock, whether the reservoir bottom is rigid [Figures 5.5(a) and 5.6(a)] or absorptive [Figures 5.5(b) and 5.6(b)]. Dam-water interaction leads to almost the same percentage reduction in the fundamental resonant frequency irrespective of the foundation-rock condition. This observation leads to the following expression:

$$\frac{\tilde{\omega}_1}{\omega_1} = \frac{\tilde{\omega}_r}{\omega_1} \frac{\tilde{\omega}_f}{\omega_1}$$

less pronounced for flexible foundation rock than for rigid foundation rock (compare the change from curve 2 to 4 with the change from curve 1 to 3).

The conclusions deduced in Section 5.3 concerning the response to vertical ground motion from response results for dams supported on rigid foundation rock are confirmed by Figures 5.5 and 5.6, in which the effects of dam-foundation rock interaction are included. The significance of the response of the dam to vertical ground motion, relative to the response to horizontal ground motion, increases because of hydrodynamic effects irrespective of whether the foundation rock is rigid or flexible. However as noted before, reservoir bottom absorption reduces the relative significance of the response to vertical ground motion.

The effects of reservoir bottom absorption on the response of the dam, supported on flexible foundation rock, due to horizontal and vertical ground motion are shown in Figures 5.7 and 5.8, respectively. The response of systems with moduli ratio $E_f/E_s=1$ is presented for four values of the wave reflection coefficient: $\alpha=1.0$ (rigid reservoir bottom), 0.75, 0.5, and 0 (Cases 12, 13, 14 and 15). Reservoir bottom absorption mainly affects the fundamental resonant peak due to horizontal ground motion (Figure 5.7), reducing its amplitude as α decreases with little change in the resonant frequency; and it essentially has no effect on the response for higher excitation frequencies, an observation noted earlier from results for rigid foundation rock (Figure 5.2). The most pronounced effects of reservoir bottom absorption on the response to vertical ground motion (Figure 5.8) are at excitation frequencies near ω_n^r, where the unbounded response peaks reduce to bounded values decreasing with α; at excitation frequencies not close to ω_n^r the effects are relatively small.

Reservoir bottom absorption has a smaller effect on the response of the dam supported on flexible foundation rock (Figures 5.7 and 5.8) than the response of the dam on rigid foundation rock (Figure 5.2). This can be explained by considering the damping due to dam-foundation rock interaction and reservoir bottom absorption. As mentioned in the previous section, where the foundation rock was assumed rigid, the primary effect of reservoir bottom absorption on dam-water interaction is to increase the effective damping at the fundamental resonant frequency, where normally no damping exists other than the material damping in the dam concrete. If foundation-rock flexibility is included, however,
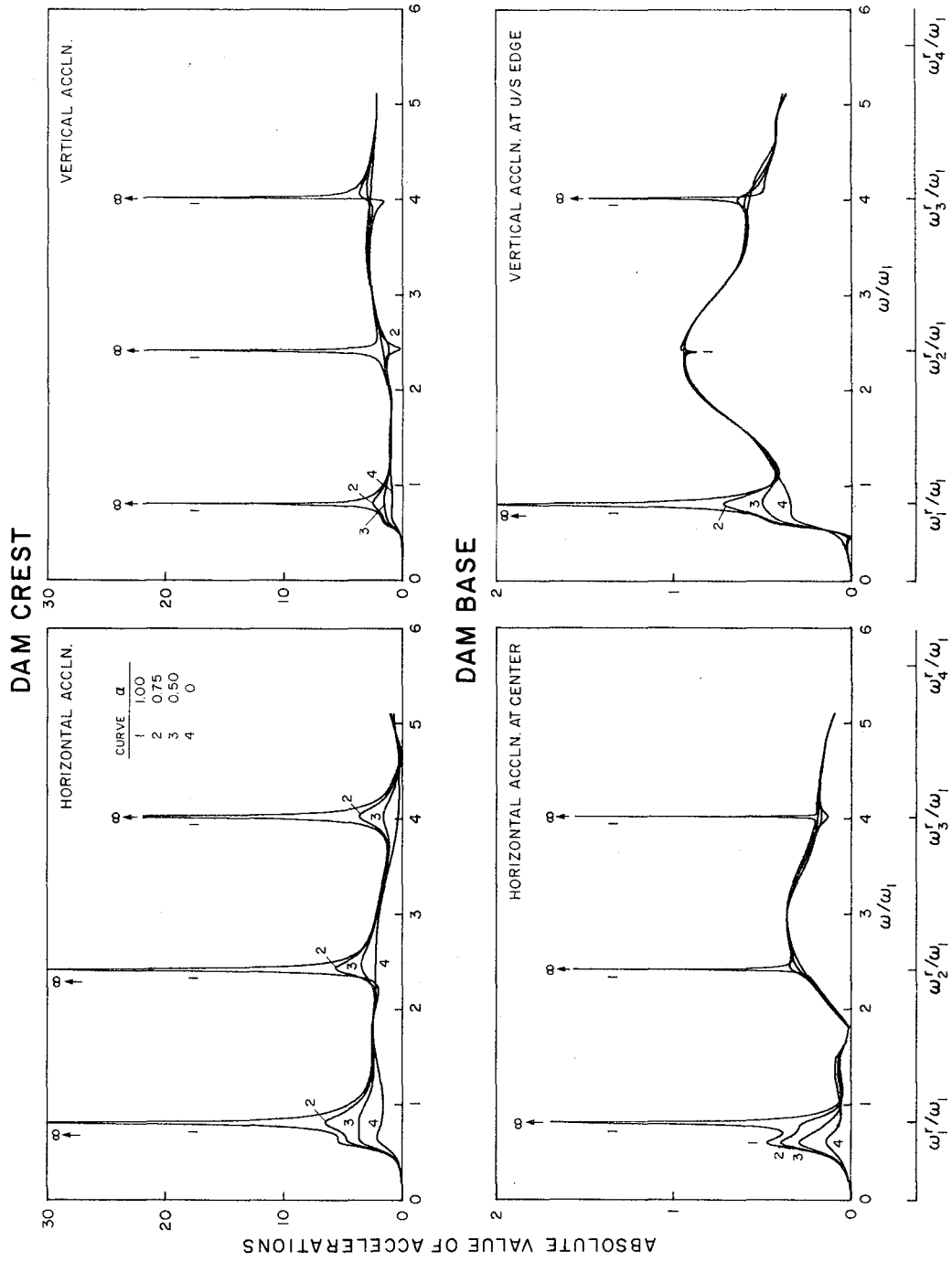
FIGURE 5.8   Influence of wave reflection coefficient α on response of dams on flexible foundation rock with full reservoir due to harmonic vertical ground motion (Cases 12, 13, 14 and 15 of Table 5.1).
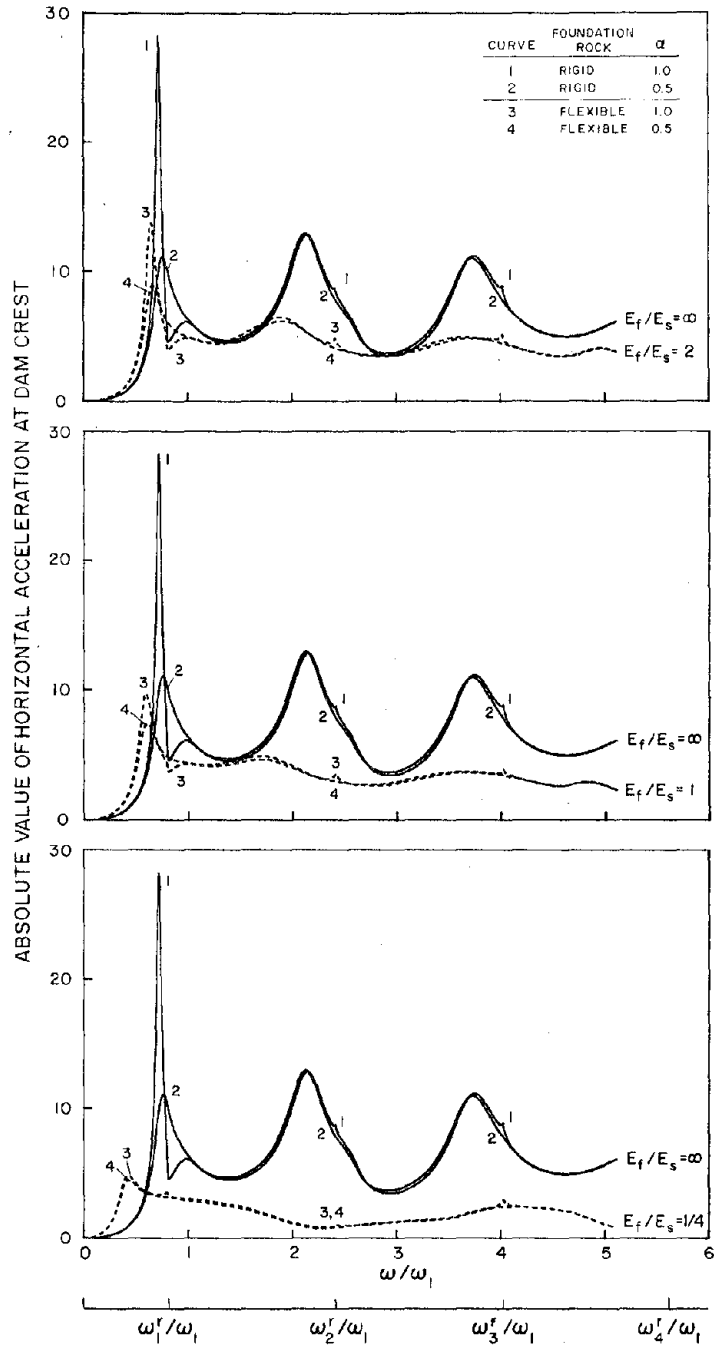
FIGURE 5.9   Effects of reservoir bottom absorption on response of dams with full reservoir due to harmonic horizontal ground motion for various values of the moduli ratio E_f/E_s.

to vertical ground motion, except at excitation frequencies near the natural vibration frequencies ω_n^r of the impounded water (Figure 5.10). The reduced importance of reservoir bottom absorption as E_f/E_s decreases was explained previously by consideration of the contributions to damping from dam-foundation rock interaction, dam-water interaction, and reservoir bottom absorption. In particular, the effects of reservoir bottom absorption are most significant if the foundation rock is rigid because, except for material damping in the dam, there is no other damping mechanism at the fundamental resonant frequency of the dam-water system. As the foundation rock becomes more flexible, more energy radiates through the foundation-rock region because of dam-foundation rock interaction, so that the additional damping due to reservoir bottom absorption is not as effective in further reducing the response.

The curves in Figures 5.9 and 5.10 are replotted in Figures 5.11 and 5.12 to show further the influence of the moduli ratio E_f/E_s on the response of the dam. As E_f/E_s decreases, which for a fixed E_s means an increasingly flexible foundation rock, the fundamental resonant frequency decreases, the dam response at this frequency decreases and the frequency bandwidth at resonance increases. These trends are the same for a rigid reservoir bottom [Figures 5.11(a) and 5.12(a)] and an absorptive reservoir bottom [Figures 5.11(b) and 5.12(b)]. It is apparent from Figures 5.11 and 5.12 that the effects of decreasing moduli ratio E_f/E_s on the fundamental resonant response of the dam are qualitatively similar, whether the reservoir bottom is rigid or absorptive; but quantitatively, the relative decrease in amplitude of the fundamental resonant peak depends on the wave reflection coefficient α, being less pronounced for an absorptive reservoir bottom.

As the moduli ratio E_f/E_s decreases, dam-foundation rock interaction introduces increased radiation damping at the higher resonant frequencies, in addition to the damping from hydrodynamic effects, thus reducing the amplitude of the the higher resonant peaks. For relatively flexible foundation rock, e.g. $E_f/E_s=1/4$, the higher resonant peaks are almost completely suppressed.
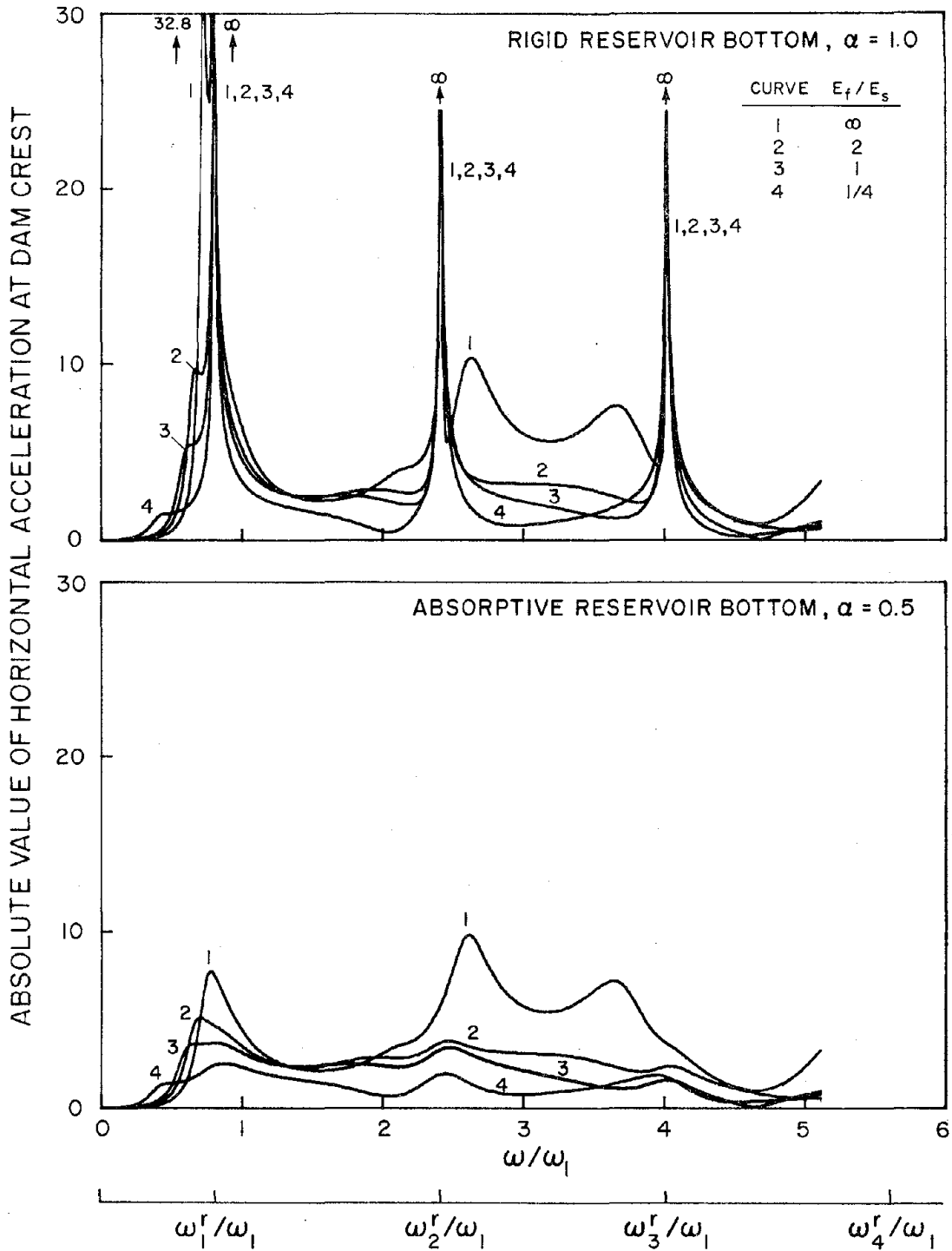
FIGURE 5.12   Influence of moduli ratio E_f/E_s on response of dams with full reservoir due to harmonic vertical ground motion.
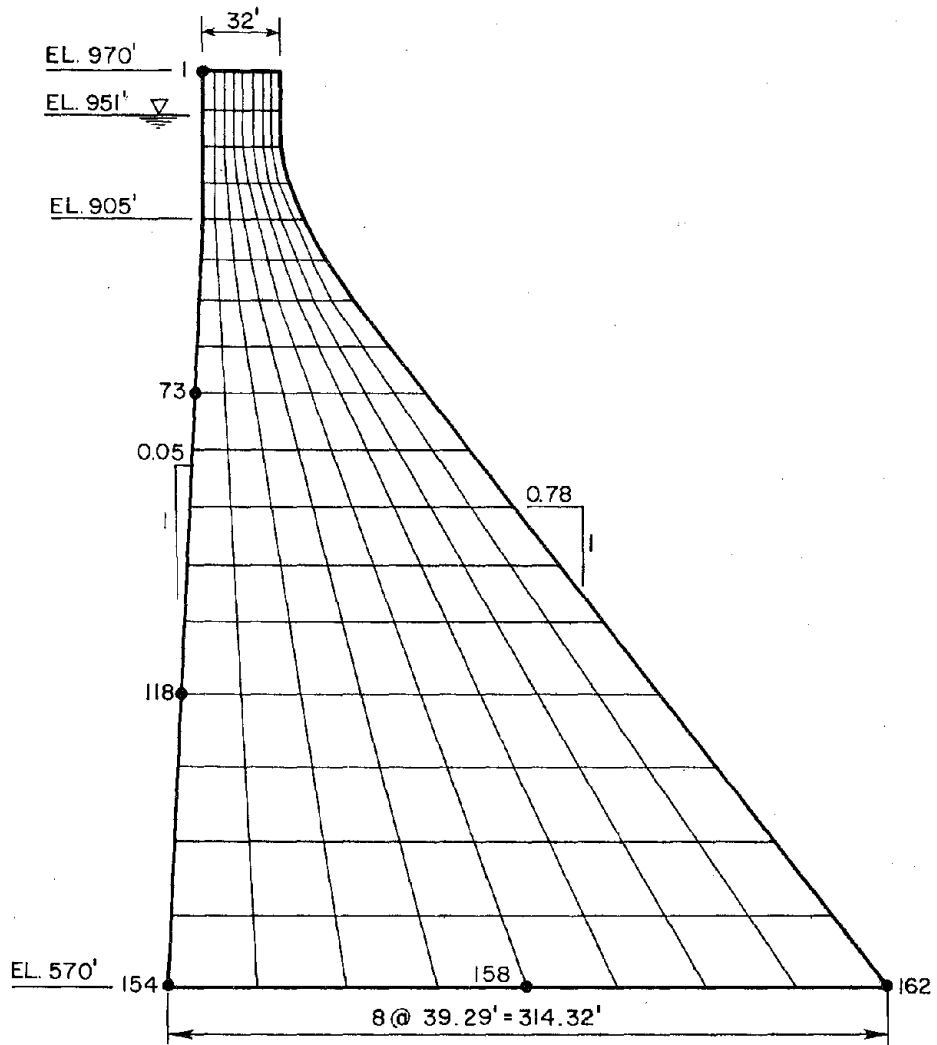
FIGURE 6.1   Finite element idealization of tallest, non-overflow monolith of Pine Flat Dam.

6.2.2 Ground Motion

The ground motion recorded at Taft Lincoln School Tunnel during the Kern County, California, earthquake of 21 July 1952 is selected as the free-field ground acceleration for the analysis of Pine Flat Dam. The Taft ground motion is a typical moderate earthquake, particularly in the short-period range of its spectrum, which is the range of interest for concrete gravity dams. The ground motion acting in the horizontal direction, transverse to the axis of the dam, and in the vertical direction is defined as the S69E and vertical components of the recorded ground motion, respectively. These two components and their maximum values of acceleration are shown in Figure 6.2.

6.3 Response Results

To evaluate the effects of reservoir bottom absorption, dam-water interaction and dam-foundation rock interaction, the tallest, non-overflow monolith of Pine Flat Dam was analyzed for the eight sets of assumptions and conditions listed in Table 6.1. For each of the eight cases, the response of the dam was computed for three excitations: S69E component, only; vertical component, only; and S69E and vertical components, simultaneously, of Taft ground motion.

The earthquake response of the dam was computed under the assumption of linear behavior of the dam-water-foundation rock system using the analytical procedure developed in Chapter 4, where the displacement history was obtained by Fourier synthesis of the complex-valued frequency response functions for the generalized coordinates. These response functions for Pine Flat Dam were computed for the excitation frequency range 0 to 25 Hz, which is adequate for the recorded Taft ground motion. To represent accurately the response of the dam in this frequency range, the analyses for Cases 1 to 4 with rigid foundation rock included the first five generalized coordinates, and the analyses for Cases 5 to 8 with flexible foundation rock included the first ten generalized coordinates. For this problem, $\omega_{max} = 157$ rad/sec and $\omega_f = 19.5$ rad/sec, so the number of included vibration modes of the impounded water $N_w = 9$ according to equation (4.47), and the eigenproperties of the impounded water were interpolated over the excitation frequency interval $\omega^* = 14.6$ rad/sec for $\alpha = 0.5$ and $\omega^* = 4.88$ rad/sec for $\alpha = 0$ according to equation (4.50). In the Fourier synthesis for the response history, 2048 time steps of

0.02 seconds were used, of which the last half-number of steps formed a "quiet zone" to reduce the aliasing error inherent in the discrete Fourier transform.

The fundamental resonant period and effective damping ratio at that period, determined by the half-power bandwidth method, both obtained from the frequency response function for horizontal ground motion, are listed in Table 6.1 for each case, along with the corresponding psuedo-acceleration $S_a(T,\xi)$ obtained from the response spectrum for the S69E component of Taft ground motion.

In a practical earthquake analysis of a dam, the displacements and stresses due to the static loads (weight of the dam and hydrostatic pressure of the impounded water) would be included in the total response. However, the effects of the static loads are *not* included in most of the results presented here because they complicate the interpretation of the effects of reservoir bottom absorption, dam-water interaction and dam-foundation rock interaction on the dynamic response of the dam. However, an example of a practical earthquake analysis, including the effects of the static loads, is presented at the end of this chapter.

The results of the computer analyses consist of the response history of horizontal and vertical displacements at the nodal points and the three components of plane stress at the centroid of the finite elements. Only a small portion of the response results are presented to highlight the important effects. The maximum horizontal displacement at the crest of the dam (nodal point 1) and maximum principal stresses at three critical locations in the dam monolith are summarized in Table 6.2 for the dam supported on rigid foundation rock (Cases 1 to 4), and in Table 6.3 for the dam supported on flexible foundation rock (Cases 5 to 8). Figures 6.3 to 6.20 show the history of horizontal displacement at the dam crest (nodal point 1) and the distribution of envelope values of the maximum principal stresses in the dam monolith (positive is maximum tensile stress, negative is minimum compressive stress) due to Taft ground motion.

6.4 Dam-Water Interaction Effects

The displacement history of Pine Flat Dam supported on rigid foundation rock with an empty reservoir due to the S69E and vertical components of Taft ground motion is shown in Figure 6.3(a). It is apparent -- consistent with common view -- that the response of the dam to vertical ground motion compared to the response to horizontal ground motion is relatively small if the reservoir is empty.

Interaction between the dam and the water impounded in the reservoir introduces frequency-dependent hydrodynamic terms into the equations of motion that affect the dynamic response of the dam. As described in Chapters 3 and 4, the hydrodynamic terms can be interpreted as an added force (different for horizontal and vertical ground motion), an added mass, and an added damping. The added hydrodynamic mass for a full reservoir and rigid reservoir bottom lengthens the fundamental resonant period of the dam from 0.317 sec to 0.394 sec (Table 6.1). The damping ratio at the fundamental resonant period decreases from 5% to 4% because of the increased added hydrodynamic force at the fundamental resonant period (Section 5.3). The ordinate of the psuedo-acceleration response spectrum for the S69E component of Taft ground motion that corresponds to the modified fundamental resonant period and damping ratio is also shown in Table 6.1. The interaction effects on the response of a dam to a specified earthquake ground motion are controlled, in part, by the change in the response spectrum ordinate for the fundamental resonant peak that corresponds to the change in the fundamental resonant period and damping. The added hydrodynamic force for horizontal ground motion has less effect on the response because it is relatively small compared to the effective earthquake force associated with the mass of the dam. It was shown in Chapter 5 that dam-water interaction has little effect on the higher resonant frequencies, but reduces the amplitude of the higher resonant peaks because of the added damping present for higher excitation frequencies.

The response of the dam with full reservoir and rigid reservoir bottom due to the S69E component of Taft ground motion is shown in Figure 6.3(b). In part, because of the lengthened fundamental resonant period and greater amplitude due to dam-water interaction effects, the maximum crest displacement increases from 1.06 in. to 1.45 in. The higher vibration modes of the dam contribute slightly less to the response because dam-water interaction reduces their corresponding resonant peaks.
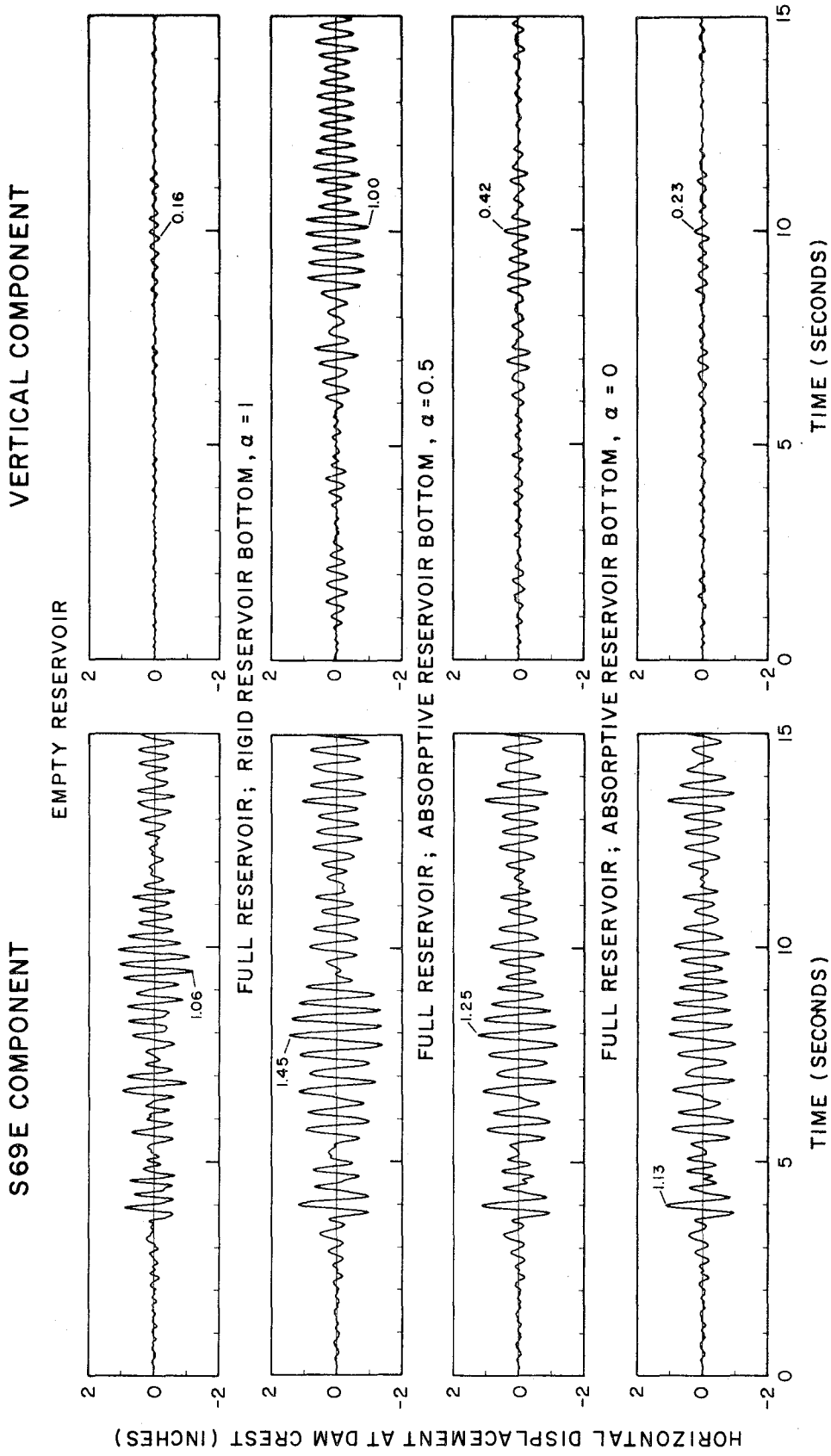
FIGURE 6.3 Displacement response of Pine Flat Dam on rigid foundation rock due to S69E and vertical components, separately, of Taft ground motion.

(a) Empty Reservoir

(b) Full Reservoir
Rigid Reservoir Bottom, $\alpha=1$

(c) Full Reservoir
Absorptive Reservoir Bottom, $\alpha=0.5$

(d) Full Reservoir
Absorptive Reservoir Bottom, $\alpha=0$
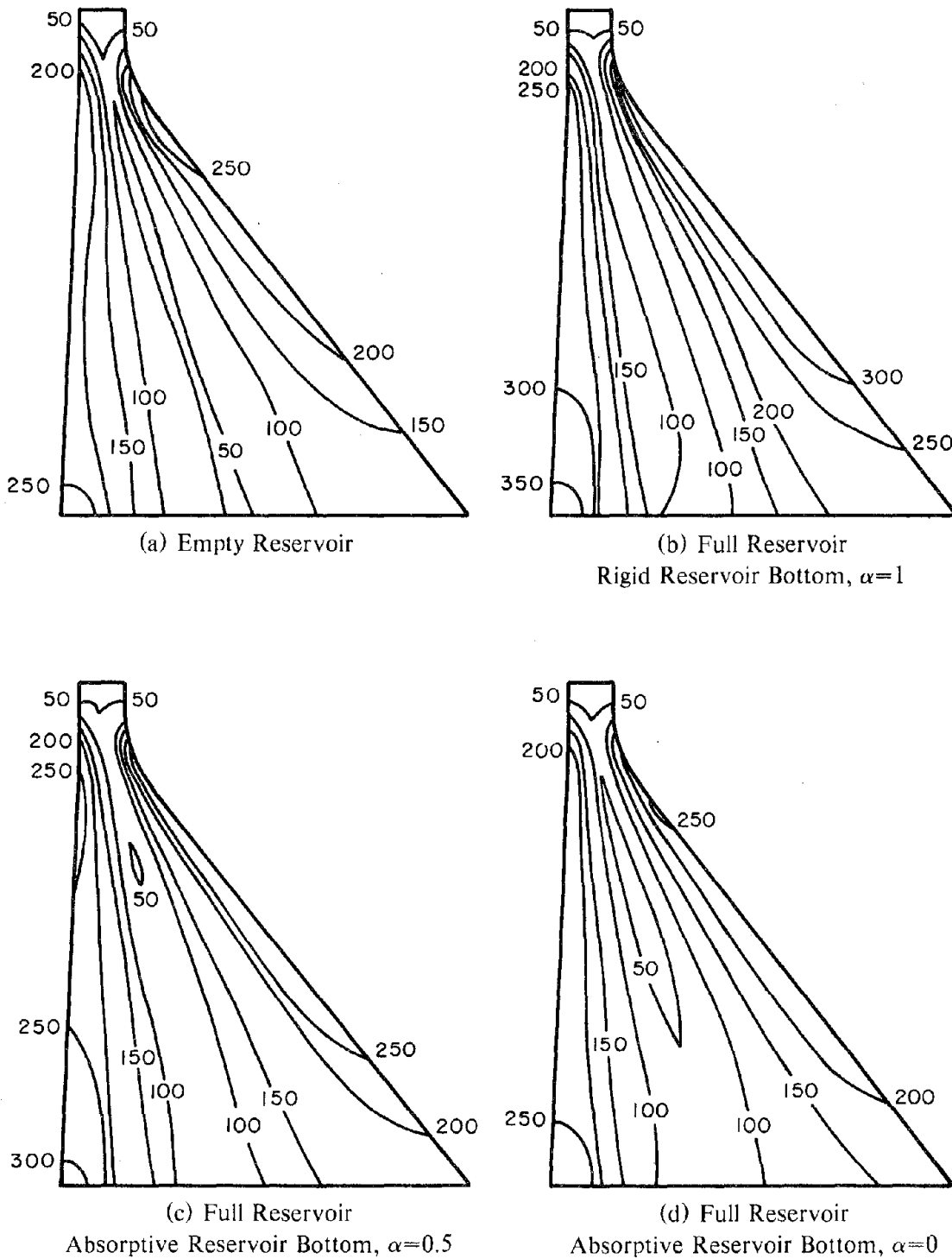
FIGURE 6.4   Envelope values of maximum principal stresses (in psi) in Pine Flat Dam on rigid foundation rock due to S69E component, only, of Taft ground motion. Initial static stresses are excluded.

with an empty reservoir (Table 6.1). As the reservoir bottom becomes more absorptive, i.e. as the wave reflection coefficient α decreases, the added damping at the fundamental resonant period increases because of increasing refraction of hydrodynamic pressure waves into the reservoir bottom materials and propagation of pressure waves upstream through the impounded water, resulting in an increased effective damping ratio (Table 6.1). As shown in Chapter 5, reservoir bottom absorption primarily affects the fundamental resonant response of the dam, and has little effect on the response to higher excitation frequencies.

The response of the dam with full reservoir due to the S69E component of Taft ground motion is shown in Figure 6.3(c)-(d) for $\alpha=0.5$ and $\alpha=0$. These results demonstrate that the main effect of reservoir bottom absorption is to reduce the larger displacement peaks without significantly changing the frequency content of the response [compare Figure 6.3(c)-(d) to Figure 6.3(b)]. Because of the added hydrodynamic damping due to reservoir bottom absorption, the maximum crest displacement of the dam with full reservoir decreases from 1.45 in. (for rigid reservoir bottom) to 1.25 in. for $\alpha=0.5$, and to 1.13 in. for $\alpha=0$; the maximum principal stress at the downstream face decreases from 335 psi (for rigid reservoir bottom) to 277 psi for $\alpha=0.5$, and to 250 psi for $\alpha=0$, and the maximum principal stress at the upstream face decreases somewhat less [Figure 6.4(b)-(d)]. The area enclosed by a particular stress contour decreases, indicating that tensile stresses exceed the value corresponding to that contour over a smaller portion of the monolith because of reservoir bottom absorption. However, the general pattern of maximum principal stresses is not substantially altered.

Reservoir bottom absorption reduces the added hydrodynamic force and the response of the dam to vertical ground motion for all excitation frequencies. In particular, it eliminates the unbounded peaks in the added hydrodynamic force and in the dam response for excitation frequencies equal to the natural vibration frequencies of the impounded water (Chapter 5). The effect of eliminating the unbounded peaks can be seen in Figure 6.3(b)-(d) for the response of the dam with full reservoir due to the vertical component of Taft ground motion. Reservoir bottom absorption drastically reduces the maximum crest displacement from 1.00 in. (for rigid reservoir bottom) to 0.42 in. for $\alpha=0.5$, and to 0.23 in. for $\alpha=0$, and similarly reduces the maximum principal stresses in the dam monolith [Figure

Table 6.3 -- Summary of Responses[*] of Pine Flat Dam,
On Flexible Foundation Rock, To Taft Ground Motion

Case	Water	α	Maximum Horizontal Crest Displacement, in inches	Maximum Tensile Stress, in psi		
				Upstream Face	Downstream Face	Heel
(a) Response to S69E Component, Only, of Taft Ground Motion						
5	none	-	1.01	172	181	200
6	full	1.0	1.71	230	245	354
7	full	0.5	1.59	218	229	331
8	full	0	1.55	213	232	321
(b) Response to Vertical Component, Only, of Taft Ground Motion						
5	none	-	0.16	23	42	34
6	full	1.0	0.96	198	196	135
7	full	0.5	0.41	79	74	59
8	full	0	0.22	41	57	40
(c) Response to S69E and Vertical Components, Simultaneously, of Taft Ground Motion						
5	none	-	1.10	186	198	230
6	full	1.0	1.73	247	238	346
7	full	0.5	1.72	242	225	346
8	full	0	1.71	240	239	348

[*]Effects of static loads are excluded.

maximum principal stresses throughout the dam monolith, as seen by comparison of Figure 6.7(a) to 6.4(a) [also compare Case 5 in Table 6.3(a) to Case 1 in Table 6.2(a)].

The effects of dam-foundation rock interaction on the frequency response function of the dam are similar for horizontal and vertical ground motion, as described in Section 5.4. The response of the dam with an empty reservoir due to the vertical component of Taft ground motion is so small, however, that it is difficult to discern the effects of dam-foundation rock interaction by comparison of Figure 6.6(a) to 6.3(a), except for the lengthening of the fundamental resonant period. Dam-foundation rock interaction slightly reduces the maximum principal stresses in the monolith due to vertical ground motion as seen by comparison of Figure 6.8(a) to 6.5(a) [also compare Case 5 in Table 6.3(b) to Case 1 in Table 6.2(b)].

6.5.2 Hydrodynamic and Reservoir Bottom Absorption Effects

As noted in the preceding sections, the fundamental resonant period of the dam is lengthened because of dam-water interaction and also because of dam-foundation rock interaction. Simultaneous consideration of the two sources of interaction results in a fundamental resonant period of the dam that is longer than the period including either interaction effect individually. In particular, dam-water interaction, with a rigid or absorptive reservoir bottom, lengthens the fundamental resonant period of the dam by almost the same percentage whether the foundation rock is rigid or flexible.

The response of the dam supported on flexible foundation rock with full reservoir and rigid reservoir bottom due to the S69E component of Taft ground motion is shown in Figure 6.6(b). Because of dam-water interaction, the maximum crest displacement increases from 1.01 in. to 1.71 in.; and the maximum principal stress increases from 172 psi to 230 psi at the upstream face, from 181 psi to 245 psi at the downstream face, and from 200 psi to 354 psi at the heel [Figure 6.7(a)-(b)]. The area enclosed by a particular stress contour increases because of dam-water interaction, with little change in the general pattern of the contours.

It was shown in Chapter 5 that if the foundation rock is rigid and the reservoir bottom is rigid, the added hydrodynamic force for vertical ground motion is infinite at the natural vibration frequencies of

(a) Empty Reservoir

(b) Full Reservoir
Rigid Reservoir Bottom, $\alpha=1$

(c) Full Reservoir
Absorptive Reservoir Bottom, $\alpha=0.5$

(d) Full Reservoir
Absorptive Reservoir Bottom, $\alpha=0$
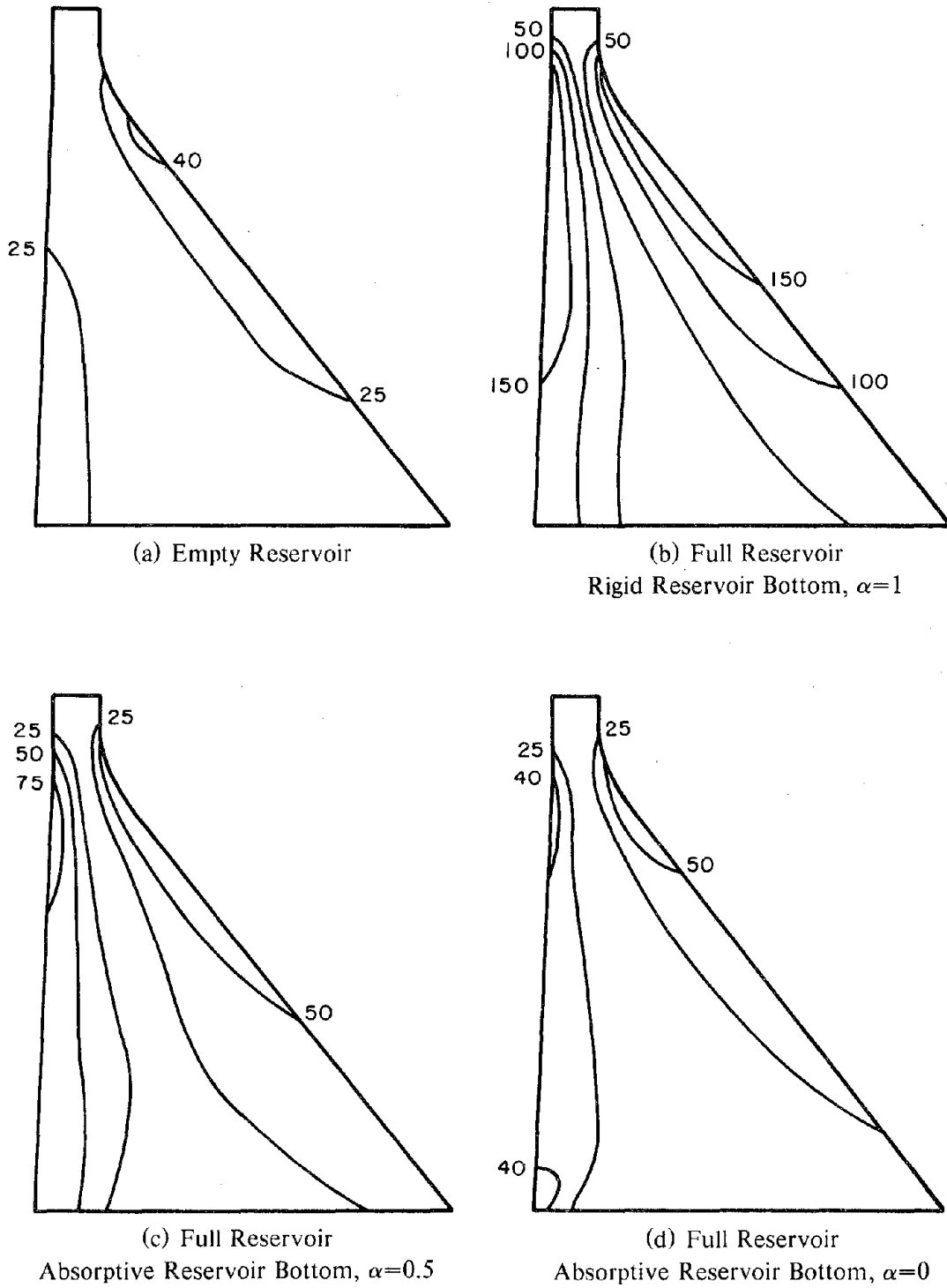
FIGURE 6.8   Envelope values of maximum principal stresses (in psi) in Pine Flat Dam on flexible foundation rock due to vertical component, only, of Taft ground motion. Initial static stresses are excluded.

6.6 Significance of the Response to Vertical Ground Motion

As seen in the preceding sections of this chapter, the earthquake response of Pine Flat Dam is increased by dam-water interaction and decreased by reservoir bottom absorption, with the magnitude of these effects depending on the condition of foundation rock, rigid or flexible, and on the component of ground motion, horizontal or vertical. In particular, both dam-water interaction and reservoir bottom absorption profoundly affect the response of the dam to vertical ground motion irrespective of the foundation rock condition, but have relatively less affect on the response to horizontal ground motion, with the magnitude of the effects decreasing further if foundation-rock flexibility is considered. Stated differently, the response of the dam with an empty reservoir due to vertical ground motion expressed as a percentage of the response to horizontal ground motion is small; the percentage greatly increases because of dam-water interaction with a rigid reservoir bottom; and from this increased value it decreases significantly because of reservoir bottom absorption.

The response of Pine Flat Dam to the S69E and vertical components, simultaneously, of Taft ground motion is presented in Figures 6.9 to 6.20 to evaluate the significance of the response to vertical ground motion in the total dynamic response of the dam. All the conclusions stated in the preceding paragraph would be fully applicable to the total response if the individual responses to the horizontal and vertical components of ground motion were exactly in phase and the maximum responses were directly additive. But this is not the case as is apparent from the response history of crest displacement in Figures 6.9 and 6.10 for rigid foundation rock and Figures 6.15 and 6.16 for flexible foundation rock. If the reservoir is empty, the contribution of the response to the vertical component is very small whether the foundation rock is rigid (Figure 6.9 for crest displacement and Figure 6.11 for stresses) or flexible (Figure 6.15 for crest displacement and Figure 6.17 for stresses).

For dams with impounded water, however, the main implication of the phase difference between the responses to horizontal and vertical ground motion is that the contribution to the maximum response from the vertical component may not be as significant as noted earlier from the dam responses to the individual ground motion components. For example, if the reservoir bottom is rigid, the increase of the maximum stresses in the dam with full reservoir is not as large (Figure 6.12 for rigid
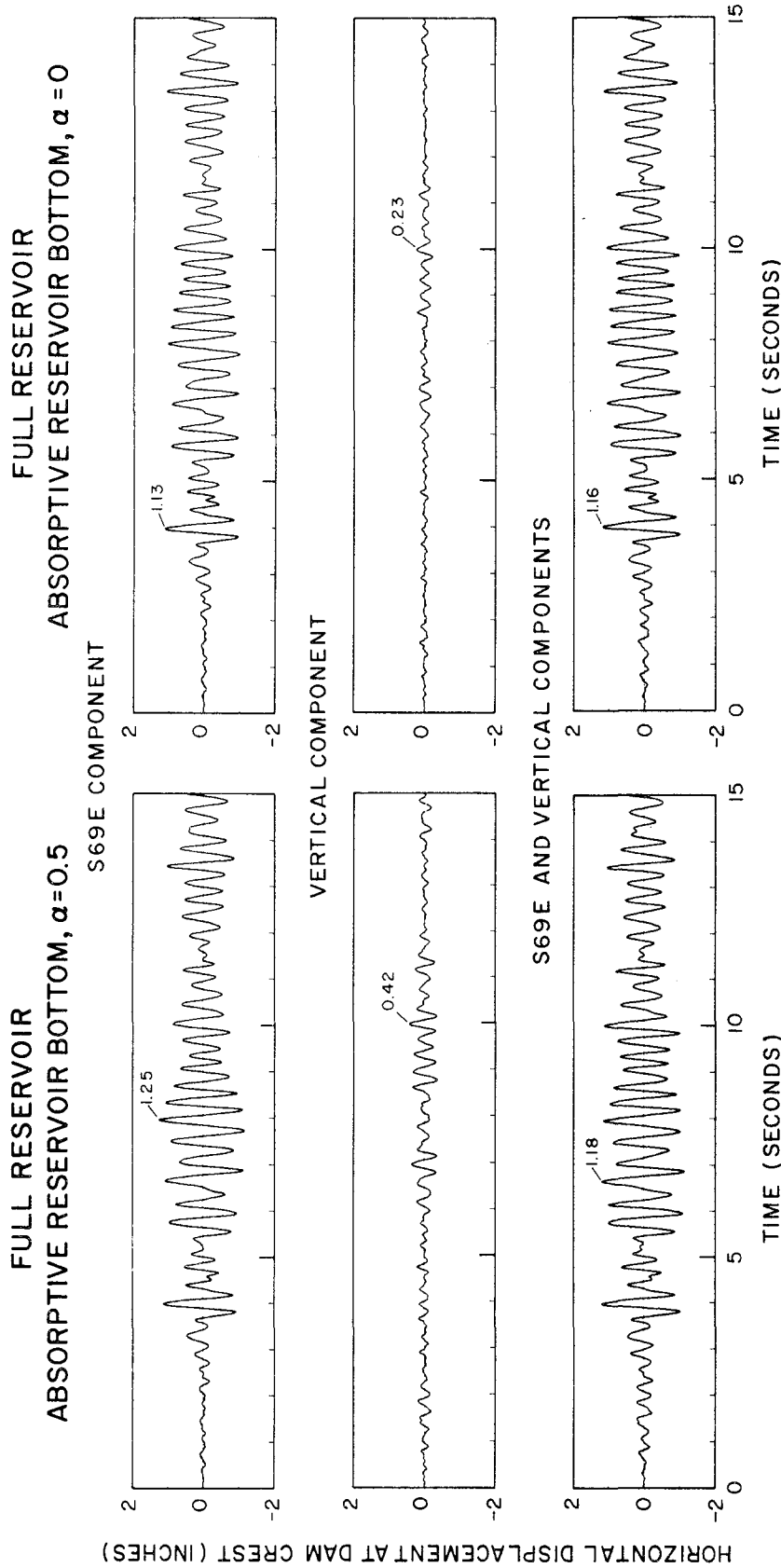
FIGURE 6.10 Displacement response of Pine Flat Dam on rigid foundation rock with full reservoir and absorptive reservoir bottom due to S69E and vertical components, separately and simultaneously, of Taft ground motion: (i) α=0.5, and (ii) α=0.

S69E and Vertical Components

Vertical Component
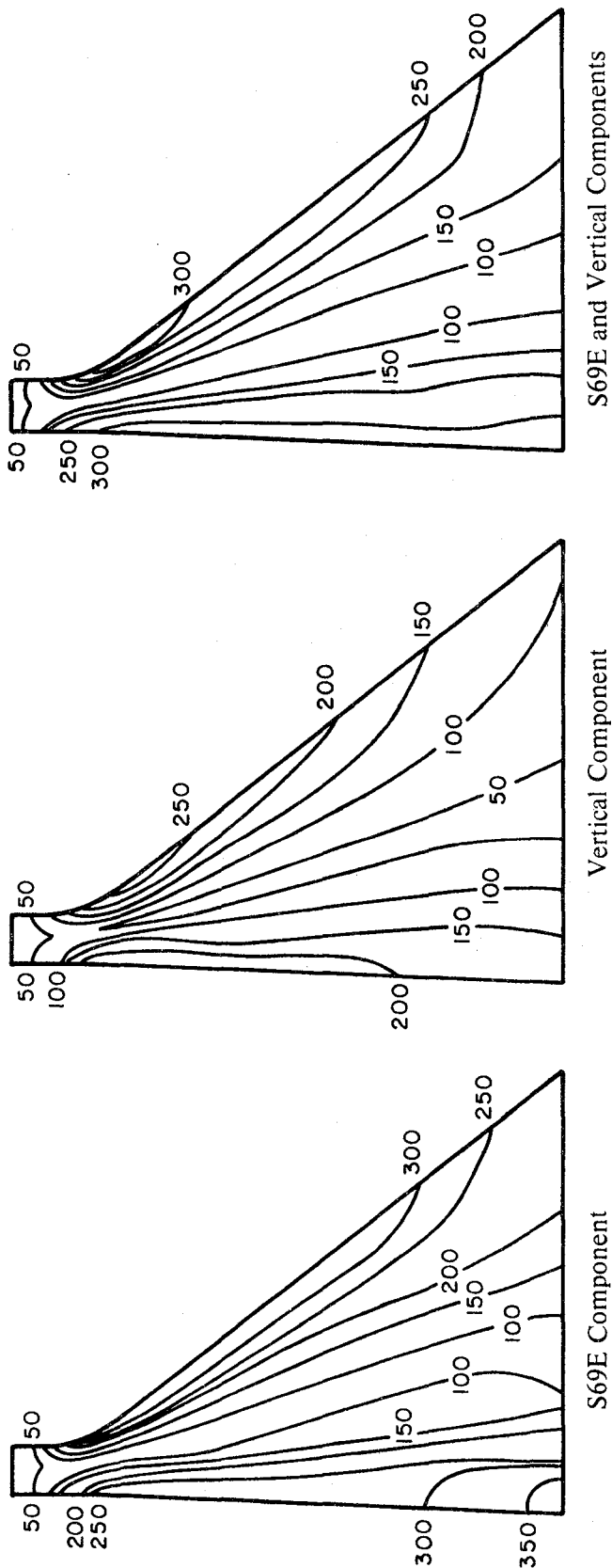
S69E Component

FIGURE 6.12 Envelope values of maximum principal stresses (in psi) in Pine Flat Dam on rigid foundation rock with full reservoir and rigid reservoir bottom ($\alpha=1$) due to S69E and vertical components, separately and simultaneously, of Taft ground motion. Initial static stresses are excluded.
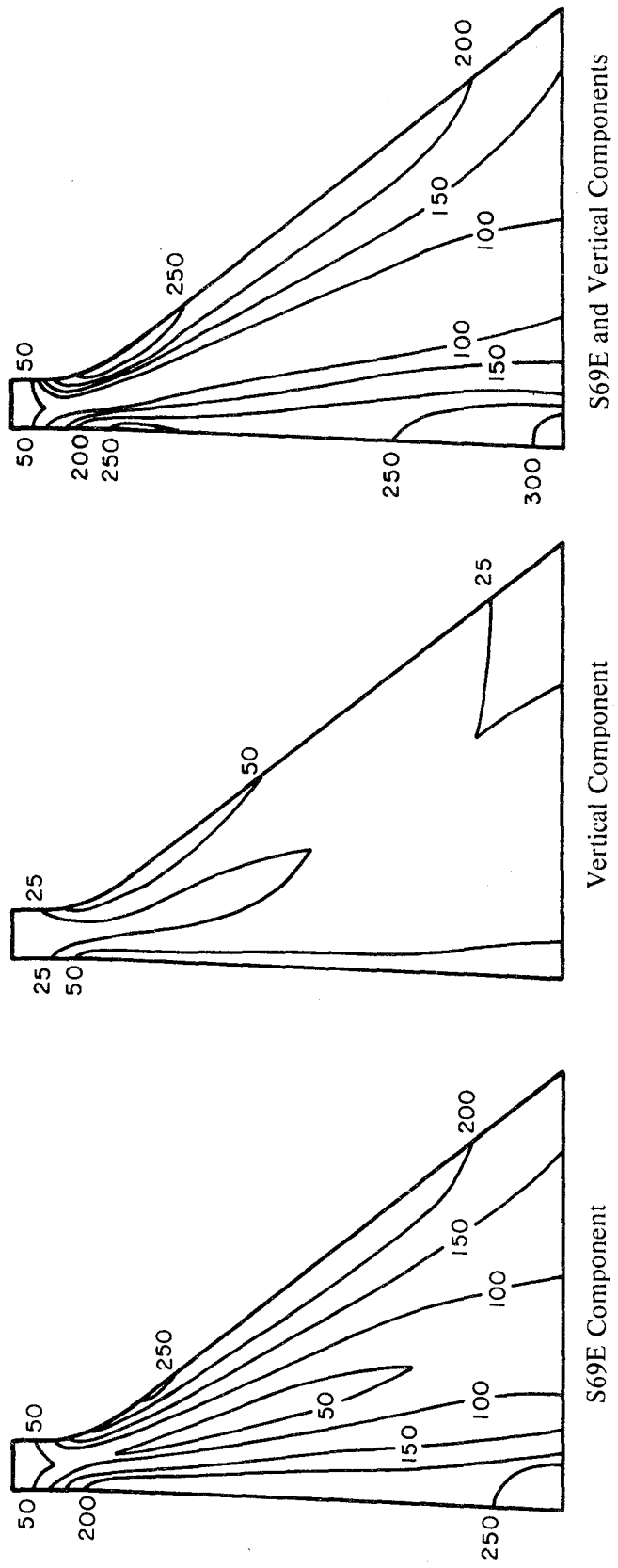
FIGURE 6.14 Envelope values of maximum principal stresses (in psi) in Pine Flat Dam on rigid foundation rock with full reservoir and absorptive reservoir bottom (with $\alpha=0$) due to S69E and vertical components, separately and simultaneously, of Taft ground motion. Initial static stresses are excluded.
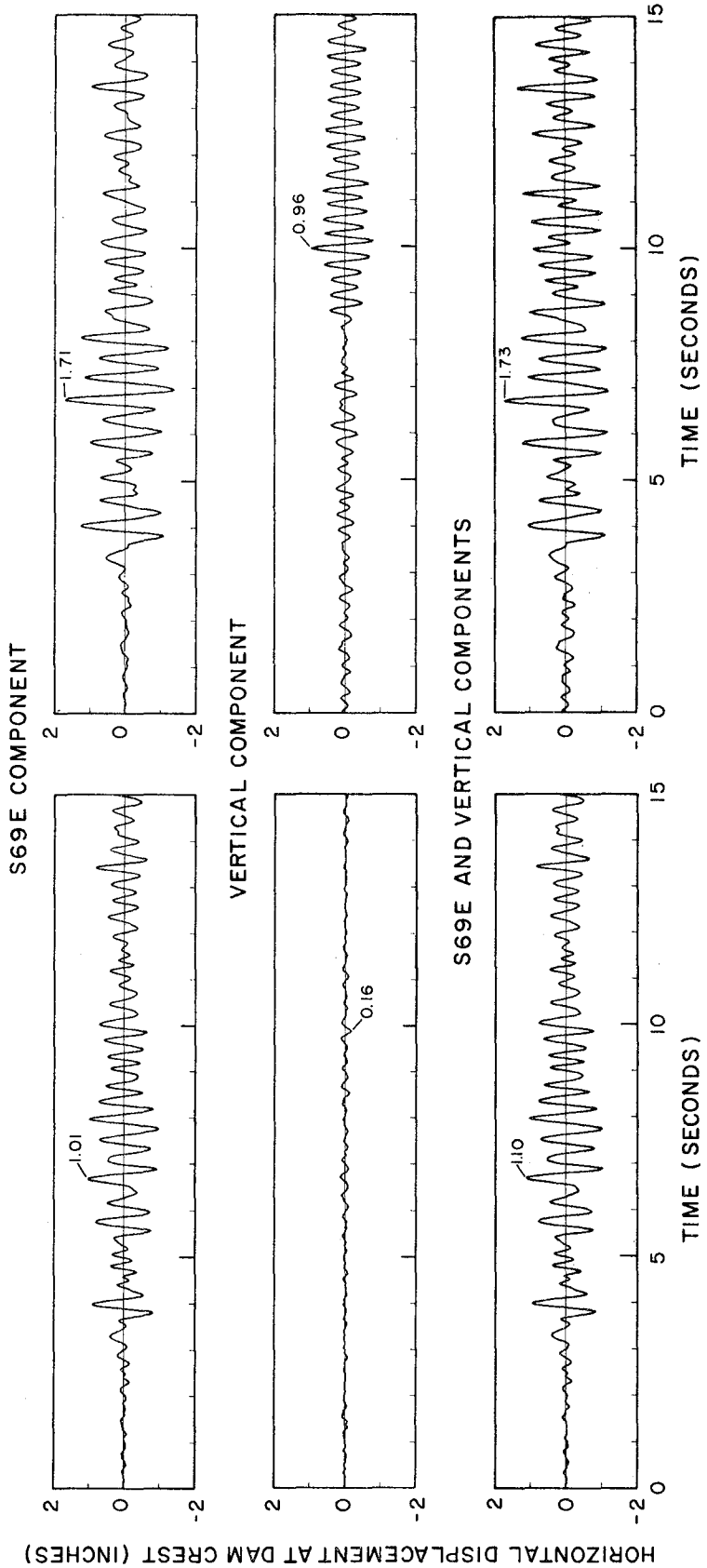
FIGURE 6.15 Displacement response of Pine Flat Dam on flexible foundation rock due to S69E and vertical components, separately and simultaneously, of Taft ground motion: (i) empty reservoir, and (ii) full reservoir with rigid reservoir bottom (α=1).
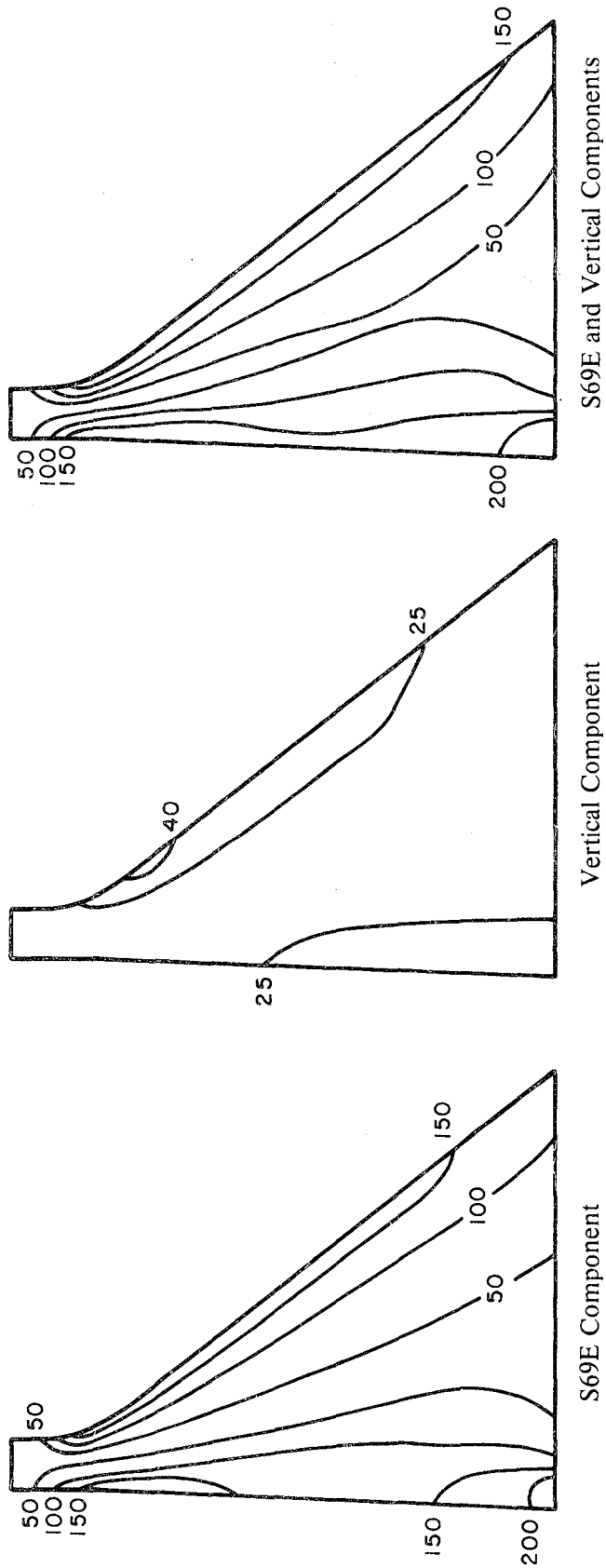
FIGURE 6.17 Envelope values of maximum principal stresses (in psi) in Pine Flat Dam on flexible foundation rock with empty reservoir due to S69E and vertical components, separately and simultaneously, of Taft ground motion. Initial static stresses are excluded.
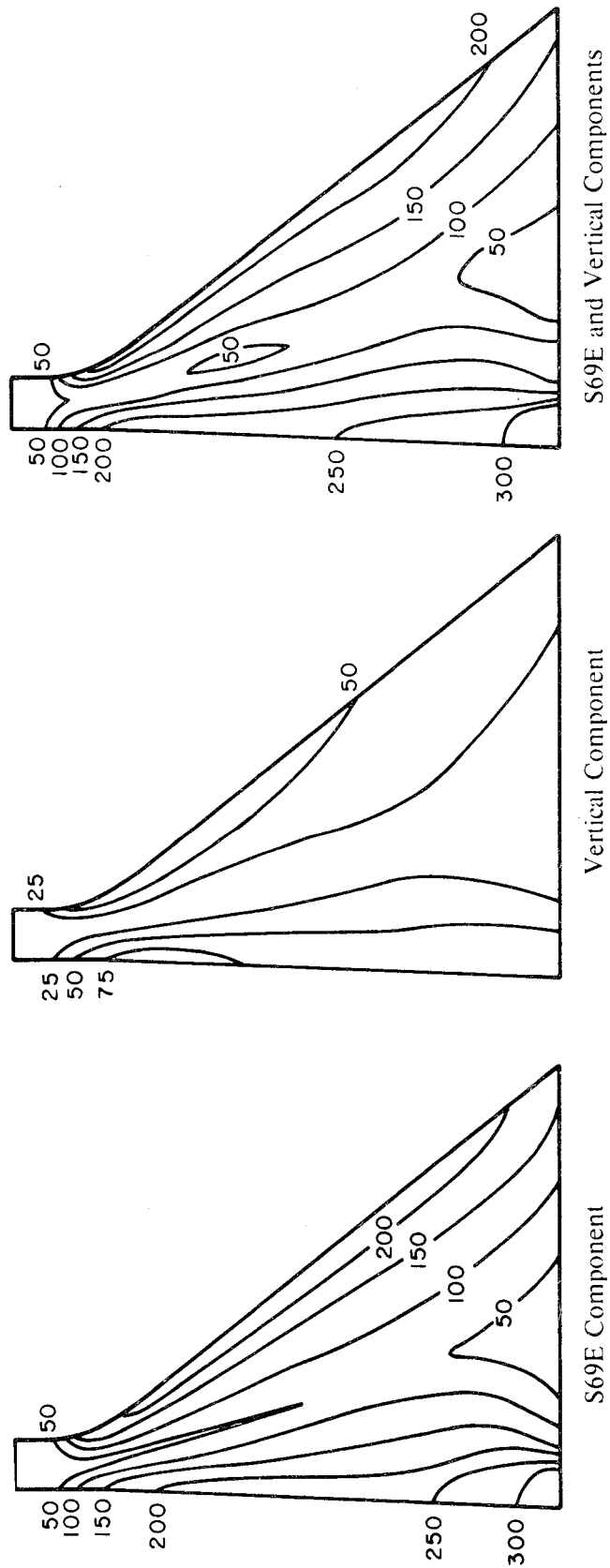
FIGURE 6.19 Envelope values of maximum principal stresses (in psi) in Pine Flat Dam on flexible foundation rock with full reservoir and absorptive reservoir bottom (with $\alpha=0.5$) due to S69E and vertical components, separately and simultaneously, of Taft ground motion. Initial static stresses are excluded.

Such a complete analysis of Pine Flat Dam was performed. A wave reflection coefficient $\alpha=0.5$ for the reservoir bottom materials was assumed in the analysis. The distribution of envelope values of the maximum principal stresses in the dam monolith due to only the static loads (weight of the dam and hydrostatic pressure of the impounded water) is shown in Figure 6.21. The horizontal and vertical displacements, relative to the free-field ground motion, at three levels on the upstream face of the dam (nodal points 1, 73 and 118) and three locations on the base (nodal points 154, 158 and 162) due to the S69E and vertical components, simultaneously, of Taft ground motion are shown in Figure 6.22. It can be seen that the horizontal and vertical motions of the dam base permitted by foundation-rock flexibility may not be inconsequential compared to the motion in the upper parts of the dam, although they are smaller. Figure 6.23 shows the distribution of envelope values of maximum principal stresses. Stress results such as these, that include the stresses due to the static loads, make it possible to identify the portions of the dam monolith that may crack during an earthquake.

The computation time required to obtain a complete history of displacements and stresses in the dam (including formation of the dynamic stiffness matrix for the foundation-rock region from the compliance data, eigenvalue analysis of the associated dam-foundation rock system, and fast Fourier transforms) is shown in Table 6.4 for Cases 7 and 8. Table 6.4 also includes the computation times required for response analyses of the dam under the other assumptions for the impounded water, the foundation rock and the reservoir bottom materials. Although each of these effects significantly complicate the analysis, the additional computation time required to include them is small. In particular, the extra cost of including reservoir bottom absorption is modest, demonstrating the efficacy of the procedures presented in Section 4.4 for the evaluation of the hydrodynamic terms. The overall efficiency of the analytical procedure, as demonstrated by the data in Table 6.4, lies in the use of the substructure method along with the transformation of displacements to generalized coordinates.
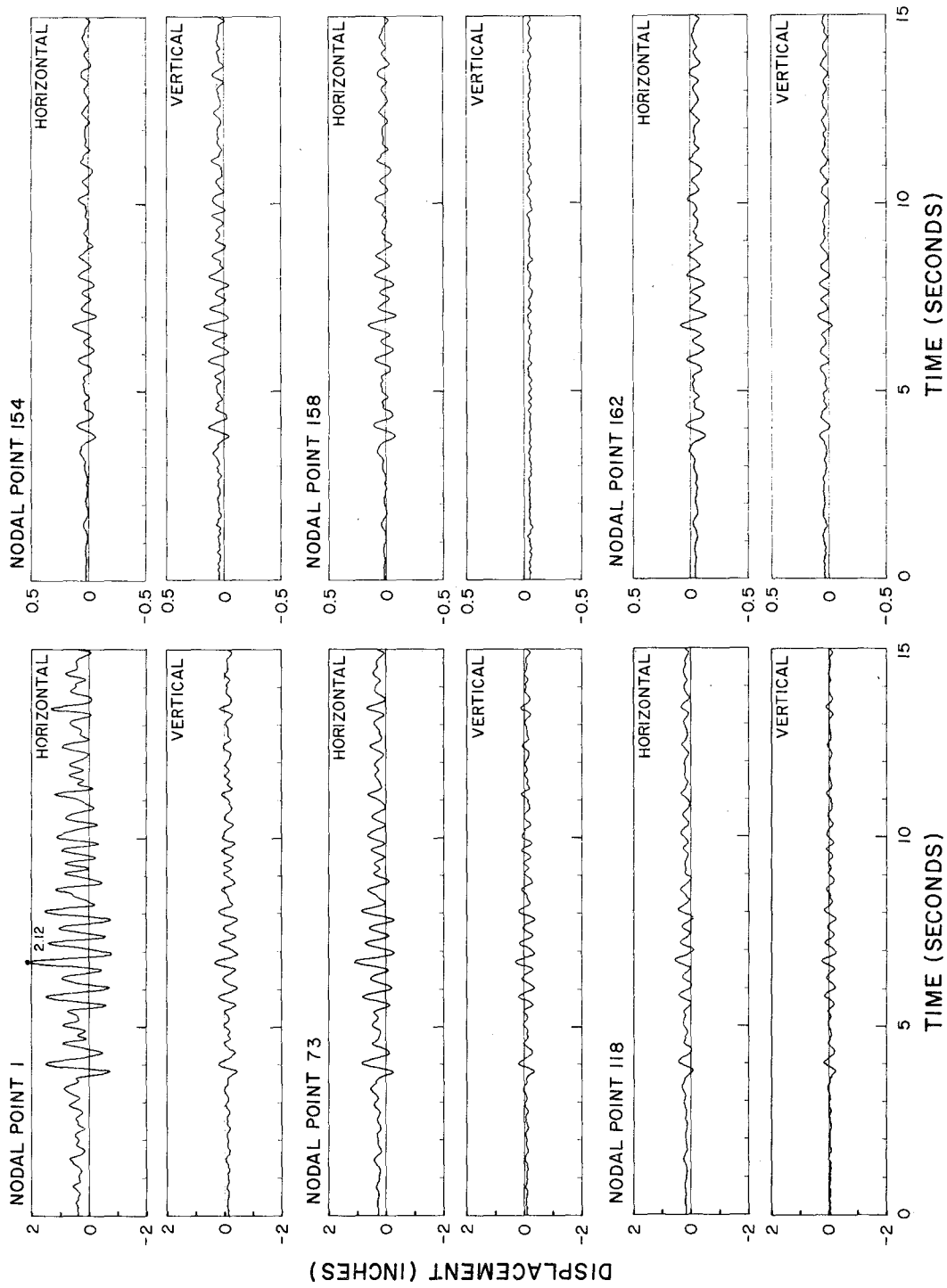
FIGURE 6.22 Displacement response of Pine Flat Dam on flexible foundation rock with full reservoir and absorptive reservoir bottom (with $\alpha=0.5$) due to S69E and vertical components, simultaneously, of Taft ground motion.

Table 6.4 -- Computation Times for Complete Analysis
of Pine Flat Dam to S69E and Vertical Components,
Simultaneously, of Taft Ground Motion

Case	Foundation Rock	Water	Reservoir Bottom	No. of Generalized Coordinates	Central Processor Time[*] (sec)
1	rigid	none	-	5	9.2
2	rigid	full	rigid	5	10.0
3-4	rigid	full	absorptive	5	10.2
5	flexible	none	-	10	13.0
6	flexible	full	rigid	10	14.5
7-8	flexible	full	absorptive	10	14.8

[*] CDC 7600 Computer

WATER

ABSORPTIVE RESERVOIR
BOTTOM MATERIAL

DAM

RIGID
BASE

$a_g(t)$
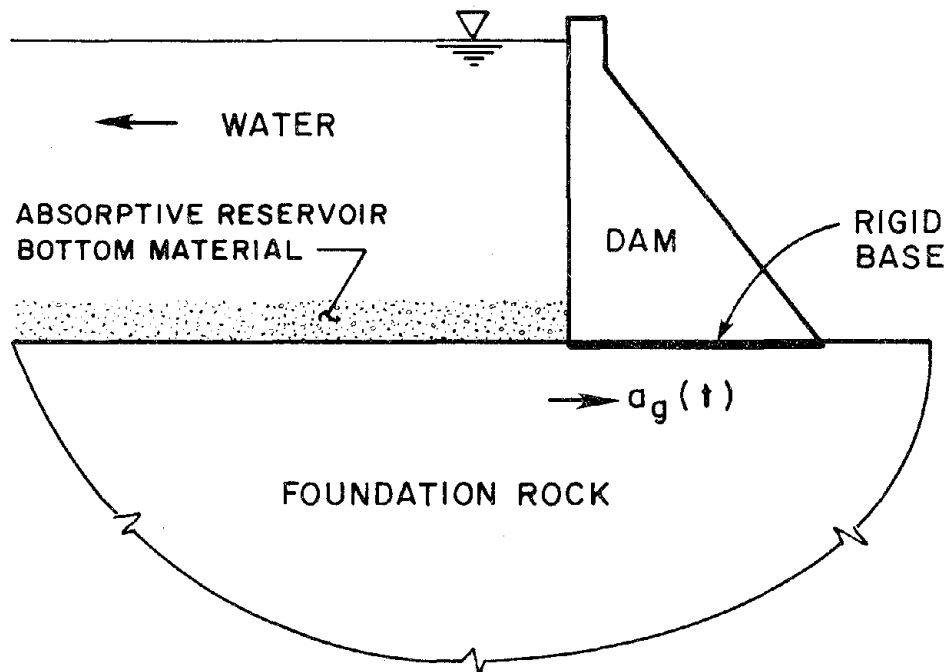
FOUNDATION ROCK

FIGURE 7.1   Dam-water-foundation rock system.

into equation (7.2) gives:

$$\bar{Y}_1(\omega) = \frac{-L_1}{-\omega^2 M_1 + i\omega\, C_1 + K_1} \tag{7.5}$$

The response history of the modal coordinate $Y_1(t)$ due to a specified earthquake ground motion can be computed from its frequency response function, equation (7.5), using standard Fourier synthesis techniques. The displacement response history of the dam is then given by equation (7.1). Furthermore, the maximum deformation and forces can be expressed directly in terms of the response spectrum for an earthquake ground motion [7,14].

The following sections of this chapter present the extensions to equation (7.5) necessary to include the effects of dam-water interaction, reservoir bottom absorption and dam-foundation rock interaction in the simplified analysis of the fundamental mode response of concrete gravity dams to earthquake ground motion.

7.4 Dams with Impounded Water

7.4.1 Exact Fundamental Mode Response

The equation of motion for the modal coordinate, equation (7.2), must be modified to include the hydrodynamic pressure due to the impounded water that acts on the upstream face of the dam (Chapter 3). The hydrodynamic pressure in the impounded water is governed by the two-dimensional wave equation subject to appropriate boundary conditions at: (a) the free surface, (b) the absorptive reservoir bottom, and (c) the upstream face of the dam. It was shown in Chapter 3 that including the interaction between the dam and compressible water results in the following complex-valued frequency response function for the modal coordinate [Equation (3.24)]:

$$\bar{Y}_1(\omega) = \frac{-[L_1 + B_0(\omega)]}{-\omega^2\{M_1 + \mathrm{Re}[B_1(\omega)]\} + i\omega\,\{C_1 - \omega\,\mathrm{Im}[B_1(\omega)]\} + K_1} \tag{7.6}$$

in which the hydrodynamic terms are defined as:

7.4.2 Approximate Fundamental Mode Response

Considering the effects of water impounded in the reservoir, the frequency response function $\bar{Y}_1(\omega)$ for the modal coordinate associated with the fundamental vibration mode of the dam, equation (7.6), is a complicated function of excitation frequency ω that contains frequency-dependent hydrodynamic terms. In a simplified analytical procedure, it is advantageous to represent the dam-water system by an equivalent single-degree-of-freedom (SDF) system with frequency-independent values for the hydrodynamic terms. This was done in reference 7 for dam-water systems with rigid reservoir bottom. If the reservoir bottom is absorptive, it is also possible to select frequency-independent hydrodynamic terms for an equivalent SDF system that approximates the fundamental mode response of the dam with impounded water.

The properties of the equivalent SDF system are defined as those of the dam with an empty reservoir modified by an added mass and an added damping that represent the hydrodynamic effects of the impounded water and reservoir bottom materials. The mass density $\tilde{m}_k(x,y)$, $k=x,y$, of the equivalent SDF system is defined as:

$$\tilde{m}_x(x,y) = m_x(x,y) + m_a(y)\,\delta(x) \tag{7.10a}$$

$$\tilde{m}_y(x,y) = m_y(x,y) \tag{7.10b}$$

where $\delta(x)$ is the Dirac delta function. Because the hydrodynamic pressure on a vertical upstream face acts in the horizontal direction, the "added mass" $m_a(y)$ only applies to the horizontal component of the dam motion and is concentrated at the upstream face of the dam. The "added mass" is defined as:

$$m_a(y) = \frac{\bar{p}_1(y,\tilde{\omega}_r)}{\phi_1^x(0,y)} \tag{7.11}$$

where the natural vibration frequency $\tilde{\omega}_r$ of the equivalent SDF system approximates the fundamental resonant frequency of the dam with impounded water. If the reservoir bottom is absorptive, $m_a(y)$ is complex-valued. Thus, it is not a mass quantity in the usual sense; only its real-valued component contributes to an added mass, whereas the imaginary-valued component leads to an added damping.

a comparison of equations (7.6) and (7.12) shows that $\overline{Y}_1(\tilde{\omega}_r) = \overline{Y}_1(\tilde{\omega}_r)$, i.e. the equivalent SDF system exactly predicts the fundamental resonant response of the dam with impounded water.

The natural vibration frequency $\tilde{\omega}_r$ of the equivalent SDF system is given by the excitation frequency that makes the real-valued component of the denominator in equation (7.12) zero:

$$\tilde{\omega}_r = \frac{\omega_1}{\sqrt{1 + \text{Re}[B_1(\tilde{\omega}_r)]/M_1}} \tag{7.16}$$

which must be evaluated iteratively for $\tilde{\omega}_r$. Hydrodynamic effects always reduce the natural vibration frequency because $\text{Re}[B_1(\omega)] > 0$ for all excitation frequencies. Equation (7.16) could have also been obtained from the exact fundamental mode response, equation (7.6), which demonstrates that the mass of the equivalent SDF system defined in equations (7.10) and (7.11) reduces the fundamental resonant frequency of the dam due to hydrodynamic effects by the proper amount.

The damping ratio of the equivalent SDF system $\tilde{\xi}_r = \tilde{C}_1 / 2\tilde{M}_1\tilde{\omega}_r$ is (Appendix F):

$$\tilde{\xi}_r = \frac{\tilde{\omega}_r}{\omega_1}\xi_1 + \xi_r \tag{7.17}$$

where the added damping due to dam-water interaction and reservoir bottom absorption is represented by the added damping ratio ξ_r, defined as:

$$\xi_r = -\frac{1}{2}\frac{1}{M_1}\left(\frac{\tilde{\omega}_r}{\omega_1}\right)^2 \text{Im}[B_1(\tilde{\omega}_r)] \tag{7.18}$$

The added damping ratio ξ_r is non-negative because $\text{Im}[B_1(\omega)] \leqslant 0$ for all excitation frequencies.

For dam-water systems with a rigid reservoir bottom ($\alpha = 1$), $\overline{p}_1(y,\tilde{\omega}_r)$ is real-valued (Chapter 3), as is $m_a(y)$. For a real-valued $m_a(y)$, equation (7.16) reduces to the earlier result [7] for the natural vibration frequency of the equivalent SDF system, and the added damping ratio ξ_r due to dam-water interaction is zero; so equation (7.17) reduces to the earlier expression for the damping ratio of the equivalent SDF system [7]. An absorptive reservoir bottom ($\alpha < 1$) results in complex-valued $m_a(y)$, which modifies the natural vibration frequency $\tilde{\omega}_r$ and increases the damping because hydrodynamic pressure waves propagate upstream and refract into the absorptive reservoir bottom at that frequency.
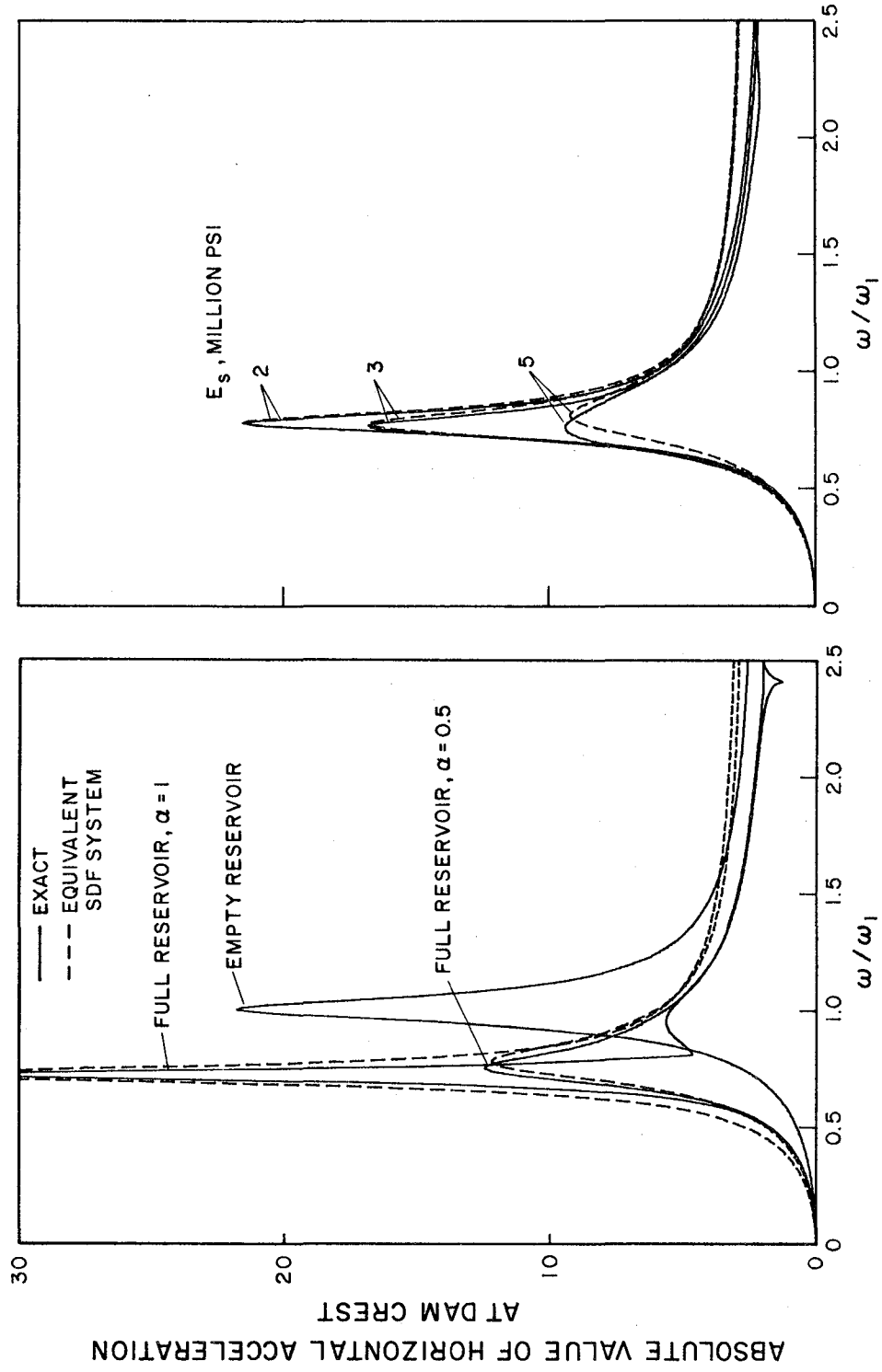
FIGURE 7.2 Comparison of exact and equivalent SDF system response of dams on rigid foundation rock with impounded water due to harmonic horizontal ground motion.

increasing rapidly with water depth. Furthermore, the vibration period ratio $\tilde{T}_r/T_1$ increases as the modulus of elasticity E_s of the concrete increases [4] because of interaction between the closely-spaced fundamental vibration frequencies of the dam and water (Chapter 3). As the reservoir bottom materials become more absorptive, i.e. as the wave reflection coefficient α decreases, the natural vibration period is reduced from its value for rigid reservoir bottom materials. This occurs because reservoir bottom absorption eliminates the unbounded peaks in the hydrodynamic terms, thus reducing the value of the added mass for excitation frequencies near the natural vibration frequencies of the impounded water. The wave reflection coefficient α has little influence on the fundamental resonant period if E_s is small, but its effect increases with E_s. However, as shown in Figure 7.3, the $\tilde{T}_r/T_1$ ratio is relatively insensitive to E_s if the reservoir bottom materials are absorptive with $\alpha \leq 0.5$.

The effects of reservoir bottom absorption on the added damping ratio ξ_r (Figure 7.4), and hence, on the damping ratio $\tilde{\xi}_r$ of the equivalent SDF system (Figure 7.5), are more complicated than its effects on the vibration period. As the wave reflection coefficient α decreases from unity, ξ_r increases monotonically from zero for small values of E_s, but the trends are more complicated for larger values of E_s. This latter unexpected behavior in ξ_r results from the previously described effects of reservoir bottom absorption on the natural vibration frequency $\tilde{\omega}_r$ of the equivalent SDF system [equation (7.16)], which is the frequency at which the added damping ratio is evaluated [equation (7.18)]. The value of the added damping ratio ξ_r depends on the relative values of $\tilde{\omega}_r$ and ω_1^r, the fundamental natural vibration frequency of the impounded water. As E_s increases, $\tilde{\omega}_r$ approaches ω_1^r, and the imaginary component of the hydrodynamic term $B_1(\tilde{\omega}_r)$ increases as α decreases from unity to zero, thus increasing ξ_r (Section 3.5). Figure 7.4 also shows that the wave reflection coefficient α has a larger effect on the added damping for large E_s values than for smaller E_s values. If the reservoir bottom materials are absorptive $(\alpha < 1)$, the added damping ratio ξ_r increases as E_s increases, with the rate of increase becoming smaller as α decreases.

Considering that $\tilde{\omega}_r$ is less than ω_1, equation (7.17) shows that dam-water interaction reduces the effectiveness of structural damping. Unless this reduction is compensated by added damping due to reservoir bottom absorption, the overall damping ratio $\tilde{\xi}_r$ will be less than ξ_1 (Figure 7.5).
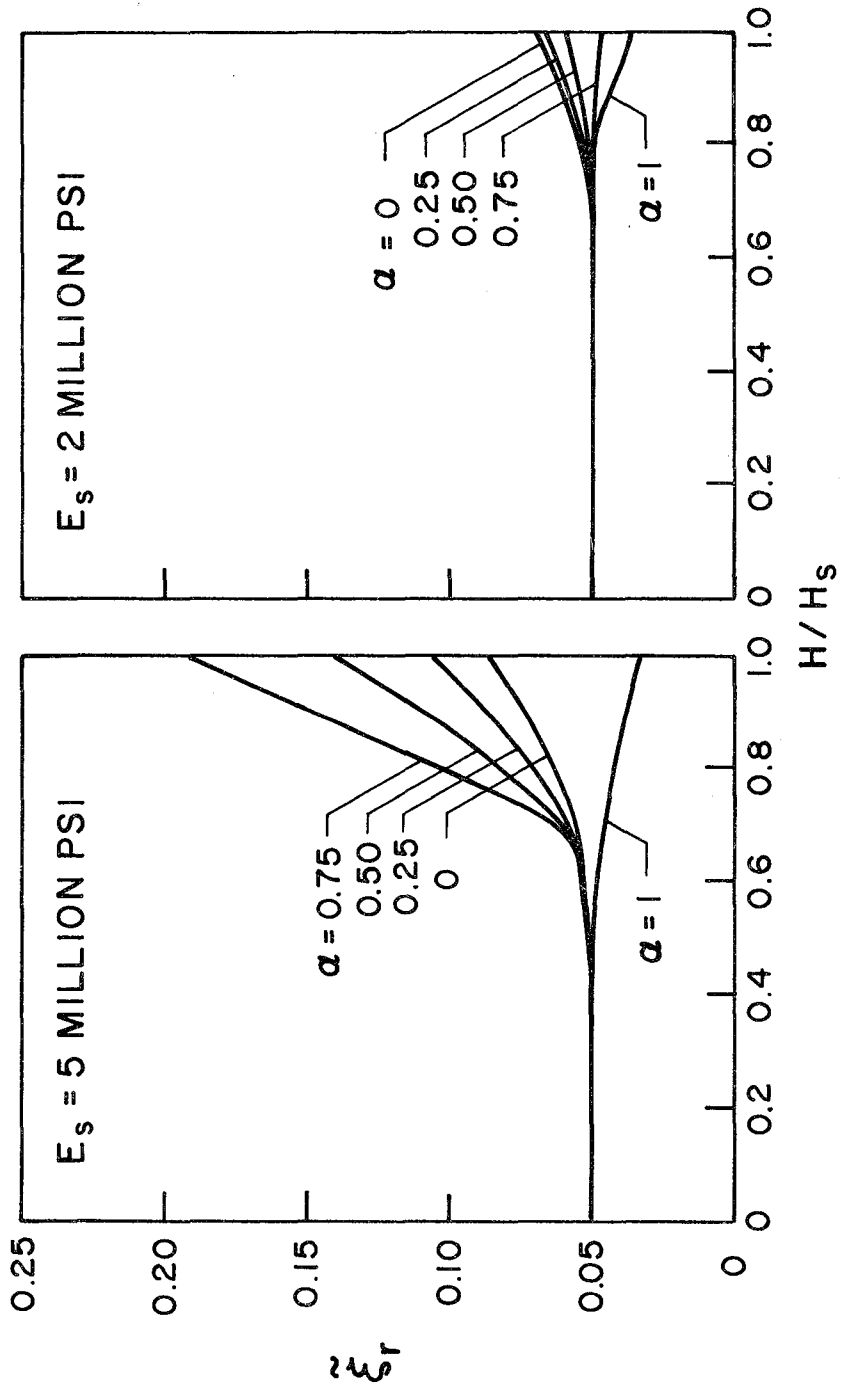
FIGURE 7.5 Damping ratio $\tilde{\xi}_r$ of the equivalent SDF system representing dams on rigid foundation rock with impounded water; $\xi_1 = 0.05$.
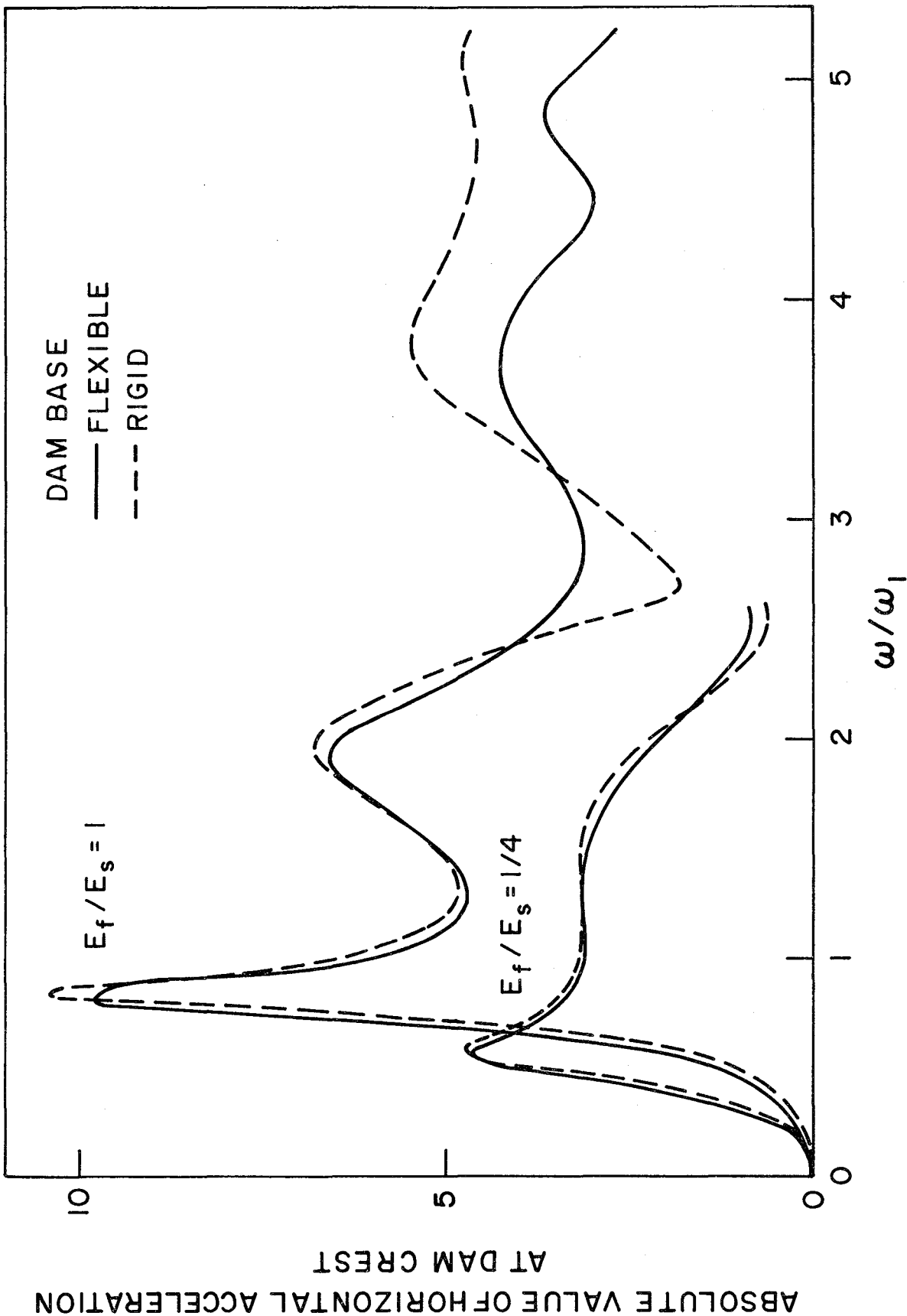
FIGURE 7.6 Effect of rigid base assumption on response of dams on flexible foundation rock with empty reservoir due to harmonic horizontal ground motion.
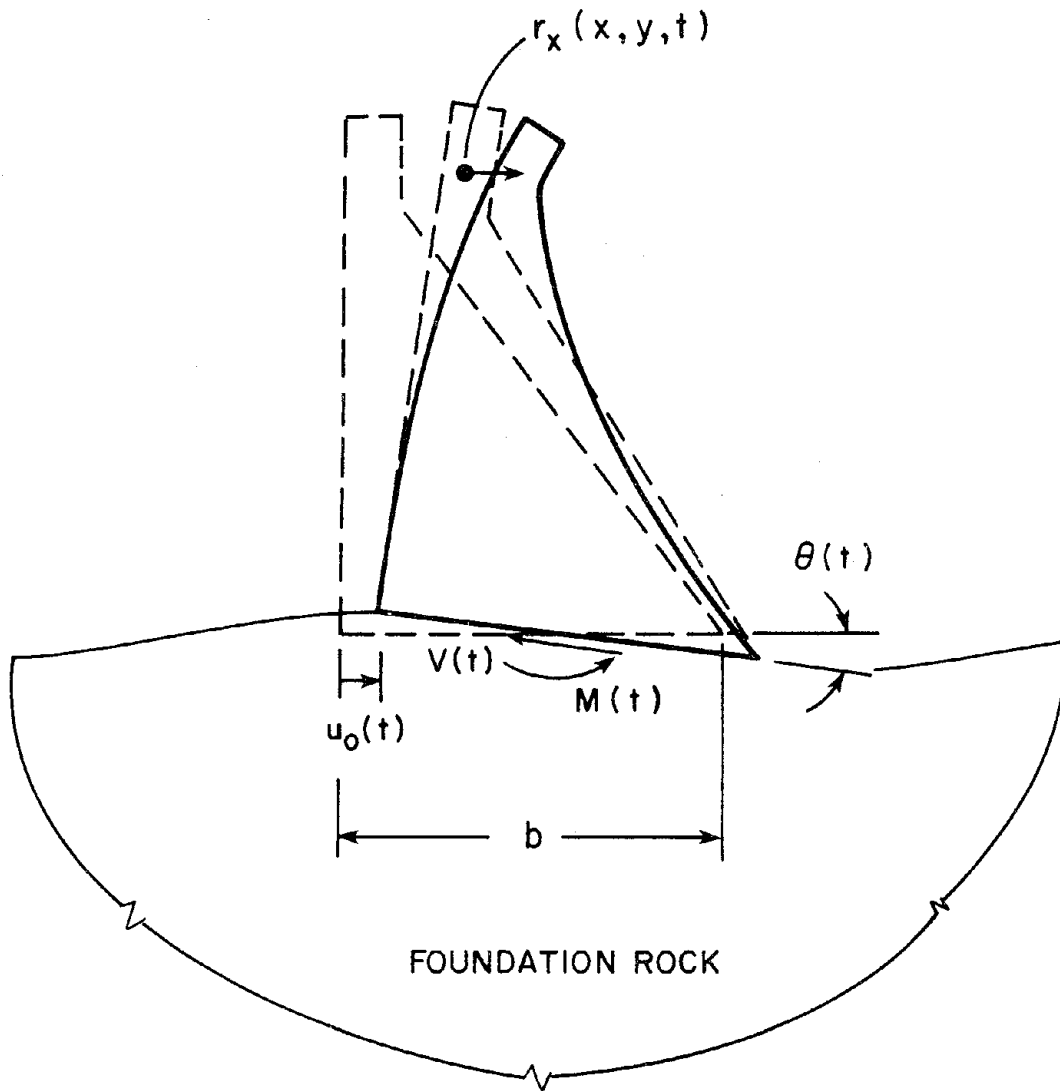
FIGURE 7.7   Displaced configuration of dam with rigid base on flexible foundation rock.

The coupling impedances $K_{VM}(\omega)$ and $K_{MV}(\omega)$ in the dynamic stiffness matrix, which are usually neglected in the analysis of multistory buildings [1,28,29], have a significant influence on the fundamental mode response of dams, as shown in Figure 7.8 for the idealized triangular dam monolith. The additional radiation damping associated with the coupling impedances is significant for a squat, heavy structure such as a concrete gravity dam because, unlike slender multistory buildings, its base translational motion is comparable in amplitude to the rotational motion.

7.5.3 Approximate Fundamental Mode Response

Following the procedure developed earlier for building-foundation systems [28,29], the contribution of the fundamental vibration mode of the dam to the earthquake response can by modelled by an equivalent SDF system on a fixed base. The properties of the equivalent system are defined to recognize the reduction in stiffness and change in damping of the dam due to dam-foundation rock interaction.

The natural vibration frequency $\tilde{\omega}_f$ of the equivalent SDF system that models the fundamental mode response of the dam on flexible foundation rock with an empty reservoir is given by the excitation frequency that makes the real-valued component of the denominator in equation (7.22) zero. Neglecting the effect of the second-order damping term, $\tilde{\omega}_f$ is given by

$$\tilde{\omega}_f = \frac{\omega_1}{\sqrt{1 + \mathrm{Re}[F(\tilde{\omega}_f)]}} \tag{7.24}$$

which must be evaluated iteratively. The vibration frequency $\tilde{\omega}_f$ will be less than ω_1 because $\mathrm{Re}[F(\omega)] > 0$ for all excitation frequencies. Substituting equation (7.23), after dropping the coupling impedance terms, into equation (7.24) gives the corresponding expression presented in reference 28 for building-foundation systems.

The frequency response function for the equivalent SDF system with natural vibration frequency $\tilde{\omega}_f$ and damping ratio $\tilde{\xi}_f$ can be shown have the following form (Appendix F):

$$\overline{Y}_1(\omega) = \left(\frac{\tilde{\omega}_f}{\omega_1}\right)^2 \cdot \frac{-L_1}{-\omega^2 M_1 + i\omega\{2\tilde{\xi}_f M_1 \tilde{\omega}_f\} + \tilde{\omega}_f^2 M_1} \tag{7.25}$$

The damping ratio $\tilde{\xi}_f$ is determined by equating the resonant response of the equivalent SDF system, from equation (7.25), to the exact fundamental mode response of the dam on flexible foundation rock, from equation (7.22), at the natural vibration frequency $\tilde{\omega}_f$: $\overline{Y}_1(\tilde{\omega}_f) = \overline{Y}_1(\tilde{\omega}_f)$. It can then be shown that the damping ratio $\tilde{\xi}_f$ is (Appendix F):

$$\tilde{\xi}_f = \left(\frac{\tilde{\omega}_f}{\omega_1}\right)^3 \xi_1 + \xi_f \tag{7.26}$$

where the added damping due to dam-foundation rock interaction is represented by the added damping ratio ξ_f, defined as:

$$\xi_f = -\frac{1}{2}\left(\frac{\tilde{\omega}_f}{\omega_1}\right)^2 \text{Im}[F(\tilde{\omega}_f)] \tag{7.27}$$

The added damping ratio ξ_f is positive because $\text{Im}[F(\omega)] < 0$ for all excitation frequencies. Equation (7.26) for the damping ratio of dam-foundation rock systems has the same form as for building-foundation systems [28,29].

7.5.4 Response Results

Figure 7.9 shows the absolute value of horizontal acceleration at the crest of the triangular dam monolith, relative to the rigid dam base, due to horizontal harmonic free-field ground acceleration, computed from equation (7.22), for several values of the moduli ratio E_f/E_s and a hysteretic damping factor for the foundation rock of $\eta_f=0.10$. As the moduli ratio E_f/E_s decreases, which for a fixed value of E_s implies a decrease in the foundation rock modulus E_f, the fundamental resonant frequency of the dam decreases and the amplitude of the resonant peak also decreases. These effects due to foundation-rock flexibility and damping, both material and radiation, have been discussed extensively for buildings [1,28,29] and for concrete gravity dams (Chapters 5 and 6). The frequency response function for the equivalent SDF system, computed from equation (7.25), with the natural vibration frequency $\tilde{\omega}_f$ and damping ratio $\tilde{\xi}_f$ given by equations (7.24) and (7.26), respectively, is also presented in Figure 7.9. These results demonstrate that, over a wide range of excitation frequencies, the equivalent SDF system accurately represents the fundamental mode response of dams supported on flexible

foundation rock.

The lengthening of the fundamental resonant period of the idealized triangular monolith due to dam-foundation rock interaction, determined from the resonant peak of $\bar{Y}_1(\omega)$, equation (7.22), is shown in Figure 7.10 for a range of E_f/E_s values. The vibration period $\tilde{T}_f$ of the equivalent SDF system, where $\tilde{T}_f = 2\pi/\tilde{\omega}_f$ is computed from equation (7.24), is close to the fundamental resonant period of the dam-foundation rock system for large values of E_f/E_s, but its accuracy decreases as E_f/E_s decreases, i.e. as the foundation rock becomes more flexible. However, the increasing error in the vibration period $\tilde{T}_f$ has little effect on the accuracy of the SDF system response, as shown in Figure 7.9, because the damping due to foundation-rock flexibility increases as E_f/E_s decreases resulting in response functions that do not resonate sharply. The added damping ratio ξ_f due to dam-foundation interaction is presented in Figure 7.11, and the damping ratio $\tilde{\xi}_f$ of the equivalent SDF system is shown in Figure 7.12, with a range of values for the hysteretic damping factor η_f for the foundation rock. The damping ratios ξ_f and $\tilde{\xi}_f$ increase with increasing foundation-rock flexibility and damping factor η_f. Considering that $\tilde{\omega}_f$ is less than ω_1, equation (7.26) indicates that dam-foundation rock interaction reduces the effectiveness of the structural damping. However, unlike for slender multistory buildings [28], for a wide range of E_f/E_s and η_f values this reduction is more than compensated by the added damping due to dam-foundation rock interaction, which leads to an increase in the overall damping of the dam, as shown in Figure 7.12.

The effects of dam-foundation rock interaction on dam response may be neglected if the moduli ratio E_f/E_s is relatively large. In particular, as shown in Figures 7.10 and 7.11, if E_f/E_s is greater than five, the increase in the vibration period is less than five percent, the increase in the damping ratio $\tilde{\xi}_f$ is less than two percent; and consequently, the foundation rock may be treated as rigid.
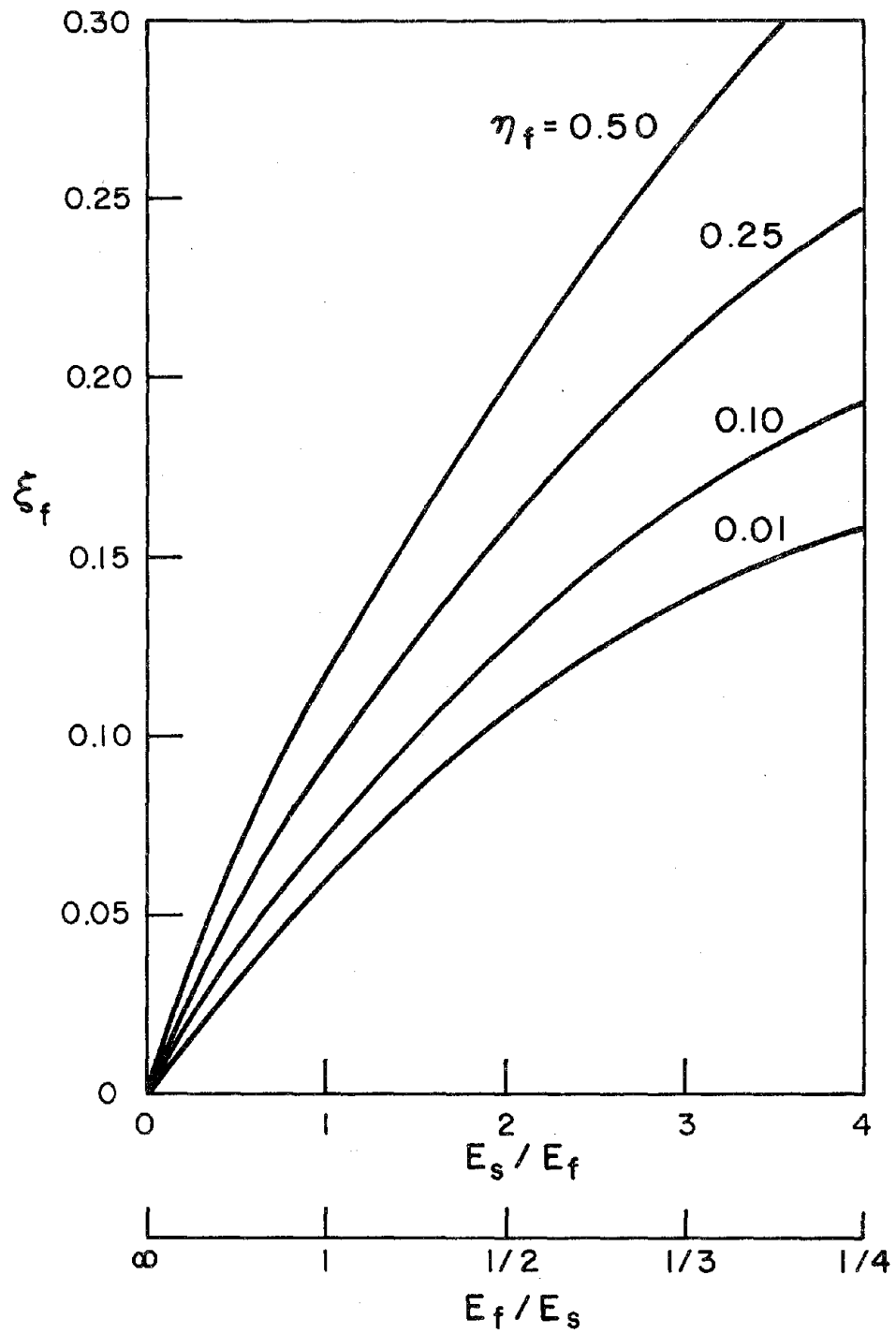
FIGURE 7.11 Added damping ratio ξ_f due to dam-foundation rock interaction for a range of E_f/E_s values and various values of η_f, the constant hysteretic damping factor for the foundation rock.

7.6 Dams on Flexible Foundation Rock with Impounded Water

7.6.1 Exact Fundamental Mode Response

When modified to include effects of dam-water interaction and reservoir bottom absorption, the frequency domain equations for the fundamental mode response of dams on flexible foundation rock, equation (7.21), become (Appendix D):

$$
\begin{bmatrix}
-\omega^2 M_1 + i\omega C_1 + K_1 - \omega^2 B_1(\omega) & -\omega^2[L_1 + B_0(\omega)] & -\omega^2[L_1^\theta + B_{\theta 1}(\omega)] \\
-\omega^2[L_1 + B_0(\omega)] & -\omega^2[m_r + B_{00}(\omega)] + K_{VV}(\omega) & -\omega^2[L_\theta^x + B_{0\theta}(\omega)] + K_{VM}(\omega)\,b \\
-\omega^2[L_1^\theta + B_{\theta 1}(\omega)] & -\omega^2[L_\theta^x + B_{0\theta}(\omega)] + K_{MV}(\omega)\,b & -\omega^2[I_r + B_{\theta\theta}(\omega)] + K_{MM}(\omega)\,b^2
\end{bmatrix}
\begin{Bmatrix}
\overline{Y}_1(\omega) \\
\overline{u}_0(\omega) \\
\overline{\theta}(\omega)
\end{Bmatrix}
$$

$$
= -\begin{Bmatrix}
L_1 + B_0(\omega) \\
m_r + B_{00}(\omega) \\
L_\theta^x + B_{0\theta}(\omega)
\end{Bmatrix}
\tag{7.28}
$$

where the hydrodynamic terms $B_0(\omega)$ and $B_1(\omega)$ are defined by equation (7.7); and the additional hydrodynamic terms associated with the rigid-body motion of the dam due to foundation-rock flexibility are:

$$
B_{00}(\omega) = \int_0^H \overline{p}_0(y,\omega)\,dy, \qquad
B_{0\theta}(\omega) = \int_0^H y\,\overline{p}_0(y,\omega)\,dy
\tag{7.29a}
$$

$$
B_{\theta\theta}(\omega) = \int_0^H y\,\overline{p}_0^\theta(y,\omega)\,dy, \qquad
B_{\theta 1}(\omega) = \int_0^H y\,\overline{p}_1(y,\omega)\,dy
\tag{7.29b}
$$

The functions $\overline{p}_0(y,\omega)$ and $\overline{p}_1(y,\omega)$ in equation (7.29) are defined in equation (7.8), and $\overline{p}_0^\theta(y,\omega)$ is the frequency response function for hydrodynamic pressure on the upstream face of a rigid dam rotating about the centroid of its base:

$$
\overline{p}_0^\theta(y,\omega) = 2\rho H \sum_{n=1}^\infty \frac{\mu_n^2(\omega)}{H[\mu_n^2(\omega) - (\omega q)^2] + i(\omega q)} \frac{I_{\theta n}(\omega)}{\sqrt{\mu_n^2(\omega) - \omega^2/C^2}} Y_n(y,\omega)
\tag{7.30}
$$

where

$$
I_{\theta n}(\omega) = \frac{1}{H} \int_0^H y\,Y_n(y,\omega)\,dy
\tag{7.31}
$$

and $\mu_n(\omega)$ and $Y_n(y,\omega)$ are defined in equations (3.20) and (3.21), respectively.

7.6.2 Approximate Fundamental Mode Response

Equivalent SDF systems have been developed in the Sections 7.4 and 7.5 to approximate the fundamental mode response of dams considering the effects of dam-water interaction and dam-foundation rock interaction separately. In a similar manner, the fundamental mode response of dams simultaneously considering the two types of interaction can be represented by an equivalent SDF system on a fixed base.

However, the parameters of the equivalent SDF system -- natural vibration frequency and damping ratio -- are especially complicated because of the hydrodynamic terms associated with the rigid-body motion of the dam in the water-foundation rock coupling term $F_r(\omega)$ defined in equation (7.33). It is therefore desirable to find an approximation to the hydrodynamic terms $B_{00}(\omega)/m_1^*$, $B_{0\theta}(\omega)/m_1^* h_1^*$ and $B_{\theta\theta}(\omega)/m_1^*(h_1^*)^2$ in $F_r(\omega)$, that permit simpler expressions for the parameters of the equivalent SDF system. For this purpose only, the hydrodynamic terms in $F_r(\omega)$ are approximated by considering only the contribution of the fundamental vibration mode to the rigid-body displacements of the upstream face of the dam: $1 \approx (L_1/M_1)\phi_1^x(0,y)$ and $y \approx (L_1^\theta/M_1)\phi_1^x(0,y)$. With this assumption each of the above hydrodynamic terms associated with the rigid-body motion of the dam is equal to the hydrodynamic term $B_1(\omega)/M_1$ associated with the fundamental vibration mode of the dam; and, $F_r(\omega)$ is then:

$$F_r(\omega) = \frac{1}{M_1} B_1(\omega) F(\omega) \qquad (7.34)$$

where $B_1(\omega)$ and $F(\omega)$ are defined in equations (7.7b) and (7.23), respectively. The effect of using the approximate expression for $F_r(\omega)$, equation (7.34), instead of the exact expression, equation (7.33), in the frequency response function $\overline{Y}_1(\omega)$, equation (7.32), is demonstrated in Figure 7.13, where the response of the idealized triangular dam monolith on flexible foundation rock with a full reservoir due to horizontal harmonic ground motion is shown for several cases. The approximation of the hydrodynamic terms in equation (7.34) for $F_r(\omega)$ introduces little error in the fundamental resonant frequency, but the fundamental resonant peak errs on the conservative side, with the errors decreasing as E_f/E_s becomes smaller.

The properties of the equivalent SDF system can now be obtained by consideration of the fundamental mode response of dams on flexible foundation rock with impounded water, as expressed in equation (7.32) and (7.34). The mass of the equivalent system is still given by equation (7.10) with the "added mass" is described by an expression similar to equation (7.11), but evaluated at a different frequency:

$$m_a(y) = \frac{\bar{p}_1(y, \tilde{\omega}_1)}{\phi_1^x(0, y)} \tag{7.35}$$

where the natural vibration frequency $\tilde{\omega}_1$ of the equivalent SDF system approximates the fundamental resonant frequency of the dam on flexible foundation rock with impounded water.

The natural vibration frequency is approximately given by the excitation frequency that makes the real-valued component of the denominator in equation (7.32) zero, which upon use of equation (7.34) for $F_r(\omega)$ and neglect of the second-order damping terms leads to (Appendix F):

$$\tilde{\omega}_1 = \omega_1 \left(\frac{1}{\sqrt{1 + \mathrm{Re}[B_1(\tilde{\omega}_1)]/M_1}} \right) \cdot \left(\frac{1}{\sqrt{1 + \mathrm{Re}[F(\tilde{\omega}_1)]}} \right) \tag{7.36}$$

The first parenthesis represents the portion of the reduction in the natural vibration frequency due to dam-water interaction, associated with the added hydrodynamic mass that arises from the "added mass" distribution given in equation (7.35), in a manner similar to that shown in Section 7.4 for dams on rigid foundation rock with impounded water. The second parenthesis represents the portion of the reduction in the natural vibration frequency due to dam-foundation rock interaction associated with the foundation-rock flexibility term $\mathrm{Re}[F(\tilde{\omega}_1)]$, in a manner similar to that shown in Section 7.5 for dams on flexible foundation rock with empty reservoirs. Because $F(\omega)$ is a slowly-varying, smooth function of excitation frequency, as is $\mathrm{Re}[B_1(\omega)]$ if the reservoir bottom materials are significantly absorptive, the foundation-rock flexibility term $\mathrm{Re}[F(\omega)]$ may be evaluated at $\tilde{\omega}_f$, and the added hydrodynamic mass $\mathrm{Re}[B_1(\omega)]$ may be evaluated with sufficient accuracy at $\tilde{\omega}_r$. Consequently, the natural vibration frequency $\tilde{\omega}_1$ from equation (7.36) may be expressed as:

$$\tilde{\omega}_1 = \omega_1 \left(\frac{1}{\sqrt{1 + \mathrm{Re}[B_1(\tilde{\omega}_r)]/M_1}} \right) \cdot \left(\frac{1}{\sqrt{1 + \mathrm{Re}[F(\tilde{\omega}_f)]}} \right) \tag{7.37}$$

evaluated at $\tilde{\omega}_1$:

$$\xi_f(\tilde{\omega}_1) = -\frac{1}{2}\left[\frac{\tilde{\omega}_1}{\omega_1}\right]^2 \text{Im}[F(\tilde{\omega}_1)] \qquad (7.42)$$

The special cases for a dam on rigid foundation rock and a dam with an empty reservoir are contained in equation (7.38) for the natural vibration frequency, in equation (7.40) for the damping ratio, and in equation (7.39) for the frequency response function for the equivalent SDF system.

7.6.3 Response Results

The effectiveness of the equivalent SDF system in representing the fundamental mode response of the triangular dam monolith on flexible foundation rock with a full reservoir is shown in Figure 7.14 for several values of the moduli ratio E_f/E_s and wave reflection coefficient α. The "exact" fundamental mode response was computed using equation (7.32) with approximate the $F_r(\omega)$ given by equation (7.34); and the response of the equivalent SDF system was computed using equation (7.39), with the natural vibration frequency $\tilde{\omega}_1$ and damping ratio $\tilde{\xi}$ computed from equations (7.38) and (7.40), respectively. The equivalent SDF system represents with an acceptable degree of accuracy the dam response including interaction with the flexible foundation rock and impounded water and the effects of reservoir bottom absorption.

The effects of dam-water interaction, reservoir bottom absorption and dam-foundation rock interaction on the fundamental resonant period are shown in Figure 7.15. For a given moduli ratio E_f/E_s, the fundamental resonant period lengthens with increasing depth of water, and the period shortens as the wave reflection coefficient α decreases. A particular case of these trends was seen in Figure 7.3 for $E_f/E_s=\infty$ (rigid foundation rock). As E_f/E_s decreases, the fundamental resonant period of the dam lengthens due to increasing flexibility of the foundation-rock relative to that of the dam. A particular case of this trend was seen in Figure 7.10 for $H/H_s=0$ (empty reservoir). It is apparent that the fundamental resonant period obtained from the the resonant peak of $\bar{Y}_1(\omega)$, equations (7.32) and (7.34), is approximately represented by the natural vibration period $\tilde{T}_1$ of the equivalent SDF system, where $\tilde{T}_1=2\pi/\tilde{\omega}_1$ is given by equation (7.38). The error between the exact and approximate values of
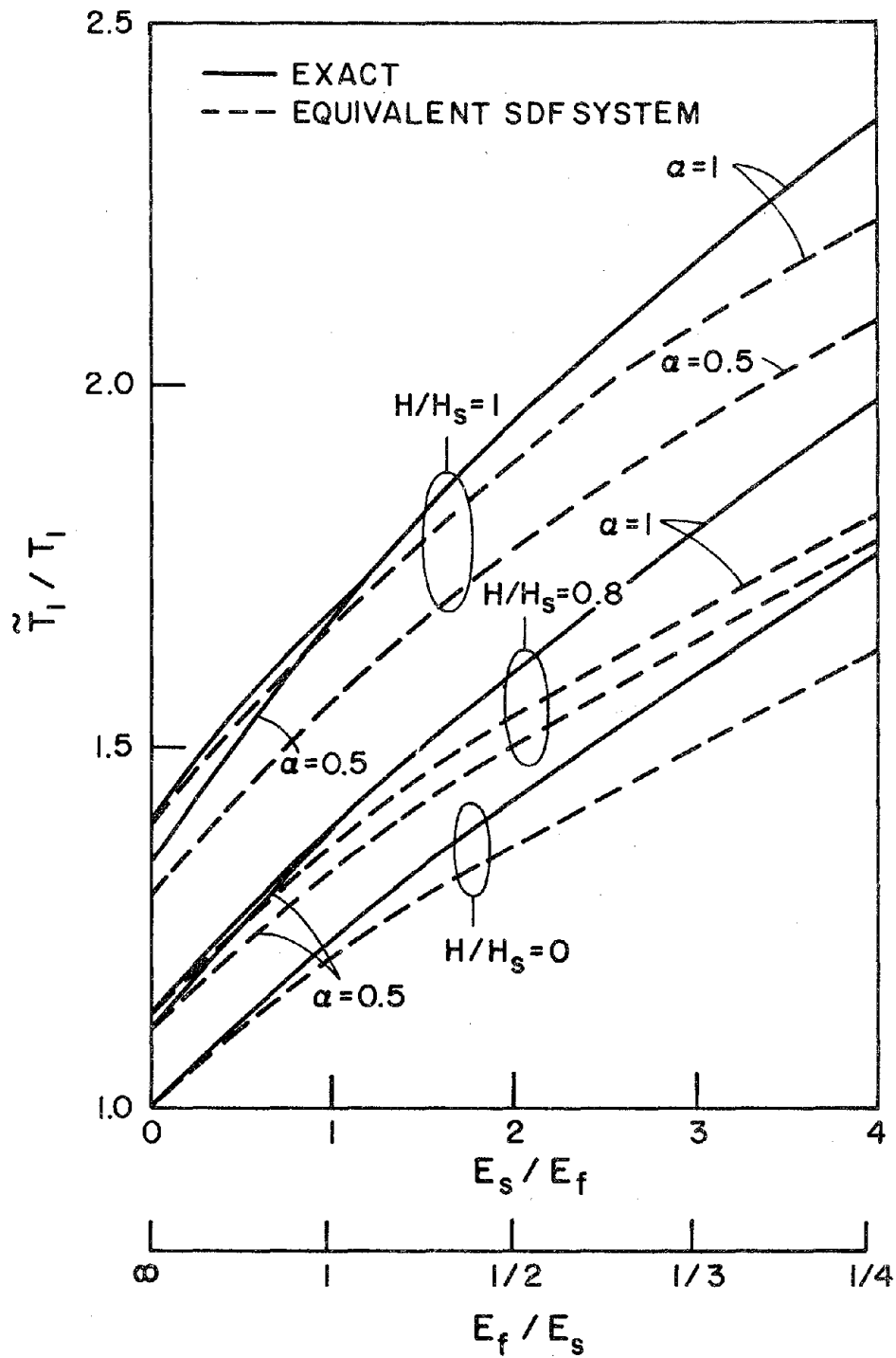
FIGURE 7.15 Comparison of exact and approximate (equivalent SDF system) values of the ratio of the fundamental vibration periods $\tilde{T}_1$ and T_1 of the dam on flexible foundation rock with impounded water and the dam on rigid foundation rock with empty reservoir. Results presented for E_s=4 million psi.
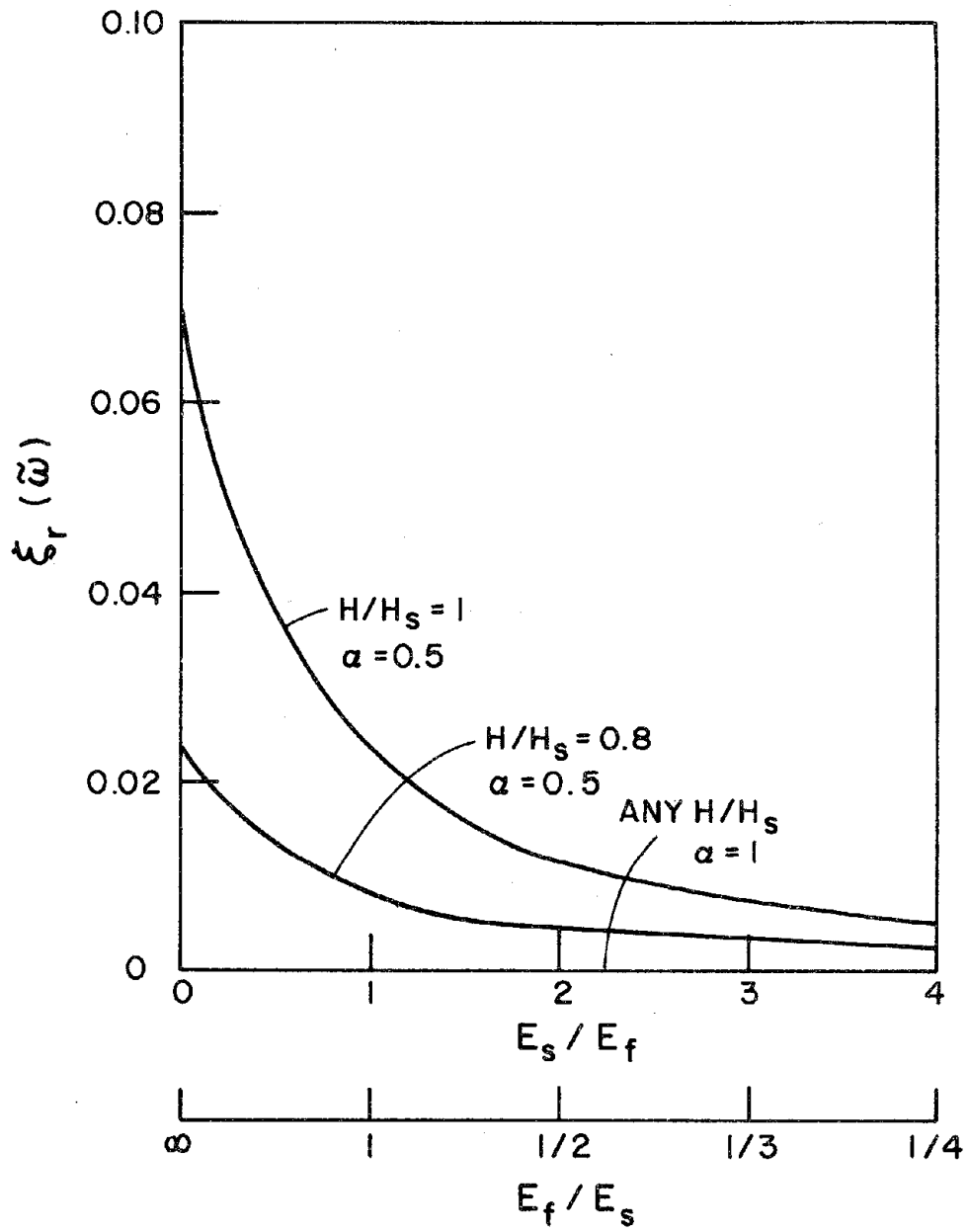
FIGURE 7.16 Added damping ratio $\xi_r(\tilde{\omega}_1)$ due to dam-water interaction and reservoir bottom absorption. Results presented for E_s=4 million psi.

reservoir bottom materials ($\alpha=1$), the reduction of the natural vibration frequency due to hydrodynamic effects results in a decreased added damping ratio $\xi_f(\tilde{\omega}_1)$ arising from foundation-rock flexibility, as shown in Figure 7.17, without contributing additional damping to $\xi_r(\tilde{\omega}_1)$ (Figure 7.16). The net effect of these trends is shown in Figure 7.18(a), where for a particular E_f/E_s value, the damping ratio $\tilde{\xi}$ decreases as the depth of the impounded water increases. For absorptive reservoir bottom materials ($\alpha<1$), the reduction in the natural vibration frequency due to hydrodynamic effects is less than for non-absorptive reservoir bottom materials (see Figure 7.3), so the reduction on $\xi_f(\tilde{\omega}_1)$ due to dam-water interaction is less (Figure 7.17), and dam-water interaction and reservoir bottom absorption contribute additional damping, as represented by the added damping ratio $\xi_r(\tilde{\omega}_1)$. The net effects of these contributions to the overall damping ratio $\tilde{\xi}$ are shown in Figure 7.18(b) for absorptive reservoir bottom materials. If the moduli ratio is relatively large ($E_f/E_s>1/2$), the increase in the added damping ratio $\xi_r(\tilde{\omega}_1)$ dominates the decrease in $\xi_f(\tilde{\omega}_1)$ (Figure 7.17), so $\tilde{\xi}$ increases as the depth of the impounded water increases. However, if the moduli ratio is relatively small ($E_f/E_s<1/2$), the added damping ratio $\xi_r(\tilde{\omega}_1)$ is very small (Figure 7.16) and the reduction of $\xi_f(\tilde{\omega}_1)$ due to dam-water interaction effects (Figure 7.17) dominates, resulting in a decrease of $\tilde{\xi}$ as the depth of the impounded water increases.

7.6.4 Simplification of the Damping Ratio

Because the damping ratio $\xi_r(\tilde{\omega}_1)$ due to dam-water interaction and reservoir bottom absorption depends on the moduli ratio E_f/E_s (Figure 7.16) and the damping ratio $\xi_f(\tilde{\omega}_1)$ due to dam-foundation rock interaction depends on the water depth ratio H/H_s, and wave reflection coefficient α (Figure 7.17), it would be cumbersome to compute these two added damping ratios in a simplified analytical procedure. It is possible, however, to uncouple the effects of dam-foundation rock interaction from the evaluation of $\xi_r(\tilde{\omega}_1)$ and the effects of dam-water interaction from the evaluation of $\xi_f(\tilde{\omega}_1)$, and still obtain a reasonable estimate of the damping ratio $\tilde{\xi}$ of the equivalent SDF system. The effects of dam-foundation rock interaction on the added hydrodynamic damping ratio $\xi_r(\tilde{\omega}_1)$ can be neglected by evaluating $\text{Im}[B_1(\omega)]$ at $\tilde{\omega}_r$, the natural vibration frequency of the dam on rigid foundation rock with

impounded water; equation (7.41) then becomes:

$$\xi_r(\tilde{\omega}_1) \approx \left[\frac{\tilde{\omega}_f}{\omega_1}\right]^2 \xi_r \tag{7.43}$$

where ξ_r is given by equation (7.18). Similarly, the effects of dam-water interaction and reservoir bottom absorption on the added damping ratio $\xi_f(\tilde{\omega}_1)$ due to dam-foundation rock interaction can be neglected by evaluating $\text{Im}[F(\omega)]$ at $\tilde{\omega}_f$, the natural vibration frequency of the dam on flexible foundation rock with an empty reservoir; equation (7.42) then becomes:

$$\xi_f(\tilde{\omega}_1) \approx \left[\frac{\tilde{\omega}_r}{\omega_1}\right]^2 \xi_f \tag{7.44}$$

where ξ_f is given by equation (7.27). The substitution of equations (7.43) and (7.44) into equation (7.40) gives the simplified expression for the damping ratio $\tilde{\xi}$:

$$\tilde{\xi} \approx \left[\frac{\tilde{\omega}_r}{\omega_1}\right]\left[\frac{\tilde{\omega}_f}{\omega_1}\right]^3 \xi_1 + \xi_r + \xi_f \tag{7.45}$$

According to equation (7.45), the contributions of dam-water interaction and dam-foundation rock interaction to the damping of the system are obtained independently and summed with the structural damping, with its effectiveness properly reduced by the interaction effects, to give the damping ratio $\tilde{\xi}$ of the equivalent SDF system. In conjunction with the approximation used to obtain equation (7.43), the effective earthquake force $\tilde{L}_1$ is evaluated at $\tilde{\omega}_r$, so that $\tilde{L}_1 \approx L_1 + B_0(\tilde{\omega}_r)$.

The equivalent SDF system's representation of the fundamental vibration mode of the triangular dam monolith is shown in Figure 7.19, where the response was computed from equation (7.39) using the two definitions of the damping ratio $\tilde{\xi}$: "exact" $\tilde{\xi}$ given by equation (7.40), and simplified $\tilde{\xi}$ given by equation (7.45). The simplified expression for the damping ratio overestimates the damping in systems with an absorptive reservoir bottom ($\alpha=0.5$), resulting in underestimation of the resonant response. The simplified damping ratio is more accurate if the reservoir bottom is rigid ($\alpha=1$) because the added damping due to dam-water interaction is zero; but the resonant response is slightly overestimated because the added force term in $\tilde{L}_1$ is overestimated in the approximation.

The final result of the series of approximations used to simplify the analysis of the fundamental mode response of dam-water-foundation rock systems is shown in Figure 7.20 for the triangular dam monolith. The exact fundamental mode response of the dam on flexible foundation rock with full reservoir was computed using equation (7.32) and the exact water-foundation rock coupling term $F_r(\omega)$ given by equation (7.33). The response of the equivalent SDF system was computed using equation (7.39) with the natural vibration frequency $\tilde{\omega}_1$ and damping ratio $\tilde{\xi}$ evaluated from equations (7.38) and (7.45), respectively. These results demonstrate that the equivalent SDF system provides a good approximation of the fundamental mode response of concrete gravity dams for a wide range of values for the moduli ratio E_f/E_s and wave reflection coefficient α. The quality of the approximation is satisfactory for preliminary design of dams, considering the complicated effects of dam-water interaction, reservoir bottom absorption and dam-foundation rock interaction that are included; the number of approximations necessary to develop the simplified expressions for the properties of the equivalent SDF system; and noting that the approximate results generally err on the conservative side.

7.7 Summary

It has been shown in this chapter that although dam-water-foundation rock interaction introduces frequency-dependent, complex-valued hydrodynamic and foundation interaction terms in the governing equations, frequency-independent values for such terms can be defined and an equivalent single-degree-of-freedom system can be developed to represent approximately the fundamental mode response of concrete gravity dams. The displacements of the dam relative to the rigid base are [equation (7.1)]:

$$r_k(x,y,t) = \phi_1^k(x,y)\, Y_1(t), \qquad k=x,y \tag{7.46}$$

The modal coordinate $Y_1(t)$ can be expressed in terms of the frequency response function $\bar{\bar{Y}}_1(\omega)$ for the equivalent SDF system given in equation (7.39):

$$\bar{\bar{Y}}_1(\omega) = \left(\frac{\tilde{\omega}_f}{\omega_1}\right)^2 \cdot \frac{-\tilde{L}_1}{-\omega^2 \tilde{M}_1 + i\omega\{2\tilde{\xi}\,\tilde{M}_1\tilde{\omega}_1\} + \tilde{\omega}_1^2 \tilde{M}_1} \tag{7.47}$$

The natural vibration frequency $\tilde{\omega}_1$ of the equivalent SDF system approximates the fundamental resonant frequency of the dam on flexible foundation rock with impounded water [equation (7.38)]:

$$\tilde{\omega}_1 = \left[\frac{\tilde{\omega}_r}{\omega_1}\right]\left[\frac{\tilde{\omega}_f}{\omega_1}\right]\omega_1 \tag{7.48}$$

in which ω_1 is the fundamental natural vibration frequency of the dam on rigid foundation rock with an empty reservoir, and $\tilde{\omega}_r$ and $\tilde{\omega}_f$ are [equations (7.16) and (7.24)]:

$$\tilde{\omega}_r = \frac{\omega_1}{\sqrt{1 + \text{Re}[B_1(\tilde{\omega}_r)]/M_1}} \tag{7.49}$$

$$\tilde{\omega}_f = \frac{\omega_1}{\sqrt{1 + \text{Re}[F(\tilde{\omega}_f)]}} \tag{7.50}$$

The damping ratio $\tilde{\xi}$ of the equivalent SDF system is [equation (7.45)]:

$$\tilde{\xi} = \left[\frac{\tilde{\omega}_r}{\omega_1}\right]\left[\frac{\tilde{\omega}_f}{\omega_1}\right]^3 \xi_1 + \xi_r + \xi_f \tag{7.51}$$

in which ξ_r represents the added damping due to dam-water interaction and reservoir bottom absorption [equation (7.18)] and ξ_f represents the added damping due to dam-foundation rock interaction [equation (7.27)]:

$$\xi_r = -\frac{1}{2}\frac{1}{M_1}\left[\frac{\tilde{\omega}_r}{\omega_1}\right]^2 \text{Im}[B_1(\tilde{\omega}_r)] \tag{7.52}$$

$$\xi_f = -\frac{1}{2}\left[\frac{\tilde{\omega}_f}{\omega_1}\right]^2 \text{Im}[F(\tilde{\omega}_f)] \tag{7.53}$$

In equation (7.47), $\tilde{M}_1$ and $\tilde{L}_1$ are the generalized mass and generalized earthquake force including hydrodynamic effects [equation (7.14)]:

$$\tilde{M}_1 = M_1 + \text{Re}\left[\int_0^H \bar{p}_1(y,\tilde{\omega}_r)\,\phi_1^x(0,y)\,dy\right] \tag{7.54a}$$

$$\tilde{L}_1 = L_1 + \int_0^H \bar{p}_1(y,\tilde{\omega}_r)\,dy \tag{7.54b}$$

where $\bar{p}_1(y,\tilde{\omega}_r)$ is the frequency response function for hydrodynamic pressure on the upstream face due to acceleration of the dam in its fundamental mode of vibration, evaluated at an excitation frequency equal to $\tilde{\omega}_r$ [equation (7.8)]:

evaluated in the following steps:

1. Compute the natural fundamental vibration frequency ω_1 and vibration mode $\phi_1^K(x,y)$ of the dam on rigid foundation rock with an empty reservoir.

2. Compute the natural fundamental vibration frequency of the dam $\tilde{\omega}_1$, as modified by dam-water interaction and dam-foundation rock interaction, using equation (7.48) where $\tilde{\omega}_r$ and $\tilde{\omega}_f$, are computed iteratively from equations (7.49) and (7.50), or more conveniently from data presented in Figures 7.3 and 7.10, respectively.

3. For an estimated damping ratio ξ_1 for the dam concrete and constant hysteretic damping factor η_f for the foundation rock, evaluate the damping ratio $\tilde{\xi}$ from equation (7.51) where ξ_r and ξ_f, can be computed from equations (7.52) and (7.53), or more conveniently from data presented in Figures 7.4 and 7.11, respectively.

4. With the known mass density of the dam and the hydrodynamic pressure function $\bar{p}_1(y,\tilde{\omega}_r)$ computed from equation (7.55), the generalized mass $\tilde{M}_1$ and earthquake force $\tilde{L}_1$ can be evaluated from equation (7.54).

5. The maximum displacement of the dam over the duration of the earthquake is then given by equation (7.56) using the response spectrum for the earthquake ground motion.

In practice, $\phi_1^K(x,y)$ would be obtained in discrete form by analysis of a finite element idealization of the dam, and $\tilde{M}_1$ and $\tilde{L}_1$ would be computed by numerically evaluating equation (7.54).

For the special case of rigid foundation rock, $\tilde{\omega}_f = \omega_1$ resulting in $\tilde{\omega}_1 = \tilde{\omega}_r$ from equation (7.48), and $\xi_f = 0$ in equation (7.51). If the reservoir is empty, $\tilde{\omega}_r = \omega_1$ resulting in $\tilde{\omega}_1 = \tilde{\omega}_f$ from equation (7.48), $\xi_r = 0$ in equation (7.51), $\tilde{L}_1 = L_1$ and $\tilde{M}_1 = M_1$. If the reservoir impounds water, but the reservoir bottom materials are non-absorptive ($\alpha=1$), then ξ_r is zero.

The maximum effects of the earthquake ground motion can be represented by equivalent lateral forces acting horizontally on the dam. The equivalent lateral forces are obtained from the maximum deformation of the dam, given by equation (7.56) [7]:

$$f_1(x,y) = \frac{\tilde{L}_1}{\tilde{M}_1} \frac{S_a(\tilde{T}_1,\tilde{\xi})}{g} \tilde{w}_x(x,y)\,\phi_1^K(x,y) \qquad (7.57)$$

8. CONCLUSIONS

The available substructure method for the analysis of the linear response of concrete gravity dams to earthquake ground motion including the effects of dam-water-foundation rock interaction has been extended to consider the effects of the alluvium and sediments invariably present at the bottom of actual reservoirs. The interaction between the water and the reservoir bottom materials is approximately modelled by a boundary condition that permits partial absorption of hydrodynamic pressure waves at the reservoir bottom.

Utilizing this analytical procedure, the response of idealized concrete gravity dams to harmonic ground motion was presented in Chapters 3 and 5 for a wide range of system parameters. Based on the frequency response functions, it was shown that the partial absorption of hydrodynamic pressure waves into the alluvium and sediments at the reservoir bottom may have a significant effect on the dynamic response of dams. Specifically, the response results in these chapters lead to the following conclusions:

1. The unbounded resonant peaks in the frequency response function for hydrodynamic force on a rigid dam due to horizontal and vertical ground motion, characteristic of a rigid reservoir bottom, are eliminated by including reservoir bottom absorption. In general, the additional energy radiation through a wave absorptive reservoir bottom smoothes the frequency response functions for hydrodynamic force.

2. Reservoir bottom absorption primarily affects the dam response of dams on rigid foundation rock for excitation frequencies less than ω_1^r, where material damping in the dam concrete is the only damping mechanism present. At higher excitation frequencies the radiation of energy through upstream propagation of hydrodynamic pressure waves dominates the energy radiation into the absorptive reservoir bottom materials, essentially eliminating its effect. However, because of reservoir bottom absorption, the response to vertical ground motion at excitation frequencies equal to ω_n^r is bounded.

3. Dam-water interaction with an absorptive reservoir bottom ($\alpha < 1$) and rigid foundation rock reduces the fundamental resonant frequency of the dam to a value less than ω_1, but not as much as for a rigid reservoir bottom ($\alpha = 1$), where the fundamental resonant frequency is

179

Therefore, the compressibility of the impounded water should be considered in the earthquake analysis of concrete gravity dams.

Utilizing the general analytical procedure of Chapter 4, the earthquake response of Pine Flat Dam to Taft ground motion was presented in Chapter 6 for a range of properties of the reservoir bottom materials and various assumptions for the impounded water and foundation rock. These response results lead to the following conclusions:

1. The earthquake response of dams is increased by dam-water interaction and decreased by reservoir bottom absorption with the magnitude of these effects depending on the flexibility of the foundation rock and on the component of ground motion.

2. Both dam-water interaction and reservoir bottom absorption have profound effect on the response of dams to vertical ground motion irrespective of the foundation-rock condition; but relatively much less effect on the response of dams to horizontal ground motion, especially if foundation-rock flexibility is considered.

3. The significance of the response of dams to vertical ground motion was overestimated in earlier studies based on the assumption of a rigid reservoir bottom. An absorptive reservoir bottom that models the alluvium and sediments at the bottom of a reservoir gives a more realistic estimate of earthquake response, especially of the response to vertical ground motion and its significance in the total response of the dam.

The effects of reservoir bottom absorption, dam-water interaction and dam-foundation rock interaction on the response of a dam depend, in part, on the particular dam and earthquake ground motion, so that the conclusions deduced in Chapter 6 from the computed response of Pine Flat Dam to Taft ground motion would not apply in their entirety to all dams and ground motions. Whereas the detailed observations may be problem dependent, the broad conclusions should be valid for many cases.

The response results presented in this investigation, and the conclusions from previous work [4,11], have demonstrated that the response of concrete gravity dams to earthquake ground motion is affected by: interaction between the dam and impounded water, compressibility of the impounded water, interaction between the dam and flexible foundation rock, and the alluvium and sediments at the

--

REFERENCES

1. Bielak, J., "Modal Analysis for Building-Soil Interaction," *Journal of the Engineering Mechanics Division*, ASCE, Vol. 102, No. EM5, Oct., 1976, pp. 771-786.

2. Chakrabarti, P., and Chopra, A.K, "Hydrodynamic Pressures and Response of Gravity Dams to Vertical Earthquake Component," *Earthquake Engineering and Structural Dynamics*, Vol. 1, No. 4, Apr.-June, 1973, pp. 325-335.

3. Chakrabarti, P., and Chopra, A.K., "Earthquake Analysis of Gravity Dams Including Hydro-dynamic Interaction," *Earthquake Engineering and Structural Dynamics*, Vol. 2, No. 2, Oct.-Dec., 1973, pp. 143-160.

4. Chakrabarti, P., and Chopra, A.K., "Hydrodynamic Effects in Earthquake Response of Gravity Dams," *Journal of the Structural Division*, ASCE, Vol. 100, No. ST6, June, 1974, pp. 1211-1224.

5. Chopra, A.K., "Hydrodynamic Pressures on Dams During Earthquakes," *Journal of the Engineering Mechanics Division*, ASCE, Vol. 93, No. EM6, Dec., 1967, pp. 205-223.

6. Chopra, A.K., "Earthquake Behavior of Reservoir-Dam Systems," *Journal of the Engineering Mechanics Division*, ASCE, Vol. 94, No. EM6, Dec., 1968, pp. 1475-1500.

7. Chopra, A.K., "Earthquake Resistant Design of Concrete Gravity Dams," *Journal of the Structural Division*, ASCE, Vol 104, No. ST6, June, 1978, pp. 953-971.

8. Chopra, A.K., and Chakrabarti, P., "Earthquake Analysis of Concrete Gravity Dams Including Dam-Water-Foundation Rock Interaction," *Earthquake Engineering and Structural Dynamics*, Vol. 9, No. 4, July-Aug., 1981, pp. 363-383.

9. Chopra, A.K., Chakrabarti, P., and Gupta, S., "Earthquake Response of Concrete Gravity Dams Including Hydrodynamic and Foundation Interaction Effects," *Report No. UCB/EERC-80/01*, Earthquake Engineering Research Center, University of California, Berkeley, California, Jan., 1980.

20. Hatano, T., "An Examination of the Resonance of Hydrodynamic Pressure During Earthquakes Due to Elasticity of Water," *Technical Report C-65001*, Central Research Institute Electric Power Industry, Tokyo, Japan, Nov., 1965.

21. Jennings, P.C., and Bielak, J., "Dynamics of Building-Soil Interaction," *Bulletin of the Seismological Society of America*, Vol. 63, No. 1, Feb., 1973, pp. 9-48.

22. Nakagawa, T., and Hatano, T., "Analytical Solution of Hydrodynamic Pressure with Reflective Condition at Reservoir Bottom During Earthquakes," *Proceedings of the Japan Society of Civil Engineers*, No. 229, Sept., 1974, pp. 119-125.

23. Pal, N., "Seismic Cracking of Concrete Gravity Dams," *Journal of the Structural Division*, ASCE, Vol. 102, No. ST9, Sept., 1976, pp. 1827-1844.

24. Rea, D., Liaw, C.Y., and Chopra, A.K, "Mathematical Models for the Dynamic Analysis of Concrete Gravity Dams," *Earthquake Engineering and Structural Dynamics*, Vol. 3, No. 3, Jan.-Mar., 1975, pp. 249-258.

25. Rosenblueth, E., "Presión Hidrodinámica en Presas Debida à al Aceleración Vertical con Refracción en el Fondo," presented at the 1968, 2nd Congreso Nacional de Ingeniería Sismica, held at Veracruz, Mexico.

26. Shul'man, S.G., "Hydrodynamic Pressure on a Dam Due to Earthquakes Under Conditions of Resonance," *Izvestiya Vsesoyuznogo Nauchno-Issledovatel'skogo Instituta Gidrotekhniki*, Vol. 91, 1969, pp. 108-112.

27. Taylor, R.L., Beresford, P.J., and Wilson, E.L., "A Non-Conforming Element for Stress Analysis," *International Journal for Numerical Methods in Engineering*, Vol. 10, No. 6, 1976, pp. 1211-1219.

28. Veletsos, A.S., "Dynamics of Structure-Foundation Systems," in *Structural and Geotechnical Mechanics*, ed. by W.J. Hall, Prentice-Hall, Clifton, New Jersey, 1977.

$a_g^l(t)$	l-component of free-field ground acceleration
$A_g^l(\omega)$	Fourier transform of $a_g^l(t)$; defined in equation (4.43)
b	breadth of the dam base
$B_0^l(\omega)$	added hydrodynamic force due to l-component of ground motion
$B_1(\omega)$	added hydrodynamic mass (real-valued component) and damping (imaginary-valued component) due to fundamental vibration mode of dam
$B_{00}, B_{0\theta}$	hydrodynamic terms defined in equation (7.29a)
$B_{\theta\theta}, B_{\theta 1}$	hydrodynamic terms defined in equation (7.29b)
$\mathbf{c}_c$	damping matrix for the finite element system
C	velocity of pressure waves in water
C_1	$= 2M_1 \xi_1 \omega_1$
$\tilde{C}_1$	defined in equation (7.15b)
C_f	$= \sqrt{E_f/\rho_f}$
C_r	$= \sqrt{E_r/\rho_r}$
C_s	$= \sqrt{E_s/\rho_s}$
$C(\omega)$	compliance function for the reservoir bottom materials, equation (4.29)
d	duration of free-field ground motion
E_f	Young's modulus of elasticity of the foundation rock
E_r	Young's modulus of elasticity of the reservoir bottom materials

$\tilde{L}_1$ defined in equation (7.15c)

$\mathbf{L}'(\omega)$ vector whose elements are defined in equation (4.18b)

L_1^θ, L_θ^x integrals defined after equation (7.19)

$\tilde{\mathbf{L}}'(\omega)$ vector whose elements are defined in equation (4.41b)

$m(x,y)$ mass density of dam concrete

$m_a(y)$ "added mass" of dam due to hydrodynamic effects; defined in equation (7.59)

$\bar{m}_k(x,y)$ mass density of equivalent SDF system, $k=x,y$; defined in equation (7.10)

m_t total mass of the dam defined after equation (7.19)

m_1^* $=(L_1)^2/M_1$, effective mass of a dam in its fundamental vibration mode

$\mathbf{m}, \mathbf{m}_b,$ submatrices of $\mathbf{m}_c$

$\mathbf{m}_c$ mass matrix for the finite element system

$M(t)$ moment at rigid base of the dam due to dam-foundation rock interaction

M_1 generalized mass of the dam in the fundamental vibration mode

$\tilde{M}_1$ generalized mass of the equivalent SDF system defined in equation (7.15a)

N number of nodal points above the base

N_b number of nodal points at the base

N_w number of vibration modes of the impounded water included in the hydrodynamic terms

$p(x,y,t)$ hydrodynamic pressure in the impounded water

$\bar{p}^l(x,y,\omega)$ frequency response function for $p(x,y,t)$ due to the l-component of ground motion

$\bar{p}_0^l(x,y,\omega)$ frequency response function for hydrodynamic pressure with a rigid dam due to l-component of ground motion

$\overline{\mathbf{r}}_f(\omega)$ — vector of frequency response functions for displacements of nodal points at the surface of the foundation rock underlying the dam

$\mathbf{r}_p(t)$ — vector of nodal displacements for finite element p

$\overline{\mathbf{R}}_0^l(\omega)$ — vector of nodal forces at the upstream face of the dam statically equivalent to $\overline{p}_0^l(0,y,\omega)$

$\mathbf{R}_b(t)$ — vector of forces at the base of the dam due to dam-foundation rock interaction

$\overline{\mathbf{R}}_b^l(\omega)$ — vector of frequency response functions for $\mathbf{R}_b(t)$ due to the l-component of ground motion

$\mathbf{R}_c(t)$ — vector containing hydrodynamic forces $\mathbf{R}_h(t)$ and dam-foundation rock interaction forces $\mathbf{R}_b(t)$

$\overline{\mathbf{R}}_c^l(\omega)$ — vector of frequency response functions for $\mathbf{R}_c(t)$ due to the l-component of ground motion

$\overline{\mathbf{R}}_f(\omega)$ — vector of frequency response functions for forces at the surface of the foundation rock underlying the dam

$\mathbf{R}_h(t)$ — vector of hydrodynamic forces at the upstream face of the dam

$\overline{\mathbf{R}}_h^l(\omega)$ — vector of frequency response functions for $\mathbf{R}_h(t)$ due to the l-component of ground motion

$\overline{\mathbf{R}}_j^h(\omega)$ — vector of nodal forces at the upstream face of the dam statically equivalent to $\overline{p}_j^h(0,y,\omega)$

$\overline{\mathbf{R}}_j^l(\omega)$ — vector of nodal forces at the upstream face of the dam statically equivalent to $\overline{p}_j^l(0,y,\omega)$

$\underline{S}(\omega)$ — matrix defined in equation (4.3)

$\underline{S}_f(\omega)$ — dynamic stiffness matrix for the foundation rock region; defined in equation (4.5b)

$\underline{\tilde{S}}_f(\omega)$ — matrix defined in equation (4.14)

$\underline{S}_{rr,rq,qq}$ — submatrices of $\underline{S}(\omega)$

$\mathbf{S}(\omega)$ — matrix whose elements are defined in equation (4.18a)

λ_n — vibration frequency for the nth mode of the associated dam-foundation rock system

$\mu_n(\omega)$ — eigenvalue for n^{th} natural vibration mode of the impounded water; defined in equation (3.20)

ξ_1 — viscous damping ratio of the dam (without water) in its fundamental vibration mode

$\tilde{\xi}$ — damping ratio of the equivalent SDF system; equation (7.40)

ξ_f — added damping ratio due to dam-foundation rock interaction; equation (7.27)

$\xi_f(\tilde{\omega})$ — added damping ratio defined in equation (7.42)

$\tilde{\xi}_f$ — damping ratio defined in equation (7.26)

ξ_r — added damping ratio due to dam-water interaction and reservoir bottom absorption; equation (7.18)

$\xi_r(\tilde{\omega})$ — added damping ratio defined in equation (7.41)

$\tilde{\xi}_r$ — damping ratio defined in equation (7.17)

ρ — density of water

ρ_f — density of the foundation rock

ρ_r — density of the reservoir bottom materials

ρ_s — density of the dam concrete

$\sigma_p(t)$ — vector of planar stress components in finite element p

$\Upsilon_n(y,\omega)$ — eigenfunction for n^{th} natural vibration mode of the impounded water; defined in equation (3.21)

$\phi_1^k(x,y)$ — fundamental natural vibration mode of the dam without water; $k = x,y$ denotes x- and y-components of modal displacements, respectively

χ_n — vector defined in equation (4.16)

APPENDIX A: BOUNDARY CONDITION AT THE RESERVOIR BOTTOM

The boundary condition at the reservoir bottom relates the hydrodynamic pressure to the sum of the vertical component of free-field ground acceleration and the acceleration due to interaction between the impounded water and the reservoir bottom materials. Because of the approximation that hydrodynamic pressure waves incident on the reservoir bottom only excite vertically propagating dilatational waves in the reservoir bottom materials, it is sufficient to consider only interaction in the y-direction. The hydrodynamic pressure $p(y,t)$ in the water is governed by the one-dimensional wave equation:

$$\frac{\partial^2 p}{\partial y^2} = \frac{1}{C^2} \frac{\partial^2 p}{\partial t^2}, \qquad y \geqslant 0 \tag{A.1}$$

Similarly, the interaction displacement $v(y,t)$ in the layer of reservoir bottom materials is governed by

$$\frac{\partial^2 v}{\partial y^2} = \frac{1}{C_r^2} \frac{\partial^2 v}{\partial t^2}, \qquad y \leqslant 0 \tag{A.2}$$

where $C_r = \sqrt{E_r/\rho_r}$, E_r is the Young's modulus of elasticity and ρ_r is the density of the reservoir bottom materials. At the reservoir bottom, the acceleration boundary condition states that the normal pressure gradient is proportional to the total acceleration:

$$\frac{\partial p}{\partial y}(0,t) = -\rho \left[a_g^y(t) \delta_{yl} + \ddot{v}(0,t) \right], \qquad l=x,y \tag{A.3}$$

where the term $a_g^y(t) \delta_{yl}$ is the vertical component of free-field ground acceleration and $\ddot{v}(0,t)$ is the acceleration of the reservoir bottom due to interaction between the impounded water and and the reservoir bottom materials. Equilibrium at the surface of the reservoir bottom materials requires that:

$$p(0,t) = -E_r \frac{\partial v}{\partial y}(0,t) \tag{A.4}$$

The D'Alembert solution to equation (A.2) is $v = g_r(y + C_r t)$ where g_r is the waveform of the refracted wave propagating vertically downward in the reservoir bottom materials. An upward propagating wave does not exist because of the radiation condition for the assumed infinitely thick layer of reservoir bottom materials. Note that $\frac{\partial v}{\partial y}(0,t) = g_r'(C_r t)$ and $\ddot{v}(0,t) = C_r^2 g_r''(C_r t)$, where the prime indicates the derivative of g_r with respect to the argument $(y + C_r t)$. Differentiating equation (A.4)

APPENDIX B: FREQUENCY RESPONSE FUNCTIONS FOR HYDRODYNAMIC PRESSURE

The frequency response functions $\bar{p}_0^x(x,y,\omega)$, $\bar{p}_0^y(x,y,\omega)$, $\bar{p}_1(x,y,\omega)$ and $\bar{p}_j^f(x,y,\omega)$ for hydrodynamic pressure in the water are solutions of the Helmholtz equation, equation (3.13), subject to the boundary conditions in equations (3.15), (3.16), (3.17) and (4.34), respectively. Because of the rectangular fluid domain and particular form of the boundary conditions, the four boundary value problems can be solved by separation of variables, where:

$$\bar{p}(x,y,\omega) = \bar{p}_x(x,\omega)\,\bar{p}_y(y,\omega) \tag{B.1}$$

The substitution of equation (B.1) into equation (3.13) and subsequent separation gives the equation for the y-direction:

$$\frac{d^2\bar{p}_y}{dy^2} + \mu^2\bar{p}_y = 0 \tag{B.2}$$

and for the x-direction:

$$\frac{d^2\bar{p}_x}{dx^2} - \kappa^2\bar{p}_x = 0 \tag{B.3}$$

where $\kappa^2 = (\mu^2 - \omega^2/C^2)$ and μ is a constant to be determined. The general solution of equation (B.2) is:

$$\bar{p}_y(y,\omega) = A(\omega)e^{i\mu y} + B(\omega)e^{-i\mu y} \tag{B.4}$$

and the general solution of equation (B.3) is:

$$\bar{p}_x(x,\omega) = C(\omega)e^{\kappa x} + D(\omega)e^{-\kappa x} \tag{B.5}$$

The radiation condition in the upstream direction (negative x-direction) is satisfied by $D(\omega) = 0$. The solutions for the four frequency response functions for hydrodynamic pressure are obtained by determining the coefficients $A(\omega)$, $B(\omega)$ and $C(\omega)$ that satisfy their respective boundary conditions.

197

The coefficients $C_n(\omega)$ that allow $\bar{p}(x,y,\omega)$ to satisfy the boundary condition at the upstream face are determined by substitution of equation (B.9) into the first boundary condition of equation (3.17):

$$\frac{\partial \bar{p}}{\partial x}(0,y,\omega) = -\rho f(y)$$

where $f(y) = \phi_1^x(0,y)$ for this case, gives

$$\sum_{n=1}^{\infty} C_n(\omega) \kappa_n Y_n(y,\omega) = -\rho \phi_1^x(0,y)$$

Multiplication of both sides of the above equation by $Y_j(y,\omega)$, integration over the depth of the water, and use of the orthogonality condition in equation (B.8) gives

$$C_n(\omega) = -2\rho H \frac{\mu_n^2(\omega)}{H[\mu_n^2(\omega) - (\omega q)^2] + i(\omega q)} \frac{I_{1n}(\omega)}{\kappa_n} \qquad (B.10)$$

where $I_{1n}(\omega)$ is defined in equation (3.19b). Substitution of equations (B.10) into equation (B.9) gives the frequency response function for hydrodynamic pressure in the impounded water due to horizontal acceleration of the dam in its fundamental vibration mode:

$$\bar{p}_1(x,y,\omega) = -2\rho H \sum_{n=1}^{\infty} \frac{\mu_n^2(\omega)}{H[\mu_n^2(\omega) - (\omega q)^2] + i(\omega q)} \frac{I_{1n}(\omega)}{\kappa_n} e^{\kappa_n x} Y_n(y,\omega) \qquad (B.11)$$

which gives equation (3.18c) if evaluated at $x=0$.

B.2 Solutions for $\bar{p}_0^x(x,y,\omega)$ and $\bar{p}_j^f(x,y,\omega)$

The frequency response functions $\bar{p}_0^x(x,y,\omega)$ and $\bar{p}_1(x,y,\omega)$ are similar because they are frequency response functions for hydrodynamic pressure due to horizontal acceleration of the dam. Repeating the steps in equations (B.6) to (B.11) with $f(y) = 1$ results in $\bar{p}_0^x(0,y,\omega)$ as given in equation (3.18a) and $I_{0n}(\omega)$ as defined in equation (3.19a).

The frequency response functions $\bar{p}_j^f(x,y,\omega)$ is similar to $\bar{p}_1(x,y,\omega)$, except that it is due to horizontal acceleration $\psi_j(y)$ of the dam that corresponds to the jth Ritz vector of the associated dam-foundation rock system. Repeating the steps in equations (B.6) to (B.11) with $f(y) = \psi_j(y)$ results in $\bar{p}_j^f(0,y,\omega)$ as given in equation (4.36c) and $I_{jn}(\omega)$ as defined in equation (4.37b).

APPENDIX C: HYDRODYNAMIC PRESSURE WITH RIGID RESERVOIR BOTTOM

The frequency response functions for hydrodynamic pressure in impounded water with rigid reservoir bottom can be obtained from equations (3.18) to (3.21) by setting the damping coefficient q for the reservoir bottom materials equal to zero. From equation (3.20), $e^{2i\mu_n(\omega)H} = -1$, which, by Euler's identity, is equivalent to $\cos 2\mu_n(\omega)H = -1$ and $\sin 2\mu_n(\omega)H = 0$. Consequently, the eigenvalues of the impounded water with rigid reservoir bottom are real-valued and given by

$$\mu_n(\omega) = \mu_n = \frac{2n-1}{2}\frac{\pi}{H}.$$

The natural vibration frequencies of the impounded water are: $\omega_n^r = \mu_n C$. The eigenfunctions of the impounded water for $q=0$ are, from equation (3.21), $Y_n(y,\omega) = \frac{1}{2}[e^{i\mu_n(\omega)y} + e^{-i\mu_n(\omega)y}]$, or: $Y_n(y,\omega) = \cos\mu_n y$.

The frequency response functions for hydrodynamic pressure are given by equation (3.18) using $q=0$ and $Y_n(y,\omega)$ defined above:

$$\bar{p}_0^x(x,y,\omega) = -2\rho \sum_{n=1}^{\infty} \frac{I_{0n}}{\kappa_n} e^{\kappa_n x} \cos\mu_n y$$

$$\bar{p}_0^y(x,y,\omega) = \frac{\rho C}{\omega} \frac{1}{\cos\dfrac{\omega H}{C}} \sin\frac{\omega(H-y)}{C}$$

$$\bar{p}_1(x,y,\omega) = -2\rho \sum_{n=1}^{\infty} \frac{I_{1n}}{\kappa_n} e^{\kappa_n x} \cos\mu_n y$$

where $\kappa_n = \sqrt{\mu_n^2 - \omega^2/C^2}$, and equation (3.19) reduces to:

$$I_{0n} = \frac{1}{H}\int_0^H \cos\mu_n y\, dy = -\frac{2}{\pi}\frac{(-1)^n}{2n-1}$$

$$I_{1n} = \frac{1}{H}\int_0^H \phi_f^x(0,y) \cos\mu_n y\, dy$$

These results for a rigid reservoir bottom were presented in references 2,3 and 25.

201

The vector $\ddot{\mathbf{r}}^t$ of total accelerations can be represented as:

$$\ddot{\mathbf{r}}^t = a_g(t)\underline{1} + \ddot{u}_0(t)\underline{1} + \ddot{\theta}(t)\underline{\epsilon}^\theta + \ddot{\mathbf{r}} \tag{D.2}$$

in which $a_g(t)$ is the horizontal component of free-field ground acceleration; $u_0(t)$ is the horizontal translation of the dam base relative to the free-field ground motion; and $\theta(t)$ is the rotation of the base about its centroid.

The fundamental mode response of the dam can be determined by expressing the displacements relative to the rigid base as:

$$\mathbf{r} = Y_1(t)\boldsymbol{\phi}_1 \tag{D.3}$$

where $\boldsymbol{\phi}_1$ is the fundamental vibration mode of the dam on a rigid base and $Y_1(t)$ is the generalized coordinate corresponding to that mode. The fundamental vibration mode of the dam is the solution of the eigenvalue problem: $\mathbf{k}\boldsymbol{\phi}_1 = \omega_1^2 \mathbf{m}\boldsymbol{\phi}_1$, where ω_1 is the fundamental natural vibration frequency of the dam on rigid base with an empty reservoir.

The substitution of equations (D.2) and (D.3) into (D.1), premultiplication of equation (D.1a) by $\boldsymbol{\phi}_1^T$, use of the orthogonality properties of $\boldsymbol{\phi}_1$ with respect to $\mathbf{m}$ and $\mathbf{k}$, and the assumption of viscous damping in the dam gives:

$$M_1 \ddot{Y}_1(t) + C_1 \dot{Y}_1(t) + K_1 Y_1(t) + L_1 \ddot{u}_0(t) + L_1^\theta \ddot{\theta}(t) = -L_1 a_g(t) + \boldsymbol{\phi}_1^T \mathbf{R}(t) \tag{D.4a}$$

$$L_1 \ddot{Y}_1(t) + m_t \ddot{u}_0(t) + L_\theta^x \ddot{\theta}(t) + V(t) = -m_t a_g(t) + \{\underline{1}\}^T \mathbf{R}(t) \tag{D.4b}$$

$$L_1^\theta \ddot{Y}_t(t) + L_\theta^x \ddot{u}_0(t) + I_t \ddot{\theta}(t) + M(t) = -L_\theta^x a_g(t) + \{\underline{\epsilon}^\theta\}^T \mathbf{R}(t) \tag{D.4c}$$

where $M_1 = \boldsymbol{\phi}_1^T \mathbf{m}\boldsymbol{\phi}_1$ is the generalized mass; $m_t = \{\underline{1}\}^T \mathbf{m}\underline{1}$ and $I_t = \{\underline{\epsilon}^\theta\}^T \mathbf{m}\underline{\epsilon}^\theta$ are the total mass of the dam and mass moment of inertia of the dam about the centroid of its base, respectively; $L_\theta^x = \{\underline{\epsilon}^\theta\}^T \mathbf{m}\underline{1}$, $L_1 = \boldsymbol{\phi}_1^T \mathbf{m}\underline{1}$, $L_1^\theta = \boldsymbol{\phi}_1^T \mathbf{m}\underline{\epsilon}^\theta$; $K_1 = \omega_1^2 M_1$; $C_1 = 2M_1\xi_1\omega_1$; and ξ_1 is the fraction of critical damping for the fundamental vibration mode. If the reservoir is empty, the vector $\mathbf{R}(t)$ of hydrodynamic forces is zero and equation (D.4) reduces to equation (7.19).

For harmonic horizontal ground acceleration $a_g(t) = e^{i\omega t}$, the displacements and forces can be represented in terms of their complex-valued frequency response functions: $Y_1(t) = \bar{Y}_1(\omega) e^{i\omega t}$,

of absorptive reservoir bottom materials, is:

$$[\frac{\partial}{\partial y} - i\omega q]\,\bar{p}(x,0,\omega) = 0 \tag{D.8}$$

where $q = \rho/\rho_r C_r$ as defined in Chapters 3 and 4. The boundary condition at the free surface is:

$$\bar{p}(x,H,\omega) = 0 \tag{D.9}$$

where H is the depth of the impounded water.

The linear form of equation (3.13) for hydrodynamic pressure, and the linear form of the above boundary conditions, allows $\bar{p}(x,y,\omega)$ to be expressed as:

$$\bar{p}(x,y,\omega) = \bar{p}_0(x,y,\omega) + \bar{p}_0(x,y,\omega)\bar{\ddot{u}}_0(\omega) + \bar{p}_0^{\theta}(x,y,\omega)\bar{\ddot{\theta}}(\omega) + \bar{p}_1(x,y,\omega)\bar{\ddot{Y}}_1(\omega) \tag{D.10}$$

The expressions for the frequency response functions for the various hydrodynamic terms are given in Chapters 3 and 7, as derived in Appendix B. The frequency response function $\bar{p}_0(x,y,\omega)$ for hydrodynamic pressure due to the horizontal component of ground motion of a rigid dam is given in equations (3.18a); the frequency response function $\bar{p}_1(x,y,\omega)$ for hydrodynamic pressure due to the horizontal acceleration $\phi_1^x(0,y)$ of the upstream face of the dam in its fundamental vibration mode is given in equation (3.18c); and the frequency response function $\bar{p}_0^{\theta}(x,y,\omega)$ for hydrodynamic pressure with a rigid dam rotating about the centroid of its base is given by equation (7.30).

The vector $\mathbf{R}(\omega)$ of frequency response functions for the hydrodynamic forces on the upstream face of the dam are, from equation (D.10):

$$\mathbf{R}(\omega) = \bar{\mathbf{R}}_0(\omega) + \bar{\ddot{u}}_0(\omega)\,\bar{\mathbf{R}}_0(\omega) + \bar{\ddot{\theta}}(\omega)\,\bar{\mathbf{R}}_0^{\theta}(\omega) + \bar{\ddot{Y}}_1(\omega)\,\bar{\mathbf{R}}_1(\omega) \tag{D.11}$$

in which the x-DOF elements of $\bar{\mathbf{R}}_0(\omega)$, $\bar{\mathbf{R}}_0^{\theta}(\omega)$ and $\bar{\mathbf{R}}_1(\omega)$ for the upstream face nodal points are the nodal forces statically equivalent to the corresponding pressure functions at the upstream face of the dam: $\bar{p}_0(0,y,\omega)$, $\bar{p}_0^{\theta}(0,y,\omega)$ and $\bar{p}_1(0,y,\omega)$, respectively. The y-DOF elements of the hydrodynamic force vectors are zero.

APPENDIX E: SOLUTION FOR FUNDAMENTAL MODE RESPONSE OF DAMS

The frequency domain equations for the fundamental mode response of dams on flexible foundation rock with impounded water are given by equation (D.12). The three-by-three system of complex-valued equations can be solved for $\bar{Y}_1(\omega)$, the frequency response function for the modal coordinate corresponding to the fundamental mode of vibration of the dam.

However, equation (D.12) contains three terms, m_t, I_t and L_θ^x that represent the inertial forces on the dam due the rigid-body motion allowed by foundation-rock flexibility, which complicate the solution for $\bar{Y}_1(\omega)$. It can shown from numerical results that the dam response is accurately represented by assuming that the mass terms m_t, I_t and L_θ^x are approximated by the contributions from only the fundamental vibration mode:

$$m_t \approx m_1^*$$

$$L_\theta^x \approx m_1^* h_1^* \tag{E.1}$$

$$I_t \approx m_1^* (h_1^*)^2$$

in which $m_1^* = (L_1)^2 / M_1$ and $h_1^* = L_1^\theta / L_1$ are the effective mass and effective height, respectively, of the dam in its fundamental mode of vibration [28]. The substitution of equation (E.1) into equation (D.12) and appropriate factorization gives a convenient non-dimensional form of the frequency domain equations:

$$
\begin{bmatrix}
-\beta^2 + i(2\xi_1\beta) + 1 - \beta^2 B_1(\omega)/M_1 & -\beta^2 \left[1 + B_0(\omega)/L_1\right] \\[2ex]
-\beta^2 \left[1 + B_0(\omega)/L_1\right] & -\beta^2 \left[1 + \dfrac{B_{00}(\omega)}{m_1^*}\right] + \dfrac{K_{VV}(\omega)}{m_1^* \omega_1^2} \\[2ex]
-\beta^2 \left[1 + B_{\theta 1}(\omega)/L_1^\theta\right] & -\beta^2 \left[1 + \dfrac{B_{0\theta}(\omega)}{m_1^* h_1^*}\right] + \dfrac{K_{MV}(\omega)}{m_1^* \omega_1^2} \left[\dfrac{b}{h_1^*}\right]
\end{bmatrix}
$$

$$
\begin{array}{c}
-\beta^2 \left[1 + B_{\theta 1}(\omega)/L_1^\theta\right] \\[2ex]
-\beta^2 \left[1 + \dfrac{B_{0\theta}(\omega)}{m_1^* h_1^*}\right] + \dfrac{K_{VM}(\omega)}{m_1^* \omega_1^2} \left[\dfrac{b}{h_1^*}\right] \\[2ex]
-\beta^2 \left[1 + \dfrac{B_{\theta\theta}(\omega)}{m_1^* (h_1^*)^2}\right] + \dfrac{K_{MM}(\omega)}{m_1^* \omega_1^2} \left[\dfrac{b}{h_1^*}\right]^2
\end{array}
\left\{
\begin{array}{c}
\dfrac{M_1}{L_1} \bar{Y}_1(\omega) \\[2ex]
\bar{u}_0(\omega) \\[2ex]
\bar{\theta}(\omega) h_1^*
\end{array}
\right\}
= -\dfrac{1}{\omega_1^2}
\left\{
\begin{array}{c}
1 + B_0(\omega)/L_1 \\[2ex]
1 + B_{00}(\omega)/m_1^* \\[2ex]
1 + B_{0\theta}(\omega)/m_1^* h_1^*
\end{array}
\right\}
\tag{E.2}
$$

in which $\beta = \omega/\omega_1$.

involve differences in hydrodynamic terms that are small; and (b) they are associated with higher-order excitation frequencies, β^2 and β^4, respectively. Neglecting the terms $G_1(\omega)$ and $G_2(\omega)$ in equation (E.3) results in equation (7.32), where $F(\omega)$ is defined in equation (7.23) and $F_r(\omega)$ is defined in equation (7.33).

$$\tilde{\omega}_1 = \omega_1 \left(\frac{1}{\sqrt{1+\text{Re}[B_1(\tilde{\omega}_1)]/M_1}} \right) \cdot \left(\frac{1}{\sqrt{1+\text{Re}[F(\tilde{\omega}_1)]}} \right) \tag{F.3}$$

Because $F(\omega)$ is a slowly-varying, smooth function of excitation frequency, as is $\text{Re}[B_1(\omega)]$ if the reservoir bottom materials are significantly absorptive, the foundation-rock flexibility term $\text{Re}[F(\omega)]$ may be evaluated at $\tilde{\omega}_f$, and the added hydrodynamic mass $\text{Re}[B_1(\omega)]$ may be evaluated with sufficient accuracy at $\tilde{\omega}_r$. Consequently, the natural vibration frequency $\tilde{\omega}_1$ from equation (F.3) is:

$$\tilde{\omega}_1 = \omega_1 \left(\frac{1}{\sqrt{1+\text{Re}[B_1(\tilde{\omega}_r)]/M_1}} \right) \cdot \left(\frac{1}{\sqrt{1+\text{Re}[F(\tilde{\omega}_f)]}} \right) \tag{F.4}$$

The natural vibration frequencies $\tilde{\omega}_r$ and $\tilde{\omega}_f$, for dams on rigid foundation rock and dams with empty reservoirs, respectively, are:

$$\frac{\tilde{\omega}_r}{\omega_1} = \frac{1}{\sqrt{1+\text{Re}[B_1(\tilde{\omega}_r)]/M_1}} \tag{F.5a}$$

$$\frac{\tilde{\omega}_f}{\omega_1} = \frac{1}{\sqrt{1+\text{Re}[F(\tilde{\omega}_f)]}} \tag{F.5b}$$

Substitution of equation (F.5) into equation (F.4) gives equation (7.38).

The frequency response function $\overline{\overline{Y}}_1(\omega)$ for the equivalent SDF system can be obtained from the frequency response function $\overline{Y}_1(\omega)$ for the fundamental mode response of the dam, equation (F.1). Evaluating the frequency-dependent terms at excitation frequency $\tilde{\omega}_1$, using equations (F.2) to (F.5) for the real-valued terms in the denominator of equation (F.1), and grouping the imaginary-valued terms gives the frequency response function $\overline{\overline{Y}}_1(\omega)$ for the equivalent SDF system:

$$\overline{\overline{Y}}_1(\omega) = \frac{-\tilde{L}_1}{-\omega^2 \left[\frac{\omega_1}{\tilde{\omega}_r} \right]^2 \left[\frac{\omega_1}{\tilde{\omega}_f} \right]^2 + \omega_1^2 M_1 + i\omega\Xi} \tag{F.6}$$

where $\tilde{L}_1 = L_1 + B_0(\tilde{\omega}_1)$ is the generalized earthquake force, and Ξ contains the imaginary-valued terms in the denominator of equation (F.1). Multiplying numerator and denominator of equation (F.6) by $(\tilde{\omega}_f/\omega_1)^2$, using equation (7.38) and recognizing that $\omega_1^2 M_1 = \tilde{\omega}_r^2 \tilde{M}_1$, where $\tilde{M}_1 = M_1 + \text{Re}[B_1(\tilde{\omega}_r)]$, results in:

$$\xi_r(\tilde{\omega}_1) = -\frac{1}{2}\frac{1}{M_1}\left[\frac{\tilde{\omega}_1}{\omega_1}\right]^2 \text{Im}[B_1(\tilde{\omega}_1)] \tag{F.11}$$

and $\xi_f(\tilde{\omega}_1)$ is the added damping ratio due to dam-foundation rock interaction, defined as:

$$\xi_f(\tilde{\omega}_1) = -\frac{1}{2}\left[\frac{\tilde{\omega}_1}{\omega_1}\right]^2 \text{Im}[F(\tilde{\omega}_1)] \tag{F.12}$$

Substituting the following identities:

$$\text{Im}[FB_1] = \text{Re}[F]\text{Im}[B_1] + \text{Im}[F]\text{Re}[B_1]$$

$$\text{Re}[FB_1] = \text{Re}[F]\text{Re}[B_1] - \text{Im}[F]\text{Im}[B_1]$$

into equation (F.10), and using the definitions in equations (F.11) and (F.12) again, gives:

$$\tilde{\xi} = \left[\frac{\tilde{\omega}_1}{\omega_1}\right]\xi_1 + \xi_r(\tilde{\omega}_1) + \xi_f(\tilde{\omega}_1) + \xi_r(\tilde{\omega}_1)\text{Re}[F] + \xi_f(\tilde{\omega}_1)\text{Re}[B_1]/M_1$$

$$- \left[\frac{\tilde{\omega}_1}{\omega_1}\right]^3 \xi_1\text{Re}[F] - \left[\frac{\tilde{\omega}_1}{\omega_1}\right]^3 \xi_1\text{Re}[F]\text{Re}[B_1]/M_1 \tag{F.13}$$

after neglecting the term $\text{Im}[F]\text{Im}[B_1]$ because it introduces a third-order damping term into $\tilde{\xi}$. The terms $\text{Re}[B_1]$ and $\text{Re}[F]$ are obtained from the approximations in equation (F.4) and the definitions in equation (F.5):

$$\text{Re}[B_1]/M_1 \approx \text{Re}[B_1(\tilde{\omega}_r)]/M_1 = \left[\frac{\omega_1}{\tilde{\omega}_r}\right]^2 - 1$$

$$\text{Re}[F] \approx \text{Re}[F(\tilde{\omega}_f)] = \left[\frac{\omega_1}{\tilde{\omega}_f}\right]^2 - 1$$

which upon substitution into equation (F.13) and grouping of damping terms gives the damping ratio $\tilde{\xi}$ of the equivalent SDF system:

$$\tilde{\xi} = \left[\frac{\tilde{\omega}_r}{\omega_1}\right]\left[\frac{\tilde{\omega}_f}{\omega_1}\right]^3 \xi_1 + \frac{1}{(\tilde{\omega}_f/\omega_1)^2}\xi_r(\tilde{\omega}_1) + \frac{1}{(\tilde{\omega}_r/\omega_1)^2}\xi_f(\tilde{\omega}_1) \tag{F.14}$$

Equation (F.14) was presented in Chapter 7 as equation (7.40).

NOTE: Numbers in parentheses are Accession Numbers assigned by the National Technical Information Service; these are followed by a price code. Copies of the reports may be ordered from the National Technical Information Service, 5285 Port Royal Road, Springfield, Virginia, 22161. Accession Numbers should be quoted on orders for reports (PB --- ---) and remittance must accompany each order. Reports without this information were not available at time of printing. Upon request, EERC will mail inquirers this information when it becomes available.

EERC 67-1 "Feasibility Study Large-Scale Earthquake Simulator Facility," by J. Penzien, J.G. Bouwkamp, R.W. Clough and D. Rea - 1967 (PB 187 905)A07

EERC 68-1 Unassigned

NA EERC 68-2 "Inelastic Behavior of Beam-to-Column Subassemblages Under Repeated Loading," by V.V. Bertero - 1968 (PB 184 888)A05

EERC 68-3 "A Graphical Method for Solving the Wave Reflection-Refraction Problem," by H.D. McNiven and Y. Mengi - 1968 (PB 187 943)A03

EERC 68-4 "Dynamic Properties of McKinley School Buildings," by D. Rea, J.G. Bouwkamp and R.W. Clough - 1968 (PB 187 902)A07

NA EERC 68-5 "Characteristics of Rock Motions During Earthquakes," by H.B. Seed, I.M. Idriss and F.W. Kiefer - 1968 (PB 188 338)A03

NA EERC 69-1 "Earthquake Engineering Research at Berkeley," - 1969 (PB 187 906)A11

NA EERC 69-2 "Nonlinear Seismic Response of Earth Structures," by M. Dibaj and J. Penzien - 1969 (PB 187 904)A08

NA EERC 69-3 "Probabilistic Study of the Behavior of Structures During Earthquakes," by R. Ruiz and J. Penzien - 1969 (PB 187 886)A06

EERC 69-4 "Numerical Solution of Boundary Value Problems in Structural Mechanics by Reduction to an Initial Value Formulation," by N. Distefano and J. Schujman - 1969 (PB 187 942)A02

EERC 69-5 "Dynamic Programming and the Solution of the Biharmonic Equation," by N. Distefano - 1969 (PB 187 941)A03

EERC 69-6 "Stochastic Analysis of Offshore Tower Structures," by A.K. Malhotra and J. Penzien - 1969 (PB 187 903)A09

NA EERC 69-7 "Rock Motion Accelerograms for High Magnitude Earthquakes," by H.B. Seed and I.M. Idriss - 1969 (PB 187 940)A02

EERC 69-8 "Structural Dynamics Testing Facilities at the University of California, Berkeley," by R.M. Stephen, J.G. Bouwkamp, R.W. Clough and J. Penzien - 1969 (PB 189 111)A04

NA EERC 69-9 "Seismic Response of Soil Deposits Underlain by Sloping Rock Boundaries," by H. Dezfulian and H.B. Seed 1969 (PB 189 114)A03

NA EERC 69-10 "Dynamic Stress Analysis of Axisymmetric Structures Under Arbitrary Loading," by S. Ghosh and E.L. Wilson 1969 (PB 189 026)A10

NA EERC 69-11 "Seismic Behavior of Multistory Frames Designed by Different Philosophies," by J.C. Anderson and V. V. Bertero - 1969 (PB 190 662)A10

NA EERC 69-12 "Stiffness Degradation of Reinforcing Concrete Members Subjected to Cyclic Flexural Moments," by V.V. Bertero, B. Bresler and H. Ming Liao - 1969 (PB 202 942)A07

NA EERC 69-13 "Response of Non-Uniform Soil Deposits to Travelling Seismic Waves," by H. Dezfulian and H.B. Seed - 1969 (PB 191 023)A03

NA EERC 69-14 "Damping Capacity of a Model Steel Structure," by D. Rea, R.W. Clough and J.G. Bouwkamp - 1969 (PB 190 663)A06

NA EERC 69-15 "Influence of Local Soil Conditions on Building Damage Potential during Earthquakes," by H.B. Seed and I.M. Idriss - 1969 (PB 191 036)A03   -

NA EERC 69-16 "The Behavior of Sands Under Seismic Loading Conditions," by M.L. Silver and H.B. Seed - 1969 (AD 714 982)A07

NA EERC 70-1 "Earthquake Response of Gravity Dams," by A.K. Chopra - 1970 (AD 709 640)A03

NA EERC 70-2 "Relationships between Soil Conditions and Building Damage in the Caracas Earthquake of July 29, 1967," by H.B. Seed, I.M. Idriss and H. Dezfulian - 1970 (PB 195 762)A05

NA EERC 70-3 "Cyclic Loading of Full Size Steel Connections," by E.P. Popov and R.M. Stephen - 1970 (PB 213 545)A04

NA EERC 70-4 "Seismic Analysis of the Charaima Building, Caraballeda, Venezuela," by Subcommittee of the SEAONC Research Committee: V.V. Bertero, P.F. Fratessa, S.A. Mahin, J.H. Sexton, A.C. Scordelis, E.L. Wilson, L.A. Wyllie, H.B. Seed and J. Penzien, Chairman - 1970 (PB 201 455)A06

*Reports marked NA are no longer available from EERC.

EERC 73-3   "Computer Aided Ultimate Load Design of Unbraced Multistory Steel Frames," by M.B. El-Hafez and G.H. Powell 1973 (PB 248 315)A09

EERC 73-4   "Experimental Investigation into the Seismic Behavior of Critical Regions of Reinforced Concrete Components as Influenced by Moment and Shear," by M. Celebi and J. Penzien - 1973 (PB 215 884)A09

EERC 73-5   "Hysteretic Behavior of Epoxy-Repaired Reinforced Concrete Beams," by M. Celebi and J. Penzien - 1973 (PB 239 568)A03

NA EERC 73-6   "General Purpose Computer Program for Inelastic Dynamic Response of Plane Structures," by A. Kanaan and G.H. Powell - 1973 (PB 221 260)A08

EERC 73-7   "A Computer Program for Earthquake Analysis of Gravity Dams Including Reservoir Interaction," by P. Chakrabarti and A.K. Chopra - 1973 (AD 766 271)A04

EERC 73-8   "Behavior of Reinforced Concrete Deep Beam-Column Subassemblages Under Cyclic Loads," by O. Küstü and J.G. Bouwkamp - 1973 (PB 246 117)A12

NA EERC 73-9   "Earthquake Analysis of Structure-Foundation Systems," by A.K. Vaish and A.K. Chopra - 1973 (AD 766 272)A07

EERC 73-10   "Deconvolution of Seismic Response for Linear Systems," by R.B. Reimer - 1973 (PB 227 179)A08

NA EERC 73-11   "SAP IV: A Structural Analysis Program for Static and Dynamic Response of Linear Systems," by K.-J. Bathe, E.L. Wilson and F.E. Peterson - 1973 (PB 221 967)A09

EERC 73-12   "Analytical Investigations of the Seismic Response of Long, Multiple Span Highway Bridges," by W.S. Tseng and J. Penzien - 1973 (PB 227 816)A10

EERC 73-13   "Earthquake Analysis of Multi-Story Buildings Including Foundation Interaction," by A.K. Chopra and J.A. Gutierrez - 1973 (PB 222 970)A03

NA EERC 73-14   "ADAP: A Computer Program for Static and Dynamic Analysis of Arch Dams," by R.W. Clough, J.M. Raphael and S. Mojtahedi - 1973 (PB 223 763)A09

EERC 73-15   "Cyclic Plastic Analysis of Structural Steel Joints," by R.B. Pinkney and R.W. Clough - 1973 (PB 226 843)A08

NA EERC 73-16   "QUAD-4: A Computer Program for Evaluating the Seismic Response of Soil Structures by Variable Damping Finite Element Procedures," by I.M. Idriss, J. Lysmer, R. Hwang and H.B. Seed - 1973 (PB 229 424)A05

EERC 73-17   "Dynamic Behavior of a Multi-Story Pyramid Shaped Building," by R.M. Stephen, J.P. Hollings and J.G. Bouwkamp - 1973 (PB 240 718)A06

EERC 73-18   Unassigned

NA EERC 73-19   "Olive View Medical Center Materials Studies, Phase I," by B. Bresler and V.V. Bertero - 1973 (PB 235 986)A06

EERC 73-20   Unassigned

EERC 73-21   "Constitutive Models for Cyclic Plastic Deformation of Engineering Materials," by J.M. Kelly and P.P. Gillis 1973 (PB 226 024)A03

NA EERC 73-22   "DRAIN - 2D User's Guide," by G.H. Powell - 1973 (PB 227 016)A05

EERC 73-23   "Earthquake Engineering at Berkeley - 1973," (PB 226 033)A11

EERC 73-24   Unassigned

NA EERC 73-25   "Earthquake Response of Axisymmetric Tower Structures Surrounded by Water," by C.Y. Liaw and A.K. Chopra 1973 (AD 773 052)A09

NA EERC 73-26   "Investigation of the Failures of the Olive View Stairtowers During the San Fernando Earthquake and Their Implications on Seismic Design," by V.V. Bertero and R.G. Collins - 1973 (PB 235 106)A13

NA EERC 73-27   "Further Studies on Seismic Behavior of Steel Beam-Column Subassemblages," by V.V. Bertero, H. Krawinkler and E.P. Popov - 1973 (PB 234 172)A06

NA EERC 74-1   "Seismic Risk Analysis," by C.S. Oliveira - 1974 (PB 235 920)A06

NA EERC 74-2   "Settlement and Liquefaction of Sands Under Multi-Directional Shaking," by R. Pyke, C.K. Chan and H.B. Seed 1974

NA EERC 74-3   "Optimum Design of Earthquake Resistant Shear Buildings," by D. Ray, K.S. Pister and A.K. Chopra - 1974 (PB 231 172)A06

NA EERC 74-4   "LUSH - A Computer Program for Complex Response Analysis of Soil-Structure Systems," by J. Lysmer, T. Udaka, H.B. Seed and R. Hwang - 1974 (PB 236 796)A05

EERC 74-5   "Sensitivity Analysis for Hysteretic Dynamic Systems: Applications to Earthquake Engineering," by D. Ray 1974 (PB 233 213)A06

217

EERC 75-20   "Dynamic Properties of an Eleven Story Masonry Building," by R.M. Stephen, J.P. Hollings, J.G. Bouwkamp and D. Jurukovski - 1975 (PB 246 945)A04

NA   EERC 75-21   "State-of-the-Art in Seismic Strength of Masonry - An Evaluation and Review," by R.L. Mayes and R.W. Clough 1975 (PB 249 040)A07

EERC 75-22   "Frequency Dependent Stiffness Matrices for Viscoelastic Half-Plane Foundations," by A.K. Chopra, P. Chakrabarti and G. Dasgupta - 1975 (PB 248 121)A07

EERC 75-23   "Hysteretic Behavior of Reinforced Concrete Framed Walls," by T.Y. Wang, V.V. Bertero and E.P. Popov - 1975 (PB 267 298)A17

EERC 75-24   Unassigned

NA   EERC 75-25   "Influence of Seismic History on the Liquefaction Characteristics of Sands," by H.B. Seed, K. Mori and C.K. Chan - 1975 (Summarized in EERC 75-28)

EERC 75-26   "The Generation and Dissipation of Pore Water Pressures during Soil Liquefaction," by H.B. Seed, P.P. Martin and J. Lysmer - 1975 (PB 252 648)A03

NA   EERC 75-27   "Identification of Research Needs for Improving Aseismic Design of Building Structures," by V.V. Bertero 1975 (PB 248 136)A05

NA   EERC 75-28   "Evaluation of Soil Liquefaction Potential during Earthquakes," by H.B. Seed, I. Arango and C.K. Chan - 1975 (NUREG 0026)A13

NA   EERC 75-29   "Representation of Irregular Stress Time Histories by Equivalent Uniform Stress Series in Liquefaction Analyses," by H.B. Seed, I.M. Idriss, F. Makdisi and N. Banerjee - 1975 (PB 252 635)A03

NA   EERC 75-30   "FLUSH - A Computer Program for Approximate 3-D Analysis of Soil-Structure Interaction Problems," by J. Lysmer, T. Udaka, C.-F. Tsai and H. B. Seed - 1975 (PB 259 332)A07

EERC 75-31   Unassigned

EERC 75-32   Unassigned

EERC 75-33   "Predicting the Performance of Structures in Regions of High Seismicity," by J. Penzien - 1975 (PB 248 130)A03

EERC 75-34   "Efficient Finite Element Analysis of Seismic Structure - Soil - Direction," by J. Lysmer, H.B. Seed, T. Udaka, R.N. Hwang and C.-F. Tsai - 1975 (PB 253 570)A03

EERC 75-35   "The Dynamic Behavior of a First Story Girder of a Three-Story Steel Frame Subjected to Earthquake Loading," by R.W. Clough and L.-Y. Li - 1975 (PB 248 841)A05

EERC 75-36   "Earthquake Simulator Study of a Steel Frame Structure, Volume II - Analytical Results," by D.T. Tang - 1975 (PB 252 926)A10

NA   EERC 75-37   "ANSR-I General Purpose Computer Program for Analysis of Non-Linear Structural Response," by D.P. Mondkar and G.H. Powell - 1975 (PB 252 386)A08

EERC 75-38   "Nonlinear Response Spectra for Probabilistic Seismic Design and Damage Assessment of Reinforced Concrete Structures," by M. Murakami and J. Penzien - 1975 (PB 259 530)A05

EERC 75-39   "Study of a Method of Feasible Directions for Optimal Elastic Design of Frame Structures Subjected to Earthquake Loading," by N.D. Walker and K.S. Pister - 1975 (PB 257 781)A06

EERC 75-40   "An Alternative Representation of the Elastic-Viscoelastic Analogy," by G. Dasgupta and J.L. Sackman - 1975 (PB 252 173)A03

EERC 75-41   "Effect of Multi-Directional Shaking on Liquefaction of Sands," by H.B. Seed, R. Pyke and G.R. Martin - 1975 (PB 258 781)A03

EERC 76-1   "Strength and Ductility Evaluation of Existing Low-Rise Reinforced Concrete Buildings - Screening Method," by T. Okada and B. Bresler - 1976 (PB 257 906)A11

EERC 76-2   "Experimental and Analytical Studies on the Hysteretic Behavior of Reinforced Concrete Rectangular and T-Beams," by S.-Y.M. Ma, E.P. Popov and V.V. Bertero - 1976 (PB 260 843)A12

EERC 76-3   "Dynamic Behavior of a Multistory Triangular-Shaped Building," by J. Petrovski, R.M. Stephen, E. Gartenbaum and J.G. Bouwkamp - 1976 (PB 273 279)A07

EERC 76-4   "Earthquake Induced Deformations of Earth Dams," by N. Serff, H.B. Seed, F.I. Makdisi & C.-Y. Chang - 1976 (PB 292 065)A08

UCB/EERC-77/01   "PLUSH - A Computer Program for Probabilistic Finite Element Analysis of Seismic Soil-Structure Inter-action," by M.P. Romo Organista, J. Lysmer and H.B. Seed - 1977 (PB81 177 651)A05

NA   UCB/EERC-77/02   "Soil-Structure Interaction Effects at the Humboldt Bay Power Plant in the Ferndale Earthquake of June 7, 1975," by J.E. Valera, H.B. Seed, C.F. Tsai and J. Lysmer - 1977 (PB 265 795)A04

NA   UCB/EERC-77/03   "Influence of Sample Disturbance on Sand Response to Cyclic Loading," by K. Mori, H.B. Seed and C.K. Chan - 1977 (PB 267 352)A04

UCB/EERC-77/04   "Seismological Studies of Strong Motion Records," by J. Shoja-Taheri - 1977 (PB 269 655)A10

UCB/EERC-77/05   Unassigned

NA   UCB/EERC-77/06   "Developing Methodologies for Evaluating the Earthquake Safety of Existing Buildings," by No. 1 - B. Bresler; No. 2 - B. Bresler, T. Okada and D. Zisling; No. 3 - T. Okada and B. Bresler; No. 4 - V.V. Bertero and B. Bresler - 1977 (PB 267 354)A08

NA   UCB/EERC-77/07   "A Literature Survey - Transverse Strength of Masonry Walls," by Y. Omote, R.L. Mayes, S.W. Chen and R.W. Clough - 1977 (PB 277 933)A07

UCB/EERC-77/08   "DRAIN-TABS: A Computer Program for Inelastic Earthquake Response of Three Dimensional Buildings," by R. Guendelman-Israel and G.H. Powell - 1977 (PB 270 693)A07

NA   UCB/EERC-77/09   "SUBWALL: A Special Purpose Finite Element Computer Program for Practical Elastic Analysis and Design of Structural Walls with Substructure Option," by D.Q. Le, H. Peterson and E.P. Popov - 1977 (PB 270 567)A05

NA   UCB/EERC-77/10   "Experimental Evaluation of Seismic Design Methods for Broad Cylindrical Tanks," by D.P. Clough (PB 272 280)A13

UCB/EERC-77/11   "Earthquake Engineering Research at Berkeley - 1976," - 1977 (PB 273 507)A09

UCB/EERC-77/12   "Automated Design of Earthquake Resistant Multistory Steel Building Frames," by N.D. Walker, Jr. - 1977 (PB 276 526)A09

NA   UCB/EERC-77/13   "Concrete Confined by Rectangular Hoops Subjected to Axial Loads," by J. Vallenas, V.V. Bertero and E.P. Popov - 1977 (PB 275 165)A06

UCB/EERC-77/14   "Seismic Strain Induced in the Ground During Earthquakes," by Y. Sugimura - 1977 (PB 284 201)A04

UCB/EERC-77/15   Unassigned

UCB/EERC-77/16   "Computer Aided Optimum Design of Ductile Reinforced Concrete Moment Resisting Frames," by S.W. Zagajeski and V.V. Bertero - 1977 (PB 280 137)A07

UCB/EERC-77/17   "Earthquake Simulation Testing of a Stepping Frame with Energy-Absorbing Devices," by J.M. Kelly and D.F. Tsztoo - 1977 (PB 273 506)A04

NA   UCB/EERC-77/18   "Inelastic Behavior of Eccentrically Braced Steel Frames under Cyclic Loadings," by C.W. Roeder and E.P. Popov - 1977 (PB 275 526)A15

NA   UCB/EERC-77/19   "A Simplified Procedure for Estimating Earthquake-Induced Deformations in Dams and Embankments," by F.I. Makdisi and H.B. Seed - 1977 (PB 276 820)A04

NA   UCB/EERC-77/20   "The Performance of Earth Dams during Earthquakes," by H.B. Seed, F.I. Makdisi and P. de Alba - 1977 (PB 276 821)A04

UCB/EERC-77/21   "Dynamic Plastic Analysis Using Stress Resultant Finite Element Formulation," by P. Lukkunapvasit and J.M. Kelly - 1977 (PB 275 453)A04

UCB/EERC-77/22   "Preliminary Experimental Study of Seismic Uplift of a Steel Frame," by R.W. Clough and A.A. Huckelbridge 1977 (PB 278 769)A08

UCB/EERC-77/23   "Earthquake Simulator Tests of a Nine-Story Steel Frame with Columns Allowed to Uplift," by A.A. Huckelbridge - 1977 (PB 277 944)A09

UCB/EERC-77/24   "Nonlinear Soil-Structure Interaction of Skew Highway Bridges," by M.-C. Chen and J. Penzien - 1977 (PB 276 176)A07

NA   UCB/EERC-77/25   "Seismic Analysis of an Offshore Structure Supported on Pile Foundations," by D.D.-N. Liou and J. Penzien 1977 (PB 283 180)A06

UCB/EERC-77/26   "Dynamic Stiffness Matrices for Homogeneous Viscoelastic Half-Planes," by G. Dasgupta and A.K. Chopra - 1977 (PB 279 654)A06

UCB/EERC-77/27   "A Practical Soft Story Earthquake Isolation System," by J.M. Kelly, J.M. Eidinger and C.J. Derham - 1977 (PB 276 814)A07

UCB/EERC-77/28   "Seismic Safety of Existing Buildings and Incentives for Hazard Mitigation in San Francisco: An Exploratory Study," by A.J. Meltsner - 1977 (PB 281 970)A05

NA   UCB/EERC-77/29   "Dynamic Analysis of Electrohydraulic Shaking Tables," by D. Rea, S. Abedi-Hayati and Y. Takahashi 1977 (PB 282 569)A04

UCB/EERC-77/30   "An Approach for Improving Seismic - Resistant Behavior of Reinforced Concrete Interior Joints," by B. Galunic, V.V. Bertero and E.P. Popov - 1977 (PB 290 870)A06

UCB/EERC-79/01   "Hysteretic Behavior of Lightweight Reinforced Concrete Beam-Column Subassemblages," by B. Forzani, E.P. Popov and V.V. Bertero - April 1979(PB 298 267)A06

NA   UCB/EERC-79/02   "The Development of a Mathematical Model to Predict the Flexural Response of Reinforced Concrete Beams to Cyclic Loads, Using System Identification," by J. Stanton & H. McNiven - Jan. 1979(PB 295 875)A10

UCB/EERC-79/03   "Linear and Nonlinear Earthquake Response of Simple Torsionally Coupled Systems," by C.L. Kan and A.K. Chopra - Feb. 1979(PB 298 262)A06

UCB/EERC-79/04   "A Mathematical Model of Masonry for Predicting its Linear Seismic Response Characteristics," by Y. Mengi and H.D. McNiven - Feb. 1979(PB 298 266)A06

UCB/EERC-79/05   "Mechanical Behavior of Lightweight Concrete Confined by Different Types of Lateral Reinforcement," by M.A. Manrique, V.V. Bertero and E.P. Popov - May 1979(PB 301 114)A06

NA   UCB/EERC-79/06   "Static Tilt Tests of a Tall Cylindrical Liquid Storage Tank," by R.W. Clough and A. Niwa - Feb. 1979 (PB 301 167)A06

UCB/EERC-79/07   "The Design of Steel Energy Absorbing Restrainers and Their Incorporation into Nuclear Power Plants for Enhanced Safety: Volume 1 - Summary Report," by P.N. Spencer, V.F. Zackay, and E.R. Parker - Feb. 1979(UCB/EERC-79/07)A09

UCB/EERC-79/08   "The Design of Steel Energy Absorbing Restrainers and Their Incorporation into Nuclear Power Plants for Enhanced Safety: Volume 2 - The Development of Analyses for Reactor System Piping,""_Simple Systems_" by M.C. Lee, J. Penzien, A.K. Chopra and K. Suzuki "_Complex Systems_" by G.H. Powell, E.L. Wilson, R.W. Clough and D.G. Row - Feb. 1979(UCB/EERC-79/08)A10

UCB/EERC-79/09   "The Design of Steel Energy Absorbing Restrainers and Their Incorporation into Nuclear Power Plants for Enhanced Safety: Volume 3 - Evaluation of Commercial Steels," by W.S. Owen, R.M.N. Pelloux, R.O. Ritchie, M. Faral, T. Ohhashi, J. Toplosky, S.J. Hartman, V.F. Zackay and E.R. Parker - Feb. 1979(UCB/EERC-79/09)A04

UCB/EERC-79/10   "The Design of Steel Energy Absorbing Restrainers and Their Incorporation into Nuclear Power Plants for Enhanced Safety: Volume 4 - A Review of Energy-Absorbing Devices," by J.M. Kelly and M.S. Skinner - Feb. 1979(UCB/EERC-79/10)A04

UCB/EERC-79/11   "Conservatism In Summation Rules for Closely Spaced Modes," by J.M. Kelly and J.L. Sackman - May 1979(PB 301 328)A03

UCB/EERC-79/12   "Cyclic Loading Tests of Masonry Single Piers; Volume 3 - Height to Width Ratio of 0.5," by P.A. Hidalgo, R.L. Mayes, H.D. McNiven and R.W. Clough - May 1979(PB 301 321)A08

UCB/EERC-79/13   "Cyclic Behavior of Dense Course-Grained Materials in Relation to the Seismic Stability of Dams," by N.G. Banerjee, H.B. Seed and C.K. Chan - June 1979(PB 301 373)A13

UCB/EERC-79/14   "Seismic Behavior of Reinforced Concrete Interior Beam-Column Subassemblages," by S. Viwathanatepa, E.P. Popov and V.V. Bertero - June 1979(PB 301 326)A10

UCB/EERC-79/15   "Optimal Design of Localized Nonlinear Systems with Dual Performance Criteria Under Earthquake Excitations," by M.A. Bhatti - July 1979(PB 80 167 109)A06

NA   UCB/EERC-79/16   "OPTDYN - A General Purpose Optimization Program for Problems with or without Dynamic Constraints," by M.A. Bhatti, E. Polak and K.S. Pister - July 1979(PB 80 167 091)A05

NA   UCB/EERC-79/17   "ANSR-II, Analysis of Nonlinear Structural Response, Users Manual," by D.P. Mondkar and G.H. Powell July 1979(PB 80 113 301)A05

UCB/EERC-79/18   "Soil Structure Interaction in Different Seismic Environments," A. Gomez-Masso, J. Lysmer, J.-C. Chen and H.B. Seed - August 1979(PB 80 101 520)A04

UCB/EERC-79/19   "ARMA Models for Earthquake Ground Motions," by M.K. Chang, J.W. Kwiatkowski, R.F. Nau, R.M. Oliver and K.S. Pister - July 1979(PB 301 166)A05

NA   UCB/EERC-79/20   "Hysteretic Behavior of Reinforced Concrete Structural Walls," by J.M. Vallenas, V.V. Bertero and E.P. Popov - August 1979(PB 80 165 905)A12

UCB/EERC-79/21   "Studies on High-Frequency Vibrations of Buildings - 1: The Column Effect," by J. Lubliner - August 1979 (PB 80 158 553)A03

UCB/EERC-79/22   "Effects of Generalized Loadings on Bond Reinforcing Bars Embedded in Confined Concrete Blocks," by S. Viwathanatepa, E.P. Popov and V.V. Bertero - August 1979(PB 81 124 018)A14

NA   UCB/EERC-79/23   "Shaking Table Study of Single-Story Masonry Houses, Volume 1: Test Structures 1 and 2," by P. Gülkan, R.L. Mayes and R.W. Clough - Sept. 1979 (HUD-000 1763)A12

NA   UCB/EERC-79/24   "Shaking Table Study of Single-Story Masonry Houses, Volume 2: Test Structures 3 and 4," by P. Gülkan, R.L. Mayes and R.W. Clough - Sept. 1979 (HUD-000 1836)A12

UCB/EERC-79/25   "Shaking Table Study of Single-Story Masonry Houses, Volume 3: Summary, Conclusions and Recommendations," by R.W. Clough, R.L. Mayes and P. Gülkan - Sept. 1979 (HUD-000 1837)A06

UCB/EERC-79/26   "Recommendations for a U.S.-Japan Cooperative Research Program Utilizing Large-Scale Testing Facilities," by U.S.-Japan Planning Group - Sept. 1979(PB 301 407)A06

UCB/EERC-79/27   "Earthquake-Induced Liquefaction Near Lake Amatitlan, Guatemala," by H.B. Seed, I. Arango, C.K. Chan, A. Gomez-Masso and R. Grant de Ascoli - Sept. 1979(NUREG-CR1341)A03

UCB/EERC-79/28   "Infill Panels: Their Influence on Seismic Response of Buildings," by J.W. Axley and V.V. Bertero Sept. 1979(PB 80 163 371)A10

UCB/EERC-79/29   "3D Truss Bar Element (Type 1) for the ANSR-II Program," by D.P. Mondkar and G.H. Powell - Nov. 1979 (PB 80 169 709)A02

UCB/EERC-80/28   "Shaking Table Testing of a Reinforced Concrete Frame with Biaxial Response," by M.G. Oliva October 1980(PB81 154 304)A10

UCB/EERC-80/29   "Dynamic Properties of a Twelve-Story Prefabricated Panel Building," by J.G. Bouwkamp, J.P. Kollegger and R.M. Stephen - October 1980(PB82 117 128)A06

UCB/EERC-80/30   "Dynamic Properties of an Eight-Story Prefabricated Panel Building," by J.G. Bouwkamp, J.P. Kollegger and R.M. Stephen - October 1980(PB81 200 313)A05

UCB/EERC-80/31   "Predictive Dynamic Response of Panel Type Structures Under Earthquakes," by J.P. Kollegger and J.G. Bouwkamp - October 1980(PB81 152 316)A04

UCB/EERC-80/32   "The Design of Steel Energy-Absorbing Restrainers and their Incorporation into Nuclear Power Plants for Enhanced Safety (Vol 3): Testing of Commercial Steels in Low-Cycle Torsional Fatigue," by P. Spencer, E.R. Parker, E. Jongewaard and M. Drory

UCB/EERC-80/33   "The Design of Steel Energy-Absorbing Restrainers and their Incorporation into Nuclear Power Plants for Enhanced Safety (Vol 4): Shaking Table Tests of Piping Systems with Energy-Absorbing Restrainers," by S.F. Stiemer and W.G. Godden - Sept. 1980(PB82 201 880)A05

UCB/EERC-80/34   "The Design of Steel Energy-Absorbing Restrainers and their Incorporation into Nuclear Power Plants for Enhanced Safety (Vol 5): Summary Report," by P. Spencer

UCB/EERC-80/35   "Experimental Testing of an Energy-Absorbing Base Isolation System," by J.M. Kelly, M.S. Skinner and K.E. Beucke - October 1980(PB81 154 072)A04

UCB/EERC-80/36   "Simulating and Analyzing Artificial Non-Stationary Earthquake Ground Motions," by R.F. Nau, R.M. Oliver and K.S. Pister - October 1980(PB81 153 397)A04

UCB/EERC-80/37   "Earthquake Engineering at Berkeley - 1980," - Sept. 1980(PB81 205 674)A09

UCB/EERC-80/38   "Inelastic Seismic Analysis of Large Panel Buildings," by V. Schricker and G.H. Powell - Sept. 1980 (PB81 154 338)A13

UCB/EERC-80/39   "Dynamic Response of Embankment, Concrete-Gravity and Arch Dams Including Hydrodynamic Interaction," by J.F. Hall and A.K. Chopra - October 1980(PB81 152 324)A11

UCB/EERC-80/40   "Inelastic Buckling of Steel Struts Under Cyclic Load Reversal," by R.G. Black, W.A. Wenger and E.P. Popov - October 1980(PB81 154 312)A08

UCB/EERC-80/41   "Influence of Site Characteristics on Building Damage During the October 3, 1974 Lima Earthquake," by P. Repetto, I. Arango and H.B. Seed - Sept. 1980(PB81 161 739)A05

UCB/EERC-80/42   "Evaluation of a Shaking Table Test Program on Response Behavior of a Two Story Reinforced Concrete Frame," by J.M. Blondet, R.W. Clough and S.A. Mahin (PB82 196 544)A11

UCB/EERC-80/43   "Modelling of Soil-Structure Interaction by Finite and Infinite Elements," by F. Medina - December 1980(PB81 229 270)A04

UCB/EERC-81/01   "Control of Seismic Response of Piping Systems and Other Structures by Base Isolation," edited by J.M. Kelly - January 1981 (PB81 200 735)A05

UCB/EERC-81/02   "OPTNSR - An Interactive Software System for Optimal Design of Statically and Dynamically Loaded Structures with Nonlinear Response," by M.A. Bhatti, V. Ciampi and K.S. Pister - January 1981 (PB81 218 851)A09

UCB/EERC-81/03   "Analysis of Local Variations in Free Field Seismic Ground Motions," by J.-C. Chen, J. Lysmer and H.B. Seed - January 1981 (AD-A099508)A13

UCB/EERC-81/04   "Inelastic Structural Modeling of Braced Offshore Platforms for Seismic Loading," by V.A. Zayas, P.-S.B. Shing, S.A. Mahin and E.P. Popov - January 1981(PB82 138 777)A07

UCB/EERC-81/05   "Dynamic Response of Light Equipment in Structures," by A. Der Kiureghian, J.L. Sackman and B. Nour-Omid - April 1981 (PB81 218 497)A04

UCB/EERC-81/06   "Preliminary Experimental Investigation of a Broad Base Liquid Storage Tank," by J.G. Bouwkamp, J.P. Kollegger and R.M. Stephen - May 1981(PB82 140 385)A03

UCB/EERC-81/07   "The Seismic Resistant Design of Reinforced Concrete Coupled Structural Walls," by A.E. Aktan and V.V. Bertero - June 1981(PB82 113 358)A11

UCB/EERC-81/08   "The Undrained Shearing Resistance of Cohesive Soils at Large Deformations," by M.R. Pyles and H.B. Seed - August 1981

UCB/EERC-81/09   "Experimental Behavior of a Spatial Piping System with Steel Energy Absorbers Subjected to a Simulated Differential Seismic Input," by S.F. Stiemer, W.G. Godden and J.M. Kelly - July 1981 (PB82 201 898)A04

UCB/EERC-81/10   "Evaluation of Seismic Design Provisions for Masonry in the United States," by B.I. Sveinsson, R.L. Mayes and H.D. McNiven - August 1981 (PB82 166 075)A08

UCB/EERC-81/11   "Two-Dimensional Hybrid Modelling of Soil-Structure Interaction," by T.-J. Tzong, S. Gupta and J. Penzien - August 1981(PB82 142 118)A04

UCB/EERC-81/12   "Studies on Effects of Infills in Seismic Resistant R/C Construction," by S. Brokken and V.V. Bertero - October 1981 (PB82 166 190)A09

225

UCB/EERC-82/19   "Experimental Studies of Multi-support Seismic Loading on Piping Systems," by J. M. Kelly and A. D. Cowell - November 1982

UCB/EERC-82/20   "Generalized Plastic Hinge Concepts for 3D Beam-Column Elements," by P. F.-S. Chen and G. H. Powell - November 1982 (PB83 247 981)A13

UCB/EERC-82/21   "ANSR-III: General Purpose Computer Program for Nonlinear Structural Analysis," by C. V. Oughourlian and G. H. Powell - November 1982 (PB83 251 330)A12

UCB/EERC-82/22   "Solution Strategies for Statically Loaded Nonlinear Structures," by J. W. Simons and G. H. Powell - November 1982 (PB83 197 970)A06

UCB/EERC-82/23   "Analytical Model of Deformed Bar Anchorages under Generalized Excitations," by V. Ciampi, R. Eligehausen, V. V. Bertero and E. P. Popov - November 1982 (PB83 169 532)A06

UCB/EERC-82/24   "A Mathematical Model for the Response of Masonry Walls to Dynamic Excitations," by H. Sucuoğlu, Y. Mengi and H. D. McNiven - November 1982 (PB83 169 011)A07

UCB/EERC-82/25   "Earthquake Response Considerations of Broad Liquid Storage Tanks," by F. J. Cambra - November 1982 (PB83 251 215)A09

UCB/EERC-82/26   "Computational Models for Cyclic Plasticity, Rate Dependence and Creep," by B. Mosaddad and G. H. Powell - November 1982 (PB83 245 829)A08

UCB/EERC-82/27   "Inelastic Analysis of Piping and Tubular Structures," by M. Mahasuverachai and G. H. Powell - November 1982 (PB83 249 987)A07

UCB/EERC-83/01   "The Economic Feasibility of Seismic Rehabilitation of Buildings by Base Isolation," by J. M. Kelly - January 1983 (PB83 197 988)A05

UCB/EERC-83/02   "Seismic Moment Connections for Moment-Resisting Steel Frames," by E. P. Popov - January 1983 (PB83 195 412)A04

UCB/EERC-83/03   "Design of Links and Beam-to-Column Connections for Eccentrically Braced Steel Frames," by E. P. Popov and J. O. Malley - January 1983 (PB83 194 811)A04

UCB/EERC-83/04   "Numerical Techniques for the Evaluation of Soil-Structure Interaction Effects in the Time Domain," by E. Bayo and E. L. Wilson - February 1983 (PB83 245 605)A09

UCB/EERC-83/05   "A Transducer for Measuring the Internal Forces in the Columns of a Frame-Wall Reinforced Concrete Structure," by R. Sause and V. V. Bertero - May 1983 (PB84 119 494)A06

UCB/EERC-83/06   "Dynamic Interactions between Floating Ice and Offshore Structures," by P. Croteau - May 1983 (PB84 119 486)A16

UCB/EERC-83/07   "Dynamic Analysis of Multiply Tuned and Arbitrarily Supported Secondary Systems," by T. Igusa and A. Der Kiureghian - June 1983 (PB84 118 272)A11

UCB/EERC-83/08   "A Laboratory Study of Submerged Multi-body Systems in Earthquakes," by G. R. Ansari - June 1983 (PB83 261 842)A17

UCB/EERC-83/09   "Effects of Transient Foundation Uplift on Earthquake Response of Structures," by C.-S. Yim and A. K. Chopra - June 1983 (PB83 261 396)A07

UCB/EERC-83/10   "Optimal Design of Friction-Braced Frames under Seismic Loading," by M. A. Austin and K. S. Pister - June 1983 (PB84 119 288)A06

UCB/EERC-83/11   "Shaking Table Study of Single-Story Masonry Houses: Dynamic Performance under Three Component Seismic Input and Recommendations," by G. C. Manos, R. W. Clough and R. L. Mayes - June 1983

UCB/EERC-83/12   "Experimental Error Propagation in Pseudodynamic Testing," by P. B. Shing and S. A. Mahin - June 1983 (PB84 119 270)A09

UCB/EERC-83/13   "Experimental and Analytical Predictions of the Mechanical Characteristics of a 1/5-scale Model of a 7-story R/C Frame-Wall Building Structure," by A. E. Aktan, V. V. Bertero, A. A. Chowdhury and T. Nagashima - August 1983 (PB84 119 213)A07

UCB/EERC-83/14   "Shaking Table Tests of Large-Panel Precast Concrete Building System Assemblages," by M. G. Oliva and R. W. Clough - August 1983

UCB/EERC-83/15   "Seismic Behavior of Active Beam Links in Eccentrically Braced Frames," by K. D. Hjelmstad and E. P. Popov - July 1983 (PB84 119 676)A09

UCB/EERC-83/16   "System Identification of Structures with Joint Rotation," by J. S. Dimsdale - July 1983 (PB84 192 210)A06

UCB/EERC-83/17   "Construction of Inelastic Response Spectra for Single-Degree-of-Freedom Systems," by S. Mahin and J. Lin - July 1983 (PB84 208 834)A05